


Spring 5-19-2010

REGULATION OF MORPHOGENESIS IN FILAMENTOUS FUNGI

Haoyu Si

University of Nebraska at Lincoln, haoyu@huskers.unl.edu

Follow this and additional works at: <http://digitalcommons.unl.edu/bioscidiss>

 Part of the [Cell Biology Commons](#), [Molecular Genetics Commons](#), and the [Other Microbiology Commons](#)

Si, Haoyu, "REGULATION OF MORPHOGENESIS IN FILAMENTOUS FUNGI" (2010). *Dissertations and Theses in Biological Sciences*. 11.

<http://digitalcommons.unl.edu/bioscidiss/11>

This Article is brought to you for free and open access by the Biological Sciences, School of at DigitalCommons@University of Nebraska - Lincoln. It has been accepted for inclusion in Dissertations and Theses in Biological Sciences by an authorized administrator of DigitalCommons@University of Nebraska - Lincoln.

REGULATION OF MORPHOGENESIS IN FILAMENTOUS FUNGI

By

Haoyu Si

A DISSERTATION

Presented to the Faculty of

The Graduate College at the University of Nebraska

In Partial Fulfillment of Requirements

For the Degree of Doctor of Philosophy

Major: Biological Sciences

Under the Supervision of Professor Steven D. Harris

Lincoln, Nebraska

August, 2010

REGULATION OF MORPHOGENESIS IN FILAMENTOUS FUNGI

Haoyu Si, Ph.D.

University of Nebraska, 2010

Adviser: Steven D. Harris

One of the distinguishing features of fungal cells is their highly polarized model of growth. Both yeast cells and hyphal cells grow by cell surface expansion at specified cortical sites. Although the same general mechanisms are likely to be involved in controlling the establishment of hyphal polarity in budding yeast and filamentous fungi, it is noticeable that hyphal cells are organized in a fundamentally different manner to yeast cells. For example, hyphal cells organize formins, septins and actins at the division site while simultaneously retain the same machinery at the tip; whereas yeast cells undergo a transient period of isotropic growth with mitosis and cell cycles. Among filamentous fungi, *Aspergillus nidulans* had been proven to be a particularly valuable model. The genetic tractability of this fungus coupled with the availability of sophisticated post-genomics resources has enabled the identification and characterization of numerous genes involved in hyphal morphogenesis. One objective of this study was to determine the extent to which components of the *S. cerevisiae* bud site selection module were conserved in filamentous fungi. We have identified and examined the function of bud site selection homologues of Bud3 (AN0113.3), Bud4 (AN6150.3), and Ax12 (AN1359.3) in *A. nidulans*, even though the sequence conservation is largely limited to domains that are presumed to be functionally important (i.e., the GEF domain of Bud3, and the anillin-like and PH domains of Bud4). We also identified homologues of Msb2 (An4701.3) and Rga1 (An1025.3), which are the small GTPase Cdc42 related proteins. In this article,

their unique functions for hyphal morphogenesis were characterized towards understanding the function of these genes and the mechanisms involved in polarized hyphal growth, septation and secondary developments in *A. nidulans*. I also highlight important areas for future investigation.

Acknowledgments

I want to thank Steven Harris for his guidance and mentorship throughout my graduate career I would like to thank Dr Richard Wilson for his kind help of proofreading my dissertation I would like to thank Camile Semighini and Bill Rittenour for their help in Harris lab I would like to give Aleks, special thanks for her friendship and scientific discussion to help me get along with the lab techniques over the beginning years of my study Lastly but not least, I want to thank my father who inspired me to pursue my interests in nature and science I want to express my thanks to my mother for her endless support and encouragement in my life I want to express my heartfelt gratitude and love to my wife, Menghan, for her constant love, patience and understanding Finally, I want to thank my son, Mouyuan, for upon his arrival he makes me understand the responsibility and happiness in my life

TABLE OF CONTENT

ACKNOWLEDGEMENTS.....	iv
LIST OF TABLES.....	xi
LIST OF FIGURES.....	xii
CHAPTER I Review of Hyphal morphogenesis in <i>Aspergillus nidulans</i>	1
Overview.	1
<i>A. nidulans</i> as a model organism.....	2
Features of hyphal morphogenesis in <i>A. nidulans</i>	3
Isotropic growth.....	4
Establishment of a polarity axis.....	6
Maintenance of a polarity axis.....	11
Septum formation.....	15
Perspectives.....	20
Reference.....	28
CHAPTER II.....	33
Abstract.....	33
Introduction.....	33
Material and Methods.....	38
Strains, media, growth conditions and staining.....	38
Construction of gene replacement strains.....	39
Genetic interaction experiments.....	39
Construction of GFP fusions to Anbud3 and Rho4.....	40
AnBud3 guanine nucleotide exchange assays.....	41
Conidiation experiments.....	43
sepA1 and sepH1 experiments.....	43

Microscopy.....	44
Δ bud3 suppressor screen.....	44
Results.....	44
The <i>A. nidulans</i> homologue of Bud3 is required for septum formation..	44
AnBud3 functions as a GEF for Rho4.....	46
AnBud3 and Rho4 localization patterns at septa.....	48
Roles of nuclear division and the SIN in AnBud3 localization.....	50
The presumptive GAP Msb1 does not regulate septum formation.....	51
Discussion.....	52
The Bud3-Rho4 GTPase module.....	53
The Bud3-Rho4 pathway	55
Reference.....	83
CHAPTER III.....	88
Abstract.....	88
Introduction.....	88
Summary of bud4 and axl2 in <i>Saccharomyces cerevisiae</i>	89
Axl2-GFP localization is determined by the cell cycle in yeast.	90
Secondary development in <i>Aspergillus nidulans</i>	90
Transcriptional factors on conidiophore development.....	91

Septins in <i>S. cerevisiae</i> and <i>A. nidulans</i>	92
Axl2 and Vac8 belongs to Cadherin and catenin families respectively....	93
Material and Methods.....	94
Strains, media, growth conditions and staining.....	94
Construction of gene replacement strains.....	95
Construction of GFP fusions to Axl2 and Bud4.....	95
The Axl2 and Bud4 promoter swap and alcA::Axl2 construct.....	97
Conidiophore observation.....	98
Spore counting for sexual development.....	98
Examining GFP localization on conidiophores.....	99
RT-PCR from RNA extracted from normal and induced culture.....	99
Microscopy.....	100
Results.....	100
Identification of <i>A. nidulans</i> Axl2 and Bud4.....	100
Role of Axl2 in <i>A. nidulans</i> morphogenesis.....	101
Axl2 localizes to the top of phialides.....	101
Roles of Bud4 in <i>A. nidulans</i> morphogenesis.....	102

Localization of Bud4 in <i>A nidulans</i>	103
Axl2 was upregulated when AbaA and BlrA expression were induced..	104
Axl2 localization under Bud4 and alcA promoter control.....	105
Bud4 localizaion under AnAxl2 promoter control.....	108
Interaction between septins and Axl2 in <i>A nidulans</i>	108
Vec8 and Axl2 are involved in sexual development.....	109
Discussion.....	110
The roles of Bud4 in septum formation.....	111
The role of Bud4 and Axl2 in conidiophore development.....	113
Proper expression of Axl2 and Bud4 is required for their localization..	113
The role of Axl2 and Vac8 in sexual development.....	114
Reference.....	148
Chapter IV.....	151
Introduction.....	151
Cdc42 GTPase signaling and the GTPase activating protein Rga1.....	151
Rga1 functions as a GAP of Cdc42.....	152
Effectors of Cdc42p for MAP kinase pathway.....	153

MAPkinase pathway in yeast and filamentous fungi.....	154
Msb2 and Sho1 is upstream of MAP kinase pathway.....	157
Material and Methods.....	158
Strains, media, growth conditions and staining.....	158
Construction of gene replacement strains.....	159
Construction of GFP fusions to AnRga1.....	160
Conidiophore observation and GFP localization on conidiophores...	161
Microscopy.....	161
Results.....	161
Identification of A nidulans Msb2 and Rag1.....	162
Rga1 is not required for vegetative growth but is essential for normal conidiophore development.....	163
Rga1 localize to the top of phialides before the spore generation.....	163
ΔAnMsb2 affects timing and structure of hyphal growth and cell wall integrity.....	164
Discussion.....	167
Reference.....	176
CHAPTER V FUTURE DIRECTION.....	182

GAP(s) of the Bud3-Rho4 module.....	182
The roles of AnAx12 and Anbud4 in septin organization.....	182
Cell cycle related AnAx12, Bud3 and Anbud4 expression.....	184
Roles of Vac8 and AnAx12 during sexual development.....	185
Further testing the function of Msb2 in cell wall integrity.....	186
Functions of GAPs in Aspergillus morphogenesis.....	187

LIST OF TABLES

Table 2-1	<i>A nidulans</i> strains used in this study.....	57
Table 3-1	<i>A nidulans</i> strains used in this study.....	145
Table 3-3	Spore counting.....	146
Table 3-4	Septum counting.....	147

LIST OF FIGURES

Figure 1-1	Genes that contribute to isotropic growth, polarity establishment and polarity maintenance during the germination of <i>Aspergillus nidulans</i> conidiospores.....	23
Figure 1-2	Molecular model of hyphal growth in <i>Aspergillus nidulans</i>	24
Figure 1-3	Pathways underlying septum formation.....	26
Figure 2-1	Organization and phylogenetic analysis of AnBud3.....	58
Figure 2-2	Effects of the <i>Anbud3</i> deletion on colony morphology, septum formation and conidiation.....	60
Figure 2-3	Dosage suppression of <i>bud3</i> growth and septation defects by <i>rho4</i>	62
Figure 2-4	Effects of the $\Delta\rho4$ mutation on growth, hyphal morphology, and development.....	64
Figure 2-5	AnBuD3 is a Rho4 exchange factor.....	66
Figure 2-6	AnBud3 is able to stimulate the GDP-GTP exchange activity of <i>N crassa</i> Rho4.....	68
Figure 2-7	Localization of GFP-AnBud3.....	70
Figure 2-8	Localization of GFP-Rho4.....	72
Figure 2-9	Absence of contractile actin rings in <i>sepA1</i> mutant hyphae grown at 37°.....	74

Figure 2-10	Recruitment of AnBud3 to septation sites does not require presence of the contractile actin ring.....	76
Figure 2-11	GFP-AnBud3 localization when nuclear division is blocked.....	78
Figure 2-12	Localization of GFP-AnBud3 in the <i>sepH1</i> mutant.....	79
Figure 2-13	Effects of the <i>msb1</i> mutation on growth and hyphal morphology.....	80
Figure 2-14	<i>Δbud3</i> suppressors.....	82
Figure 3-1	The life cycle of <i>Aspergillus nidulans</i>	116
Figure 3-2	Amino acid sequence and domains of AnBud4 and AnAxl2.....	117
Figure 3-3	Effects of the <i>ΔAnaxl2</i> deletion on colony morphology.....	118
Figure 3-4	Effect of <i>ΔAnaxl2</i> on conidiophore morphology.....	120
Figure 3-5	Drawing for AnAxl2::GFP C-terminal fusion and GFP::AnBud4 N-terminal fusion.....	121
Figure 3-6	Localization of AnAxl2-GFP.....	122
Figure 3-7	Effects of the <i>ΔAnbud4</i> deletion on colony morphology and conidiation.....	123
Figure 3-8	AnBud4 is involved in septum formation.....	125
Figure 3-9	Localization of GFP-AnBud4 in hyphae.....	126
Figure 3-10	GFP-AnBud4 ring dynamics.....	128

Figure 3-11	Localization of GFP-AnBud4 during asexual development.....	130
Figure 3-12	RT-PCR of <i>AnAxl2</i> expression.....	132
Figure 3-13	Constructs for <i>AnAxl2</i> and <i>AnBu4</i> promoter swap.....	133
Figure 3-14	<i>AnAxl2</i> expression under different promoters during hyphal growth...	134
Figure 3-15	Localization of <i>AnAxl2</i> -GFP under <i>pAnbud4</i> promoter control.....	136
Figure 3-16	Effects of hyper-expression of <i>AnAxl2</i> on colony morphology.....	138
Figure 3-17	Colony morphology of septin mutants, $\Delta Anaxl2$ deletion mutants and their crossed double mutants.....	140
Figure 3-18	Sexual spore production of WT, $\Delta Anvac8$ and $\Delta AnAxl2$ grown on minimal media for 9 days in dark.....	142
Figure 3-19	Schematic illustration of <i>AnAxl2</i> -GFP and GFP-AnBud4 localization..	143
Figure 4-1	Function and regulation in MAPK signaling pathways.....	167
Figure 4-2	Amino acid sequence of <i>AnRga1</i>	168
Figure 4-3	Effect of the <i>Anrga1</i> deletion on colony morphology.....	169
Figure 4-4	Effect of the <i>Anrga1</i> deletion on conidiophore development.....	170
Figure 4-5	Localization of <i>AnRga1</i> -GFP in conidiophore development.....	172
Figure 4-6	Effect of the <i>Anmsb2</i> deletion on colony morphology.....	174
Figure 4-7	Cell wall integrity test on <i>Anmsb2</i> deletion mutants.....	175

Chapter I Hyphal morphogenesis in *Aspergillus*

Overview

Despite their apparent simplicity, fungal hyphae are remarkable structures that allow filamentous fungi to colonize a diverse array of habitats. The characteristic feature of a hypha is the localization of growth to the extreme tip, leading to the formation of an elongated tube capable of impressive extension rates. The formation of apical and lateral branches increases the surface area colonized by a hyphal network. The partitioning of hyphae into cellular units by cross-walls known as septa permit compartmentalization of functions and is thought to play a key role in supporting the development of reproductive structures that bear spores. A deeper understanding of the molecular basis of hyphal morphogenesis is important at two levels. First, it would yield meaningful insight that could be exploited to allow better control of fungal growth, whether limiting the growth of a pathogen or optimizing the growth of an industrial strain that produces valuable compounds. Second, it would permit comparison to analogous processes in animals and plants. This might be particularly relevant to other highly polarized cell types in these kingdoms, including neurons and pollen tubes, with a view towards the elucidation of common principles underlying this unique mode of growth. Accordingly, there is increasing interest in the identification and characterization of functions required for the establishment and maintenance of hyphal polarity, the formation of branches, and septation. One of the fungi that has proven to be a veritable “workhorse” in this effort is *Aspergillus nidulans*, which is a widely recognized model fungus known for its genetic tractability and ease of manipulation. In this review, we summarize progress towards understanding the molecular basis of hyphal morphogenesis in *A. nidulans*.

***A. nidulans* as a model organism**

A. nidulans (teleomorph *Emericella nidulans*) is an ascomycete fungus that belongs to the class *Eurotiomycetes* and the order *Eurotiales*. Over the past ~50 years, the seminal efforts of a long list of notable research scientists have elevated *A. nidulans* to the status of a model organism. Befitting this status, numerous methods have been developed to facilitate the efficient analysis of gene function in *A. nidulans*. Foremost amongst these is the ability to use classical genetic approaches to identify and characterize interesting sets of mutants (Todd et al, 2007ab), including conditional mutations that affect essential functions. Additional methods, such as PCR-mediated gene replacement and heterokaryon rescue, permit the targeted analysis of specific genes, including those whose deletion might be lethal (Osmani et al., 2006; Szewczyk et al., 2006). Finally, a diverse collection of fluorescent reagents and probes (i.e., GFP-based markers) enable the real-time imaging of several important proteins in growing hyphae. Collectively, through the use of these methods, numerous *A. nidulans* proteins have been functionally implicated in some aspect of hyphal morphogenesis (Harris, 2008; Fischer et al., 2008). In many cases, these proteins were selected based on their homology to proteins known to be involved in the polarized morphogenesis of other organisms, primarily the yeasts *Saccharomyces cerevisiae* and *Schizosaccharomyces pombe*. In other examples, the proteins were identified as a result of unbiased genetic screens that focused on mutants that exhibit defects in polarity establishment, polarity maintenance, septum formation, or nuclear division. Notably, these screens often lead to the identification of proteins with no previously suspected role in hyphal morphogenesis.

Features of hyphal morphogenesis in *A. nidulans*

Like most filamentous fungi, *A. nidulans* initiates a new round of growth through the process of spore germination. The events underlying the germination of asexual conidiospores leading to the growth of a mature hypha have been characterized extensively (Trinci; Harris1997; d'Enfert1997; OsherovMay2001, Momany2002, Harris2006). It is presumed that a similar sequence of events accompanies the germination of sexual ascospores, though this has not been investigated in any detail.

In *A. nidulans*, the first step in spore germination is the breaking of dormancy, which is accompanied by spore re-hydration, initiation of translation, resumption of metabolic activity, and isotropic expansion of the cell surface. The next step is the establishment of a polarity axis upon which subsequent cell surface expansion and cell wall deposition are directed. The stabilization of this axis results in the maintenance of polarity and enables the formation of a germ tube that ultimately matures into a hypha.

Hyphae are populated by multiple nuclei due to a series of parasynchronous nuclear divisions (note that conidiospores are uninucleate, whereas ascospores are binucleate). Nuclear division is coordinated with growth such that each division is coupled to a doubling of cell mass, and the entire process is referred to as the duplication cycle (Trinci; Harris1997). Once hyphae reach a certain volume, which appears to vary depending on growth conditions, they are partitioned by the formation of the first septum. Notably, septation is coordinated with nuclear division and the first septum typically forms nears the basal end of a hypha near the junction with the conidiospore. Following the first septation event, each passage through the duplication cycle is terminated by the

formation of septa in the hyphal tip compartment. On the other hand, sub-apical compartments enter a period of mitotic quiescence that is eventually broken by the formation of a branch that generates a new hypha. Branch formation requires the establishment and maintenance of a new polarity axis, and likely recapitulates many of the events involved in spore germination.

For the remainder of this review, we will focus on specific features of hyphal morphogenesis in *A. nidulans*, with emphasis placed on what is known about the underlying mechanisms.

Isotropic growth

The primary trigger for conidiospore germination in *A. nidulans* appears to be glucose, whereas nitrogen and phosphorus are dispensable (it is not known if this is also true for ascospores). The presence of glucose is seemingly sensed by a G protein-coupled receptor (GPCR), because a constitutively active (i.e. GTP bound) G protein GanB causes precocious germination of conidia, even in the absence of a carbon source (Chang, Chae et al. 2004). One downstream effector of GanB is likely to be CyaA, an adenylate cyclase necessary for cyclic AMP (cAMP) production. cAMP acts as a secondary messenger that binds to the regulatory subunit of protein kinase A (PKA), thereby activating the catalytic subunit. In *A. nidulans*, both CyaA and PKA are required for efficient spore germination (Fillinger, Chaverocche et al. 2002). Additional studies also implicate a Ras signaling pathway in glucose sensing. In particular, a dominant activating mutation in the Ras homologue RasA enables conidiospores to initiate germination in the absence of a carbon source. Although mutant spores undergo isotropic expansion and nuclear condensation/division, they do not proceed to germ tube emergence (Osheroov and

May 2000). This implies that the level of active RasA must diminish for later stages of germination to proceed, and suggests that Ras activity might determine the extent of isotropic expansion based on nutrient conditions. The upstream activator of RasA remains unknown, though likely candidates include GPCRs as well as glucose transporters (Fig 1-1).

What are the physiological responses necessary for isotropic expansion that rely on the above signaling pathways? During the isotropic growth phase of conidiospores, water uptake is likely necessary to increase the volume of the spore and maintain turgor pressure. However, the mechanisms underlying the transport of water, and whether aquaporins are specifically involved, have not yet been investigated. One strategy that fungi use to increase water uptake is the synthesis or uptake of compatible solutes (osmolytes) that increase the water potential of the spore. Trehalose metabolism has been linked to glycerol accumulation in germinating spores of *A. nidulans*, suggesting the possibility that glycerol serves as an osmolyte (d'Enfert and Fontaine 1997; d'Enfert, Bonini et al. 1999; Fillinger, Chaverroche et al. 2002). However, glycerol cannot be the sole osmolyte contributing to the water potential of swelling conidia because the deletion of glycerol dehydrogenase genes and subsequent reduction in intracellular glycerol levels does not preclude isotropic expansion and spore germination (Fillinger, Ruitijter et al. 2001; de Vries, Flitter et al. 2003). Cellular mannitol, trehalose, and perhaps proline may serve as additional osmolytes. Indeed, a gene encoding the proline transporter *prnB* is upregulated during conidial germination (Tazebay, Sophianopoulou et al. 1995; Tazebay, Sophianopoulou et al. 1997).

Common housekeeping functions also appear to be strongly associated with isotropic expansion. Multiple genetic screens for conditional polarity mutants have revealed that disruption of protein translation and folding arrests conidiospore germination during the isotropic expansion phase (OsherovMay; OsherovMay; LinMomany). Similar effects are observed when conidiospores are treated with inhibitors of translation (OsherovMay). These observations suggest that increased metabolic activity is needed to support isotropic expansion. The TOR signaling pathway is an attractive candidate for mediating this effect. In *S. cerevisiae*, TOR appears to act in combination with PKA to regulate the growth response to nutrient repletion (Slattery2008). Coupled with the known capacity of TOR to regulate actin organization (REF), this observation hints at a possible mechanism for the coordination of cell surface expansion with metabolism in germinating conidiospores.

Establishment of a polarity axis

A prerequisite for the successful emergence of a germ tube from a swollen spore is the establishment of a polarity axis. Polarity establishment encompasses the processes of specifying a new polarity axis and using the resulting positional information to spatially organize the morphogenetic machinery. This results in the termination of isotropic expansion, such that cell wall deposition no longer occurs around the entire circumference of the spore, and is instead confined to a specific site that will eventually become the hyphal tip. Despite considerable interest in the mechanisms underlying polarity establishment in *A. nidulans*, they remain poorly defined. Nevertheless, genetic analyses have provided some insight into how new polarity axes are specified and have also implicated several cellular functions in the establishment of polarity.

The best understood paradigm for the specification of a polarization site in fungi is the *S. cerevisiae* bud site selection system. This system is based on the use of distinct cortical markers that specify one of two possible budding patterns. The resulting positional information is subsequently relayed to the GTPase Cdc42 via a Ras-related GTPase Rsr1/Bud1. Locally active Cdc42 then promotes recruitment of the morphogenetic machinery to the presumptive bud site. Critical components of this regulatory system are either absent from the *A. nidulans* genome (e.g., Bud8, Bud9) or, if present, are very poorly conserved (i.e., Ax12, Bud3, Bud4, Ax11). Furthermore, functional characterization of the poorly conserved homologues shows that they have no obvious role in the establishment or maintenance of hyphal polarity (H. Si and S. Harris, manuscript submitted). Based on this evidence, the bud site selection system does not appear to perform an analogous function during spore germination in *A. nidulans*. Nevertheless, results from studies using *A. fumigatus* implicate a Ras GTPase, RasB, in the spatial regulation of polarized hyphal growth, and cortical markers that generate positional information in *A. nidulans* have also been identified (i.e., TeaR; see below for more detail). Accordingly, a cortical marking system might yet specify the polarity axis in swollen *A. nidulans* spores, though the potential involvement of RasB and TeaR, as well as the identification of other vital components, remains to be investigated (Figure 1-2).

An alternative paradigm for the specification of the polarity axis is provided by the *S. cerevisiae* mating pheromone response. Binding of mating pheromone to its cognate GPCR leads to activation of an associated heterotrimeric G protein, such that the liberated complex is able to serve as a positional marker that locally recruits

components of the Cdc42 GTPase module. Local activation of Cdc42 then reorganizes the morphogenetic machinery in a manner that overrides existing bud site selection signals. Most components of the pheromone response pathway are conserved in *A. nidulans*, and furthermore, at least one GPCR and a heterotrimeric G protein have been implicated in the regulation of spore germination. Thus, it is entirely conceivable that a GPCR involved in glucose detection could also mark the eventual polarization site. At this time, there is no experimental evidence that supports this idea, though heterotrimeric G proteins do regulate the orientation of hyphal growth and control lateral branch formation in other filamentous fungi.

Although the preceding models implicate specific landmarks (i.e., bud site selection proteins, GPCRs) in the selection of new polarity axes, studies of polarity establishment in *S. cerevisiae* suggest that these markers are not needed *per se*. Notably, yeast cells can still switch from isotropic expansion to polarized growth despite the absence of all known landmarks. Under these circumstances, polarity establishment becomes reliant upon a set of positive and negative feedback loops that reinforce initially stochastic fluctuations in local Cdc42 levels until they exceed a given threshold at a random site. Key elements of these feedback loops include filamentous actin and the modular scaffold protein Bem1, which act in a complementary manner to promote localized vesicle exocytosis towards the presumptive polarized site, whereas endocytosis enables retrieval of “polarity factors” from other sites. A similar spontaneous polarization mechanism could conceivably operate during spore germination and/or branch formation in *A. nidulans*. For example, current evidence implies that the polarity axis that directs formation of the first germ tube from swollen spores is randomly selected. One the other

hand, the second germ tube almost always emerges from the pole opposite the first (i.e., the bipolar germination pattern), which would be consistent with the idea that a specific marking system only comes into play once the first polarity axis is specified. Candidate landmarks for this system could include cortical markers or GPCRs, though the possible role of the mitotic spindle and its resident proteins should perhaps be considered as well.

Surprisingly few functions are known to be required for polarity establishment in *A. nidulans*. It is generally thought that the actin cytoskeleton and vesicle trafficking machinery (i.e., the morphogenetic machinery) are needed to establish a polarity axis. In the latter case, the phenotypes of mutants such as *copA* and *podB*, which affect proteins required for normal organization of the Golgi apparatus, support this view. By contrast, there is no direct evidence that demonstrates actin filaments are required for polarity establishment in *A. nidulans*. Mutations that block formation of a sub-class of actin filaments (i.e., mutations affecting the formin SepA) only delay polarity establishment. Deletions of genes that encode actin and key regulators such as α -actinin and Bud6 are lethal, but it is not known whether this reflects a failure to establish polarity. Treatment with cytochalasin A dramatically affects polarity maintenance (see below), but its effects on polarity establishment have not been reported. Although functional actin filaments would seem to be an obvious requirement for the localized delivery of regulatory factors (i.e., landmark proteins?) and components needed for cell wall deposition to the polarization site, it is not inconceivable that cytoplasmic microtubules provide a back-up mechanism that enables polarity establishment in their absence. The observation that microtubules become essential for polarity establishment in the absence of SepA provides some evidence for this idea.

A theme that has emerged from genetic screens for polarity mutants in *A. nidulans* is the importance of post-translational modification of proteins to the process of polarity establishment. The observation that a temperature sensitive (Ts) mutation affecting the N-myristoyltransferase SwoF prevents the establishment of a polarity axis implies that at least one protein requires this modification to perform its morphogenetic function. Because of their known requirement for lipid modification, obvious candidates include GTPases such as RasA, Cdc42, and Rac1, which are each involved in some aspect of polarity establishment in *A. nidulans*. However, a bioinformatics approach identified several additional potential targets (i.e., the "myristoylome"), of which the most interesting are the Arf GTPases. A combination of genetic and biochemical evidence suggests that ArfA and ArfB are indeed targets of SwoF. The lethality of an *arfA* gene disruption precluded analysis of its role in polarity establishment, which nevertheless seems likely given its localization to endomembranes and its presumed role in vesicle transport. On the other hand, genetic analysis of an insertion mutation in *arfB* documented clear defects in both the establishment and maintenance of polarity axes, and further showed that these are likely caused by reduced endocytosis.

Nuclear division is generally not viewed as a strict requirement for successful establishment of a polarity axis during spore germination in *A. nidulans*, primarily because most never-in-mitosis (*nim*) and blocked-in-mitosis (*bim*) mutants are able to form germ tubes, albeit after a delay in some cases. However, three mitotic mutants, *nimL*, *nimM*, and *nimN*, fail to establish polarity under all conditions tested. Notably, these mutants each exhibit sensitivity to the DNA replication inhibitor hydroxyurea (HU), and moreover, exposure of wildtype conidiospores to HU also prevents polarity establishment.

These observations raise the possibility that once DNA replication is initiated, it must be completed for polarity establishment to occur. This effect does not appear to be due to the action of DNA replication or DNA damage checkpoints (S. Harris, unpublished). Instead, it is intriguing to consider the possibility that passage through a specific point in S phase of the cell cycle is required for the establishment of a polarity axis. This might be conceptually similar to “new end take-off” (NETO) in *S. pombe*, which is a point during S phase that must be passed before the new polarity axis is established to enable bipolar growth.

Maintenance of a polarity axis

Once a polarity axis has been established, it must be stabilized in order for a germ tube or branch to emerge and form a mature hypha that grows by apical extension. Indeed, it is this ability to maintain a polarity axis for a considerable distance that defines filamentous fungi such as *A. nidulans*. Both forward and reverse genetic approaches have resulted in the identification and characterization of numerous genes required for polarity maintenance in *A. nidulans*. Important functions revealed by these studies include protein O-glycosylation, sphingolipid biosynthesis and organization, the Spitzenkorper, and vesicle trafficking.

In addition to revealing the importance of post-translational modification to polarity establishment, genetic screens for Ts morphological mutants also showed that they have a role in maintaining polarity axes. In particular, results from temperature shift experiments suggest that the *swoA* mutant is able to establish polarity when grown at the

restrictive temperature, but cannot maintain the signals required to sustain polar growth (Momany, Westfall et al. 1999). The *swaA* phenotype was shown to be complemented by the *pmtA* O-mannosyltransferase gene (Shaw and Momany 2002). Accordingly, it seems likely that one or more yet-to-be identified surface protein(s) that contribute to polar growth are modified by O-glycosylation in a manner that affects their function.

The first evidence of the importance of sphingolipids in polarity maintenance came from the characterization of serine palmitoyltransferase (SPT) function in *A. nidulans*. SPT catalyzes the first committed step in sphingolipid biosynthesis, and is thereby required for the formation of all sphingolipid derivatives (i.e., sphingoid bases, ceramides, etc.). Mutational or chemical (i.e., myriocin) inactivation of SPT prevented polarity establishment without adversely affecting growth or nuclear division. It was also found that the absence of sphingolipids terminates existing polarity axes and leads to profuse branching of the hyphal tip. This study highlighted the key role of compounds such as sphingoid bases and ceramides in multiple aspects of polarized hyphal morphogenesis. Subsequent studies have further analyzed the respective roles of these two compounds. BasA, which is a homologue of *S. cerevisiae* Sur2, is a sphinganine hydroxylase responsible for the synthesis of sphingoid bases. Deletion of *basA* causes severe defects in polarity establishment and maintenance. LagA and BarA are two distinct ceramide synthases whose combined function is required for the maintenance of polarity axes, but not their establishment. Notably, BarA appears to generate a pool of glucosylceramides that promote localization of the formin SepA at hyphal tips (Rittenour et al., unpublished). Taken together, these studies suggest that the surface of hyphal tips might consist of a patchwork of lipid domains that differ in ceramide composition and

mediate recruitment of different complexes that stabilize polarity axes (e.g., Viag and Harris 2006a). Sphingoid bases may have an additional set of functions, presumably involved in lipid signaling, that separately promote polarity establishment.

The Spitzenkorper (SPK) is a phase-dark structure present at the extreme apex of fungal hyphae that has been shown to have an intimate role in promoting efficient polar growth. The concept of the SPK as a vesicle trafficking center and the modeling of its function have been previously described. The polarisome is a seemingly distinct structure at the hyphal tip that regulates formin-based assembly of actin filaments. In *A. nidulans*, localization of the formin SepA suggests that the polarisome exists as a surface crescent at the hyphal tip, whereas the SPK sits just behind the tip and appears as a spot. Further refinement of hyphal tip organization has emerged from a recent study that describes the “tip growth apparatus” of *A. nidulans*. Results from this study suggest that the SPK and polarisome are components of a dynamic apparatus that localizes to the tip and mediates the delivery of exocytic vesicles to the apex. This apparatus consists of an apical actin cluster embedded within a larger cluster of vesicles that are presumably delivered by kinesin-dependent transport on cytoplasmic microtubules. Within the apparatus, vesicles are likely transferred from microtubules to actin filaments that are nucleated by SepA, followed by transport to a discrete exocytic zone at the extreme apex. Although it has yet to be demonstrated, it seems possible that the polarisome might play a role in formation of the SPK.

Results from several recent studies have highlighted the importance of endocytosis in the maintenance of polarity axes in *A. nidulans*. Whereas exocytosis relies on filamentous actin cables for delivery of vesicles to the apex, endocytosis has been

shown to rely on branched actin patches for internalization of vesicles from a distinct cylindrical region located just behind the apex, but still within the “tip growth apparatus” (Araujo-Bazan, Penalva et al. 2008; Taheri-Talesh, Horio et al. 2008; Upadhyay and Shaw 2008). A number of conserved endocytic marker proteins (i.e., AbpA, SlaB, FimA) have been shown to interact with and to stabilize these actin patches. Mutations that eliminate these proteins cause severe defects in polarity maintenance, and in some cases, polarity establishment as well (Araujo-Bazan, Penalva et al. 2008; Taheri-Talesh, Horio et al. 2008; Upadhyay and Shaw 2008). These observations demonstrate that the presence of an endocytic zone flanking the apex is just as critical for polarity maintenance as is vesicle exocytosis. It is quite likely that plasma membrane components and important cell surface proteins are recycled via endocytosis within this zone as hyphae expand. It is tempting to speculate that the septins, which have a known role in the compartmentalization of distinct cell surface domains, might play a role in demarcating the endocytic and exocytic zones within the “tip growth apparatus”. Furthermore, the localization and characterization of MesA, a predicted cell surface protein initially identified on the basis of genetic interaction with SepA, suggests that it could facilitate organization of the endocytic zone.

An elegant series of experiments have described a microtubule-dependent regulatory complex that contributes to the maintenance of polarity axes in *A. nidulans* by stabilizing the position of the position of SPK within hyphal tips. In particular, deletion of the kinesin KipA perturbs the position and size of the SPK, as well as the distribution of microtubules. Whereas the plus ends of microtubules converge at one point in the tips of wildtype hyphae, they often end in two or more points in the tips of *kipA* mutants,

suggesting that *kipA* delivers proteins that contribute to the organization of microtubules at hyphal tips and stabilize the SPK. Indeed, KipA is required for the proper localization of cortical marker TeaR, which is a putative prenylated membrane protein that interacts with and is required for proper localization of TeaA (Takeshita, Higashitsuji et al. 2008). TeaA is also required for proper convergence of microtubules at the hyphal tip and for SPK stabilization, though it does not appear to depend upon KipA for its localization. In addition, TeaA interacts with and co-localizes with the formin SepA. These observations outline a pathway by which a cortical marker directs the organization of both microtubules and actin filaments, and thereby stabilizes the position of the SPK. It will be interesting to determine what role different lipid domains might play in the localization of TeaR at the hyphal tip.

Septum formation

A. nidulans hyphae are partitioned by septa via a process that shares similarity with cytokinesis in animal cells (Harris et al 1994; Harris 2001). This includes the formation and constriction of a cytokinetic actin ring (CAR) in a manner that is coordinated with the completion of nuclear division (Momany and Hamer 1997). Deposition of the septum occurs concomitant with constriction of the CAR, which in all likelihood provides a landmark for recruitment of the vesicle trafficking machinery as well as chitin synthetases. Notably, septa do not form a complete barrier between hyphal cells, as a pore (i.e., the septal pore, Tenney et al 2000) remains that presumably facilitates intercellular communication and nutrient translocation within a hypha. Woronin bodies positioned near the pore provide a mechanism for sealing hyphal cells should they experience osmotic or other forms of stress capable of causing lysis. Septum formation

shares certain functions in common with hyphal tip growth (e.g., formin-mediated actin nucleation, localized chitin synthesis), and the two processes can even occur simultaneously in the hyphal tip cell (Harris 1997). At the same time, there are important distinctions, of which the most important might be tight temporal and spatial coordination with nuclear division (Figure 1-3).

The multinucleate nature of hyphal cells in *A. nidulans* implies that unlike uninucleate yeast cells, not every nuclear division is associated with cytokinesis. Indeed, it was established very early on that multiple rounds of nuclear division precede formation of the first septum in germinating conidiospores (Clutterbuck 1970; Harris et al 1994). This appears to reflect the operation of a size control mechanism that regulates activation of the cyclin-dependent kinase NimX (Wolkow et al 1996; Kraus and Harris 2001). Once the size threshold has been exceeded, each subsequent round of nuclear division in the hyphal tip cell is followed by the formation of one or more septa within its basal half (Clutterbuck 1970). The positioning of each septum is largely guided by mitotic nuclei (Wolkow et al 1996); there is no evidence yet for the existence of cortical markers that specify septation sites independent of nuclei (though the recently characterized TeaC represents an attractive possibility; Higashitsuji et al 2009). Evidence suggests that as in animal cells, the mitotic spindle generates a signal that is relayed to the cortex and triggers assembly of the CAR. However, because hyphae are not uninucleate, this cannot occur for every spindle. Whether this means that only certain cortical regions are competent to receive the mitotic signal, or, randomly specified sites are able to suppress signal reception in flanking regions, remain important ideas for future investigation. In addition, the basis for suppression of septum formation in the apical

region of hyphal tips cells, which can be subverted by activation of developmental programs (Sewall 1994), is not known.

The septation initiation network (SIN) is a well-characterized signaling pathway that regulates assembly and constriction of the CAR in *S. pombe* (Simanis 2003). The analogous pathway in *S. cerevisiae*, the mitotic exit network (MEN), controls the exit from mitosis in addition to formation of the CAR (Simanis 2003). The first SIN component characterized in *A. nidulans* is SepH, which is a homologue of *S. pombe* Cdc7 that is essential for CAR assembly but not for any apparent feature of mitosis (Bruno et al 2001). Accordingly, as in *S. pombe*, SIN function appears to be restricted to septation in *A. nidulans*. Recent studies have characterized additional components of the *A. nidulans* SIN and confirmed their role in regulating the assembly and constriction of the CAR (Kim et al 2006). Surprisingly, the scaffolds that anchor SIN components to the spindle pole bodies (SPBs) are not required for septation in *A. nidulans* (Kim et al 2009). Moreover, neither the terminal SIN kinase SidB nor its associated regulator MobA needs to associate with the SPB prior to their recruitment to the septation site (Kim et al 2009). Therefore, unlike *S. pombe*, where SPB localization represents a key step in activation of the SIN (Simanis 2003), the *A. nidulans* SIN is likely activated in the cytoplasm. It remains to be determined whether a Tem1/Spg1-like GTPase activates the *A. nidulans* SIN as in either yeast, and if the localization of this GTPase changes during passage through mitosis. In addition, the identity of the relevant SIN target(s) required for CAR assembly and constriction has yet to be discovered.

The CAR is assembled at the septation site and undergoes constriction simultaneously with centripetal deposition of the septum. In *S. pombe*, the anillin-like

protein Mid1 plays a pivotal role in the spatial and temporal coordination of CAR assembly with nuclear division (Chang et al 1996; Glotzer 2005). However, there is no obvious Mid1 homologue in *A. nidulans*, and the only anillin-like protein, Bud4, appears to function at a later stage of septation (Si and Harris, unpublished). Instead, by analogy to the filamentous fungus *Neurospora crassa*, it seems likely that a Rho GTPase module may act downstream of nuclear signals to direct CAR assembly. In *N. crassa*, Rho-4 is necessary for CAR assembly and its inappropriate hyper-activation triggers the formation of spurious CARs (Rasmussen 2005). Although the nature of the nuclear signals that might lead to activation of Rho-4 are not known, the SIN network represents an obvious and attractive candidate. Several components of the *A. nidulans* CAR have been identified and characterized, including the formin SepA (Sharpless and Harris 2002), the tropomyosin TpmA (Pearson 2004), the α -actinin AcnA (Wang et al 2009), the myosin I MyoA (McGoldrick et al 1995), the formin-associated protein Bud6 (Virag and Harris 2006), and multiple chitin synthases (see below). The order in which these components are recruited, and the dynamics of their interactions within the CAR, have not yet been investigated. For example, it would be interesting to determine whether they initially form multiple small nodes that coalesce into a ring as observed in *S. pombe* (Pollard 2008). In addition, it will be important to understand how these proteins are recruited to the CAR when many of them function concurrently at the hyphal tip to build a different set of actin polymers. The possible role of localized translation in mediating the formation of spatially distinct pools of these proteins should be considered.

The septins are a conserved family of proteins with well-established roles in yeast cytokinesis (Longtine et al 1996). *A. nidulans* possesses at least five septins (Momany et

al 2001), one of which, AspB, has been characterized in detail (Westfall and Momany 2002). AspB initially localizes as a ring that co-localizes with the CAR at septation sites. Notably, formation of this ring is dependent upon the SIN pathway as well as the presence of the CAR. The AspB ring subsequently splits into two rings that flank the septum. It is tempting to speculate that these rings may define a membrane compartment that facilitates the targeting of chitin synthases and other components needed for deposition of the septum. Finally, the basal AspB ring (relative to the hyphal tip) disappears, whereas the apical ring persists following the completion of septation. This observation leads to the intriguing suggestion that the latter ring might serve as a directional marker in hyphal cells (Westfall and Momany 2002). Functional characterization of a Ts *aspB* mutant revealed that the apparent absence of AspB does not block septum formation *per se*, but does lead to the formation of faint abnormally thin septa. It will be important to determine whether the other *A. nidulans* septins exhibit the same function and localization patterns as AspB.

Chitin synthesis represents the final step in septum formation, and requires the activity of chitin synthases, which are membrane-associated enzymes that catalyze the polymerization of N-acetylglucosamine. *A. nidulans* possesses eight distinct chitin synthases, including at least one member from each of the seven classes of this enzyme known to exist in fungi. Of these eight chitin synthases, ChsA, ChsC, CsmA and CsmB have each been implicated in septum formation. ChsA and ChsC appear to function in a redundant manner during septation, as inactivation of both chitin synthases (but neither alone) leads to defects in the ultrastructure of the septum as well as its aberrant placement (Ichinomiya et al., 2005). Results from localization studies are consistent with the notion

that ChsA and ChsC associate with the CAR as it constricts, though they do not strictly co-localize with each other (Ichinomiya et al., 2005). CsmA and CsmB are novel chitin synthases that possess an N-terminal myosin motor-like domain implicated in interactions with actin filaments (Takeshita et al 2005; Takeshita et al., 2006). Both enzymes localize to septa in a pattern that suggests they associate with the CAR. Nevertheless, although their localization is indistinguishable from each other, there is no evidence that they physically interact. Instead, it has been proposed that they belong to distinct classes of exocytic vesicles that localize to septa (Takeshita et al., 2006). The combined inactivation of CsmA and CsmB does not prevent septum formation, but might compromise proper formation of the septal pore (Takeshita et al., 2006). According to this model, ChsA and ChsC are primarily responsible for synthesis of the septum, whereas CsmA and CsmB have a more specific function in regulating chitin deposition around the septal pore (Takeshita et al., 2006; Horiuchi 2008).

Perspectives

Due to their highly polarized mode of growth and their importance to the fungal lifestyle, hyphae have long attracted the interest of fungal researchers. With the increasing availability of sophisticated post-genomics tools and resources, new insights into the mechanisms underlying different aspects of hyphal morphogenesis are emerging with much greater frequency. Many of these advances have been achieved using filamentous fungi other than *A. nidulans*, including *Candida albicans*, *Ashbya gossypii*, and *N. crassa*. Indeed, because different fungi possess different attributes that make them

useful for the study of hyphal morphogenesis, the best chance for making real progress towards understanding processes such as polarity establishment, polarity maintenance, and septum formation is to exploit as diverse a set of fungi as is practical. Nevertheless, *A. nidulans* should continue to serve at the vanguard of these efforts. For example, the regularity of the duplication cycle in *A. nidulans* should make it relatively easier to characterize the mechanisms that coordinate the aforementioned processes with growth and nuclear division.

Although there are a myriad of interesting questions pertaining to hyphal morphogenesis that warrant deeper investigation, a somewhat biased sample is presented below. Notably, the answers to many of these questions will not necessarily emerge from studies that use the yeasts *S. cerevisiae* and *S. pombe* as a guiding model. In many cases, it might be more fruitful to consider observations made using migrating animal cells or neurons as a source for relevant ideas. Some of the more important questions include;

1. What is the composition and dynamics of the SPK? Given the importance of the SPK to polarized hyphal growth, a detailed description of its components, their functions, and their interactions is needed. In addition, the functional relationship of complexes such as the polarisome and exocyst to the SPK remains a mystery.

2. How is the polarity axis first established in germinating spores? Is there a set of specific landmark proteins that await identification, or is this an example of spontaneous polarization?

3. What roles do mRNA transport and localized translation play in the spatial coordination of hyphal morphogenesis? For example, do these processes generate distinct spatially segregated pools of SepA that are used for hyphal extension and septum formation?

4. How is septum formation spatially and temporally coordinated with nuclear division? Does the SIN specify when and where the CAR is assembled, and how is assembly at other sites prevented?

It should not be long before attempts to answer these and other questions yield exciting new insights that significantly advance our understanding of hyphal morphogenesis in *A. nidulans*. Because many related Aspergilli impact humans as pathogens and producers of useful compounds, these insights should also have immense practical value.

Figure 1-1

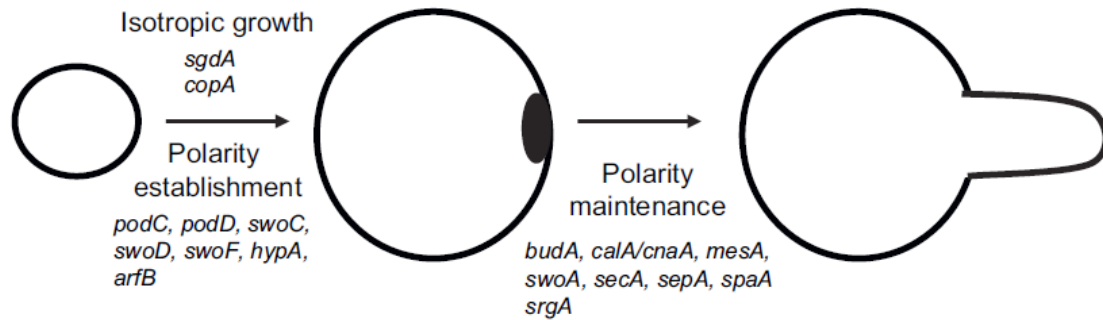


Fig. 1-1 Genes that contribute to isotropic growth, polarity establishment and polarity maintenance during the germination of *Aspergillus nidulans* conidiospores. Conidiospores undergo a period of isotropic expansion before a polarity axis is established (black spot) upon which the incipient germ tube will be released. The release of the germ tube and its subsequent growth are dependent upon the ability of *A. nidulans* to maintain several protein complexes at the point of polarity establishment (see text for details).

Figure 1-2

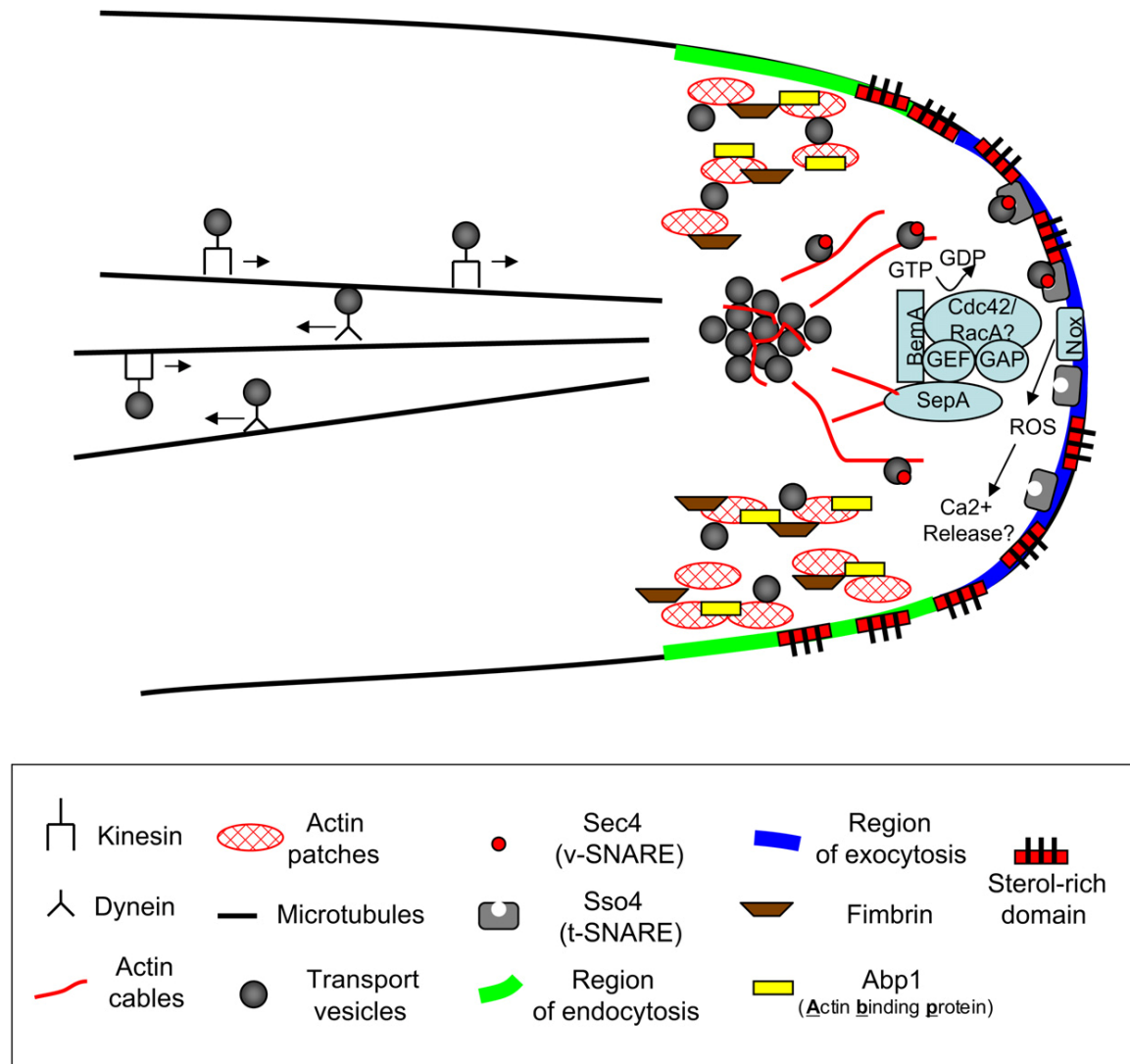


Fig. 1-2 Molecular model of hyphal growth in *Aspergillus nidulans*. Vesicles are delivered from the Golgi-like organelles to the apical vesicle cluster (i.e. Spitzenkörper) along microtubules. Vesicular transport on microtubules is powered by motor proteins in the kinesin (anterograde direction) and dynein (retrograde direction) families. From the apical vesicle cluster, the vesicles are transported along actin cables to the plasma membrane. The actin cables at the hyphal tip are nucleated by the formin SepA, which may be activated by small GTPases Cdc42 and/or RacA. Vesicle fusion with the membrane is mediated by t-SNARE and v-SNARE proteins. The hyphal tips of several fungi contain sterol-rich membrane domains. Although the protein content of sterol-rich domains is unclear, they likely represent signaling complexes that contribute to the molecular mechanisms to hyphal growth. The extreme apex of hyphal tips undergoes extensive exocytosis, whereas flanking regions undergo endocytosis to recycle membrane components. Endocytosis at the hyphal tip is dependent upon actin patches, actin binding protein, and fimbrin.

Figure 1-3

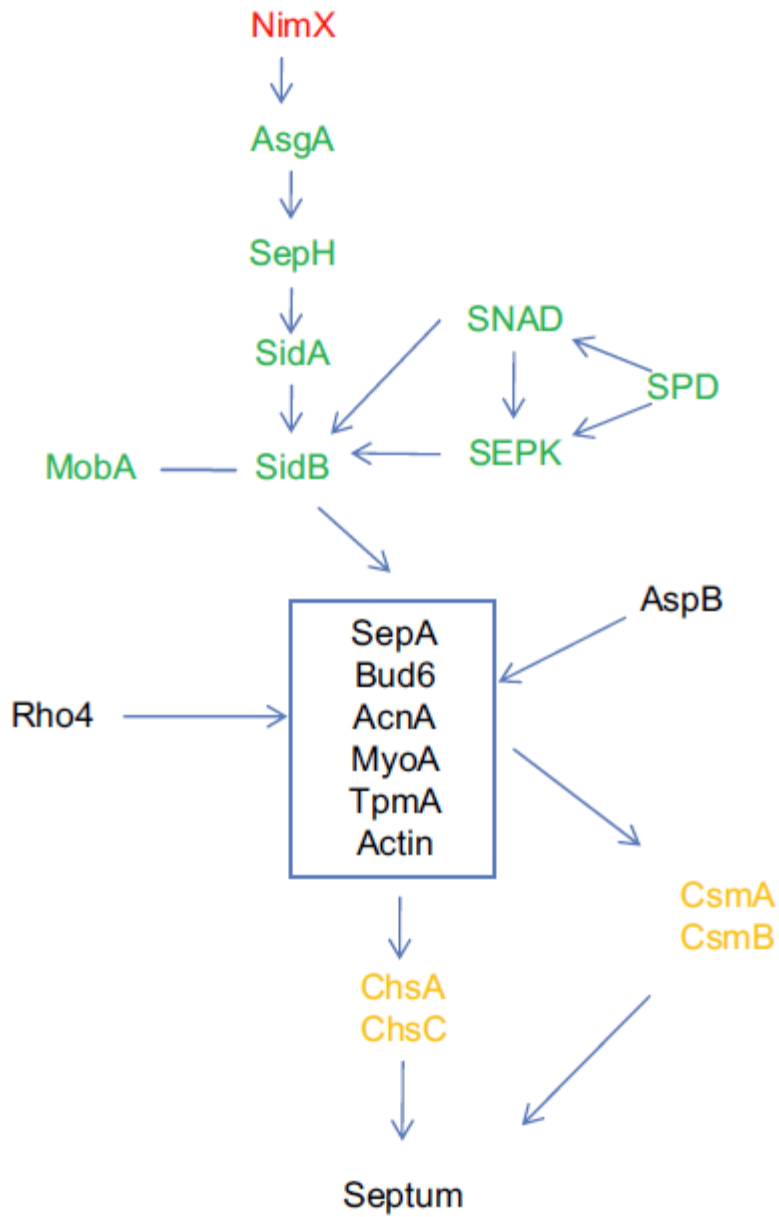


Fig. 1-3 Pathways underlying septum formation. Gene products involved in cell cycle regulation (red), the SIN (green), CAR assembly and function (black), and chitin synthesis (brown) are indicated. NimX is proposed to work in conjunction with mitotic signals and a possible cortical landmark to activate the SIN via ApgA and SepH. SnaD and SepK anchor the SIN to spindle pole bodies (SPB). The SIN is proposed to regulate the assembly and constriction of the CAR, which in turn likely serves as a landmark to direct deposition of the septum. See text for details.

References

- Araujo-Bazan L, Penalva MA, Espeso EA, 2008. Preferential localization of the endocytic internalization machinery to the hyphal tips underlies polarization of the actin cytoskeleton in *Aspergillus nidulans*. *Mol. Microbiol.* 67: 891–905.
- Barral Y, Mermall V, Mooseker MS, Snyder M, 2000. Compartmentalization of the cell cortex by septins is required for maintenance of cell polarity in yeast. *Mol. Cell* 5: 841–851.
- Bartnicki-Garcia S, Hergert F, Gierz G, 1989. Computer simulation of fungal morphogenesis and the mathematical basis for hyphal tip growth. *Protoplasma* 153: 46–57.
- Breakspear A, Langford KJ, Momany M, Assinder SJ, 2007. CopA: GFP localizes to putative golgi equivalents in *Aspergillus nidulans*. *FEMS Microbiol. Lett.* 277: 90–97.
- Bruno KS, Morrell JL, Hamer JE, Staiger CJ, 2001. SEPH, a Cdc7p orthologue from *Aspergillus nidulans*, functions upstream of actin ring formation during cytokinesis. *Mol. Microbiol.* 42: 3–12.
- Chang F, Woollard A, Nurse P, 1996. Isolation and characterization of fission yeast mutants defective in the assembly and placement of the contractile actin ring. *J Cell Sci.* 109: 131–142.
- Chang M-H, Chae K-S, Han D-M, Jahng K-Y, 2004. The GanB Ga-protein negatively regulates asexual sporulation and plays a positive role in conidial germination in *Aspergillus nidulans*. *Genetics* 167: 1305–1315.
- Cheng J, Park T-S, Fishl AS, Ye XS, 2001. Cell cycle progression and cell polarity require sphingolipid biosynthesis in *Aspergillus nidulans*. *Mol. Cell. Biol.* 21: 6198–6209.
- Clutterbuck AJ, 1970. Synchronous nuclear division and septation in *Aspergillus nidulans*. *J. Gen. Microbiol.* 60: 133–135.
- d'Enfert C, 1997. Fungal spore germination: insights from the molecular genetics of *Aspergillus nidulans* and *Neurospora crassa*. *Fungal Genet. Biol.* 21: 163–172.
- d'Enfert C, Bonini BM, Zapella PDA, Fontaine T, da Silva AM, Terenzi HF, 1999. Neutral trehalases catalyse intracellular trehalose breakdown in the filamentous fungi *Aspergillus nidulans* and *Neurospora crassa*. *Mol. Microbiol.* 32: 471–483.
- d'Enfert C, Fontaine T, 1997. Molecular characterization of the *Aspergillus nidulans* *treA* gene encoding an acid trehalase required for growth on trehalose. *Mol. Microbiol.* 24: 203–216.
- de Vries RP, Flitter SJ, van de Vondervoort PJ, Chaverroche M-K, Fontaine T, Fillinger S, Ruitijter G, d'Enfert C, Visser J, 2003. Glycerol dehydrogenase, encoded by *gldB* is essential for osmotolerance in *Aspergillus nidulans*. *Mol. Microbiol.* 49: 131–141.
- Fiddy C, Trinci AP, 1976. Mitosis, septation, branching and the duplication cycle in *Aspergillus nidulans*. *J. Gen. Microbiol.* 97:169–184.
- Fillinger S, Chaverroche M-K, Shimizu K, Keller N, d'Enfert C, 2002. cAMP and ras signalling independently control spore germination in the filamentous fungus *Aspergillus nidulans*. *Mol. Microbiol.* 44: 1001–1016.

- Fillinger S, Ruitijter G, Tamas MJ, Visser J, Thevelein JM, d'Enfert C, 2001. Molecular and physiological characterization of the NAD- dependent glycerol 3-phosphate dehydrogenase in the filamentous fungus *Aspergillus nidulans*. *Mol. Microbiol.* 39: 145–157.
- Fortwendel JR, Zhao W, Bhabhra R, Park S, Perlin DS, Askew DS, Rhodes JC, 2005. A fungus-specific Ras homolog contributes to the hyphal growth and virulence of *Aspergillus fumigatus*. *Eukaryot. Cell* 4: 1982–1989.
- Girbardt M, 1957. Der Spitzenkörper von *Polystictus versicolor*. *Planta* 50: 47–59.
- Glotzer M, 2005. The molecular requirements for cytokinesis. *Science* 307: 1735–1739.
- Haak D, Gable K, Beeler T, Dunn T, 1997. Hydroxylation of *Saccharomyces cerevisiae* ceramides requires Sur2p and Scs7p. *J. Biol. Chem.* 272: 29704–29710.
- Harris SD, 1997. The duplication cycle in *Aspergillus nidulans*. *Fungal Genet. Biol.* 22: 1–12.
- Harris SD, 1999. Morphogenesis is coordinated with nuclear division in germinating *Aspergillus nidulans* conidiophores. *Microbiology* 145: 2747–2756.
- Harris SD, 2001. Septum formation in *Aspergillus nidulans*. *Curr. Opin. Microbiol.* 4: 736–739.
- Harris SD, 2006. Cell polarity in filamentous fungi. *Int. Rev. Cytol.* 251: 41–77.
- Harris SD, Hamer L, Sharpless KE, Hamer JE, 1997. The *Aspergillus nidulans* sepA gene encodes an FH1/2 protein involved in cytokinesis and the maintenance of cellular polarity. *EMBO J* 16: 3473–3483.
- Harris SD, Momany M, 2004. Polarity in filamentous fungi: moving beyond the yeast paradigm. *Fungal Genet. Biol.* 41: 391–400.
- Harris SD, Morrell JL, Hamer JE, 1994. Identification and characterization of *Aspergillus nidulans* mutants defective in cytokinesis. *Genetics* 136: 517–532.
- Harris SD, Turner G, Meyer V, Espeso EA, Specht T, et al., 2009. Morphology and development in *Aspergillus nidulans*: a complex puzzle. *Fungal Genet. Biol.* 46: S82–92.
- Horiuchi H, 2008. Functional diversity of chitin synthases of *Aspergillus nidulans* in hyphal growth, conidiophore development and septum formation. *Med. Mycology* 47: S47–S52.
- Higashitsuji Y, Herrero S, Takeshita N, Fischer R, 2009. The cell end marker protein TeaC is involved in both growth directionality and septation in *Aspergillus nidulans*. *Eukaryot. Cell* 8: 957–967.
- Ichinomiya M, Yamada E, Yamashita S, Ohta A, Horiuchi H, 2005. Class I and class II chitin synthases are involved in septum formation in the filamentous fungus *Aspergillus nidulans*. *Eukaryot. Cell* 4: 1125–1136.
- Kim JM, Lu L, Shao R, Chin J, Liu B, 2006. Isolation of mutations that bypass the requirement of the septation initiation network for septum formation and conidiation in *Aspergillus nidulans*. *Genetics* 173: 685–696.
- Kim JM, Zeng CJ, Nayak T, Shao R, Huang AC, Oakley BR, Liu B, 2009. Timely septation requires SNAD-dependent spindle pole body localization of the septation initiation network components in the filamentous fungus *Aspergillus*

- nidulans. *Mol. Biol. Cell* 20: 2874–2884.
- Kraus PR, Harris SD, 2001. The *Aspergillus nidulans* *snt* genes are required for the regulation of septum formation and cell cycle checkpoints. *Genetics* 159: 557–569.
- Lee SC, Schmidtke SN, Dangott LJ, Shaw B, 2008. *Aspergillus nidulans* ArfB plays a role in endocytosis and polarized growth. *Eukaryot. Cell* 7: 1278–1288.
- Lee SC, Shaw BD, 2008. Localization and function of ADP ribosylation factor A in *Aspergillus nidulans*. *FEMS Microbiol. Lett.* 283: 216–222.
- Li S, Du L, Yuen G, Harris SD, 2006. Distinct ceramide synthases regulate polarized growth in the filamentous fungus *Aspergillus nidulans*. *Mol. Biol. Cell* 17: 1218–1227.
- Lin X, Momany M, 2003. The *Aspergillus nidulans* *swoC1* shows defects in growth and development. *Genetics* 165: 543–554.
- Longtine MS, DeMarini DJ, Valencik ML, Al-Awar OS, Fares H, et al., 1996. The septins: roles in cytokinesis and other processes. *Curr. Opin. Cell. Biol.* 8: 106–119.
- Martin SG, Chang F, 2005. New end take off: regulating cell polarity during the fission yeast cell cycle. *Cell Cycle* 4: 1046–1049.
- McGoldrick CA, Gruver C, May GS, 1995. *myoA* of *Aspergillus nidulans* encodes an essential myosin I required for secretion and polarized growth. *J. Cell Biol.* 128: 577–587.
- Momany M, 2002. Polarity in filamentous fungi. *Curr. Opin. Microbiol.* 5: 580–585.
- Momany M, Hamer JE, 1997. Relationship of actin, microtubules, and crosswall synthesis during septation in *Aspergillus nidulans*. *Cell Motil. Cytoskeleton* 38: 373–384.
- Momany M, Westfall PJ, Abramowsky G, 1999. *Aspergillus nidulans* *swo* mutants show defects in polarity establishment, polarity maintenance and hyphal morphogenesis. *Genetics* 151: 557–567.
- Momany M, Zhao J, Lindsey R, Westfall PJ, 2001. Characterization of the *Aspergillus nidulans* septin (*asp*) gene family. *Genetics* 157: 969–977.
- Oshero N, May G, 2000. Conidial germination in *Aspergillus nidulans* requires RAS signalling and protein synthesis. *Genetics* 155: 647–656.
- Oshero N, May G, 2001. Molecular mechanisms of conidial germination. *FEMS Microbiol. Lett.* 1999: 153–160.
- Osmani AH, Oakley BR, Osmani SA, 2006. Identification and analysis of essential *Aspergillus nidulans* genes using the heterokaryon rescue technique. *Nat. Protocol* 1: 2517–2526.
- Park HO, Bi E, 2007. Central roles of small GTPases in the development of cell polarity in yeast and beyond. *Microbiol. Mol. Biol. Rev.* 71: 48–96.
- Pearson CL, Xu K, Sharpless KE, Harris SD, 2004. *MesA*, a novel fungal protein required for the stabilization of polarity axes in *Aspergillus nidulans*. *Mol. Biol. Cell* 15: 3658–3672.
- Pollard TD, 2008. Progress towards understanding the mechanism of cytokinesis in fission yeast. *Biochem. Soc. Trans.* 36: 425–430.

- Rasmussen CG, Glass NL, 2005. A Rho-type GTPase, rho-4, is required for septation in *Neurospora crassa*. *Eukaryot. Cell* 4:1913–1925.
- Sewall TC, 1994. Cellular effects of misscheduled *brlA*, *abaA*, and *wetA* expression in *Aspergillus nidulans*. *Can. J. Microbiol* 40:1035–1042.
- Schmidt A, Kunz J, Hall MN, 1996. TOR2 is required for the organization of the actin cytoskeleton. *Proc. Nat. Acad. Sci. U.S.A* 93:13780–13785.
- Sharpless KE, Harris SD, 2002. Functional characterization and localization of *Aspergillus nidulans* formin SepA. *Mol. Biol. Cell* 13: 469–479.
- Shaw B, Momany C, 2002. *Aspergillus nidulans* polarity mutant *swoA* is complemented by protein O-mannosyltransferase *pmtA*. *Fungal Genet. Biol.* 37: 263–270.
- Shaw B, Momany C, Momany M, 2002. *Aspergillus nidulans swoF* encodes an N-myristoyl transferase. *Eukaryot. Cell* 1: 241–248.
- Shi X, Sha Y, Kaminskyj S, 2004. *Aspergillus nidulans hypA* regulates morphogenesis through the secretion pathway. *Fungal Genet. Biol.* 41: 75–88.
- Simanis V, 2003. Events at the end of mitosis in the budding and fission yeasts. *J. Cell Sci.* 116: 4263–4275.
- Slattery MG, Liko D, Heideman W, 2008. Protein kinase A, TOR, and glucose transport control the response to nutrient repletion in *Saccharomyces cerevisiae*. *Eukaryot. Cell* 7: 358–367.
- Szewczyk E, Nayak T, Oakley CE, Edgerton M, Xiong Y, et al., 2006. Fusion PCR and gene targeting in *Aspergillus nidulans*. *Nat. Protocol* 1: 3111–3120.
- Taheri-Talesh N, Horio T, Araujo-Bazan L, Dou X, Espeso EA, et al., 2008. The tip growth apparatus of *Aspergillus nidulans*. *Mol. Biol. Cell* 19: 1439–1449.
- Takeshita N, Higashitsuji Y, Konzack S, Fischer R, 2008. Apical sterol-rich membranes are essential for localizing cell end markers that determine growth directionality in the filamentous fungus *Aspergillus nidulans*. *Mol. Biol. Cell* 19:339–351.
- Takeshita N, Ohta A, Horiuchi H, 2005. CsmA, a class V chitin synthase with a myosin motor-like domain, is localized through direct interaction with the actin cytoskeleton in *Aspergillus nidulans*. *Mol. Biol. Cell* 16: 1961–1970.
- Takeshita N, Yamashita S, Ohta A, Horiuchi H, 2006. *Aspergillus nidulans* class V and VI chitin synthases CsmA and CsmB, each with a myosin motor-like domain, perform compensatory functions that are essential for hyphal tip growth. *Mol. Microbiol.* 59: 1380–1394.
- Tazebay UH, Sophianopoulou V, Cubero B, Scazzocchio C, Diallinas G, 1995. Post-transcriptional control and kinetic characterization of proline transport in germinating conidiospore of *Aspergillus nidulans*. *FEMS Microbiol. Lett.* 132: 27–37.
- Tazebay UH, Sophianopoulou V, Scazzocchio C, Diallinas G, 1997. The gene encoding the major proline transporter of *Aspergillus nidulans* is upregulated during conidiospore germination and in response to proline induction and amino acid starvation. *Mol. Microbiol.* 24: 105–117.
- Tenney K, Hunt I, Sweigard J, Pounder JI, McClain C, Bowman EJ, Bowman BJ, 2000.

- Hex-1, a gene unique to filamentous fungi, encodes the major protein of the woronin body and functions as a plug for septal pores. *Fungal Genet. Biol.* 31: 205–217.
- Todd RB, Davis MA, Hynes MJ, 2007a. Genetic manipulation of *Aspergillus nidulans*: meiotic progeny for genetic analysis and strain construction. *Nat. Protocol* 2: 811–821.
- Todd RB, Davis MA, Hynes MJ, 2007b. Genetic manipulation of *Aspergillus nidulans*: heterokaryons and diploids for dominance, complementation, and haploidization analyses. *Nat. Protocol* 2: 822–830.
- Upadhyay S, Shaw B, 2008. The role of actin, fimbrin and endocytosis in growth of hyphae in *Aspergillus nidulans*. *Mol. Microbiol.* 68: 690–705.
- Virag A, Harris SD, 2006a. Functional characterization of *Aspergillus nidulans* homologues of *Saccharomyces cerevisiae* Spa2 and Bud6. *Eukaryot. Cell* 5: 881–895.
- Virag A, Harris SD, 2006b. The Spitzenkörper: a molecular perspective. *Mycol. Res.* 110: 4–13.
- Virag A, Lee MP, Si H, Harris SD, 2007. Regulation of hyphal morphogenesis by cdc42 and rac1 homologues in *Aspergillus nidulans*. *Mol. Microbiol.* 66: 1579–1596.
- Wang J, Hu H, Wang S, Shi J, Chen S, Wei H, Xu X, Lu L, 2009. The important role of actinin-like protein (AcnA) in cytokinesis and apical dominance of hyphal cells in *Aspergillus nidulans*. *Microbiology* 155: 2714–2725.
- Wedlich-Soldner R, Altschuler S, Wu L, Li R, 2003. Spontaneous cell polarization through actomyosin-based delivery of the Cdc42 GTPase. *Science* 299: 1231–1235.
- Westfall PJ, Momany M, 2002. *Aspergillus nidulans* septin AspB plays pre- and postmitotic roles in septum, branch, and conidiophore development. *Mol. Biol. Cell* 13: 110–118.
- Whittaker SL, Lunness P, Milward KJ, Doonan JH, Assinder SJ, 1999. sodV1C is an aCOP-related gene which is essential for establishing and maintaining polarized growth in *Aspergillus nidulans*. *Fungal Genet. Biol.* 26: 236–252.
- Wolkow TD, Harris SD, Hamer JE, 1996. Cytokinesis in *Aspergillus nidulans* is controlled by cell size, nuclear positioning and mitosis. *J. Cell Sci.* 109: 2179–2188

Chapter II Regulation of septum formation by Bud3-Rho4 GTPase module in *Aspergillus nidulans*

ABSTRACT

The ability of fungi to generate polarized cells with a variety of shapes likely reflects precise temporal and spatial control over the formation of polarity axes. The bud site selection system of *Saccharomyces cerevisiae* represents the best-understood example of such a morphogenetic regulatory system. However, the extent to which this system is conserved in the highly polarized filamentous fungi remains unknown. Here, we describe the functional characterization and localization of the *Aspergillus nidulans* homologue of the axial bud site marker Bud3. Our results show that AnBud3 is not required for polarized hyphal growth *per se*, but is involved in septum formation. In particular, our genetic and biochemical evidence implicates AnBud3 as a guanine nucleotide exchange factor for the GTPase Rho4. Additional results suggest that the AnBud3-Rho4 module acts downstream of the septation initiation network to mediate recruitment of the formin SepA to the site of contractile actin ring assembly. Our observations provide new insight into the signaling pathways that regulate septum formation in filamentous fungi.

Introduction

The filamentous fungi form mycelial colonies that consist of networks of branched hyphae that grow by apical extension. In the higher fungi (i.e., *Ascomycota* and *Basidiomycota*), hyphae are compartmentalized by the formation of cross-walls, or septa. It has long been suspected that the presence of septa allows filamentous fungi to partition cellular environments within a hypha to support colony homeostasis and reproductive development (GULL 1978). The process of septum formation is similar to cytokinesis of

animal cells, in that it is coordinated with mitosis and requires formation of a contractile actin ring (CAR; BALASUBRAMANIAN et al 2004). By analogy to the yeasts *Saccharomyces cerevisiae* and *Schizosaccharomyce pombe*, the CAR likely provides a landmark that guides deposition of the septal wall material. However, unlike these yeasts, the septum is not subsequently degraded and cells remain attached. Furthermore, in most filamentous fungi, a small pore is retained to enable communication between adjacent hyphal compartments. Septum formation has been studied in several filamentous fungi, including *Aspergillus nidulans* (HARRIS 2001; WALTHER and WENDLAND 2003). Upon germination of asexual conidiospores in *A. nidulans*, the first few rounds of parasynchronous nuclear division are not accompanied by septation until cells reach an appropriate size/volume (HARRIS et al 1994; WOLKOW et al 1996). Subsequently, the first septum forms near the junction of the spore and germ tube (HARRIS et al 1994). Deposition of the septal wall material is tightly coupled to assembly and constriction of the CAR, which in turn requires persistent signals from mitotic nuclei (MOMANY and HAMER 1997). As *A. nidulans* hyphae continue to grow by apical extension, each parasynchronous round of mitosis in multinucleate tip cells is followed by formation of septa in the basal region of the compartment (CLUTTERBUCK 1970). Because tip and intercalary hyphal cells are multinucleate, not all of the individual mitotic events within the tip cell are capable of triggering septation.

Genetic analyses have identified several functions required for septum formation in *A. nidulans*, including the septation initiation network (SIN), the septins, and a formin (HARRIS 2001). The SIN is a cascade of three protein kinases that is activated by a small GTPase (KRAPP and SIMANIS 2008). In *A. nidulans*, the component kinases of the SIN

are arranged in the pathway SepH→SepL→SidB, with SepM and MobA serving as co-factors that regulate SepL and SidB, respectively (KIM et al 2006; KIM et al 2009).

Although SIN components localize to the spindle pole bodies, this does not appear to be a pre-requisite for their subsequent recruitment to the septation site (KIM et al 2009).

Functional analysis of SepH, ModA, and SidB demonstrate that the SIN is required for assembly of the CAR (BRUNO et al 2001; KIM et al 2006). Nevertheless, the upstream activators of the SIN and its downstream effectors remain unknown. However, localization of the septin AspB and the formin SepA to the septation site have been shown to require SepH (WESTFALL and MOMANY 2002; SHARPLESS and HARRIS 2002). AspB initially appears as a single ring that does not constrict, but splits into a double ring flanking the septum (WESTFALL and MOMANY 2002). AspB is not required *per se* for assembly of the CAR (WESTFALL and MOMANY 2002). On the other hand, SepA is a dynamic component of the CAR that is required for its assembly (SHARPLESS and HARRIS 2002), presumably because of its ability to nucleate actin filaments.

In *S. cerevisiae* and *S. pombe*, formins such as SepA are typically activated by Rho GTPases, such as Rho1 and Cdc42 (e.g., DONG et al 2003, MARTIN et al 2007).

However, neither Cdc42 nor Rac1 is required for septum formation in *A. nidulans*, and Cdc42 does not localize to septation sites (VIRAG et al 2007). One promising candidate for a GTPase that could activate SepA is Rho4, which appears to be specific to filamentous fungi (RASMUSSEN and GLASS 2005). In *Neurospora crassa*, Rho4 is a dynamic component of the CAR; its absence prevents CAR assembly, whereas constitutive activation permits spurious formation of extra CARs (RASMUSSEN and

GLASS 2005). Based on these results, it was suggested that Rho4 is a likely activator of formins such as SepA at septation sites. Because SepA simultaneously localizes to hyphal tips and septation sites in *A. nidulans* (SHARPLESS and HARRIS 2002), we have been interested in the identification of functions that determine patterns of cell wall deposition in hyphal cells. In this context the bud site selection system of *S. cerevisiae* provides an important paradigm. *S. cerevisiae* cells display two distinct budding patterns that are controlled by mating type (FREIFELDER 1960; CHANT 1999). Mating type a or α cells employ an axial budding pattern whereby the previous bud site serves as a template for the next bud. As a result, a chain of chitinous bud scars decorates the cell surface. In contrast, mating type a/ α cells employ a bipolar budding pattern whereby buds emerge from either the distal or proximal pole of the cell (the proximal pole is defined by the presence of the birth scar, CHANT and PRINGLE 1995). Accordingly, bud scars cluster at either pole but are not necessarily adjacent to each other. Extensive genetic analyses have provided a fairly detailed understanding of the molecular mechanisms that underlie the axial and bipolar budding patterns. For the axial pattern, the cell wall protein Axl2 serves as a landmark whose function is facilitated by its association with Axl1 and the septin-interacting proteins Bud3 and Bud4 (CHANT and HERSKOWITZ 1991; CHANT et al 1995; CHANT 1999; LORD et al 2002; GAO et al. 2007; PARK and BI 2007). For the bipolar pattern, the paralogous cell wall proteins Bud8 and Bud9, which bear no homology to Axl2, serve as distal and proximal pole markers, respectively (CHANT 1999; HARKINS et al 2001; KANG et al 2004; PARK and BI 2007). Furthermore, the membrane proteins Rax1 and

Rax2 form complexes with Bud8 and Bud9 that facilitates their function (KANG et al 2004). The positional information generated by the landmark proteins Axl2, Bud8, or Bud9 is subsequently relayed to the Ras-like Bud1/Rsr1 GTPase module via the guanine nucleotide exchange (GEF) factor Bud5 (KANG et al 2001; KANG et al 2004; KRAPPMANN et al 2007). This results in localized activation of the Rho-like GTPase Cdc42, which acts via multiple effectors to recruit components of the morphogenetic machinery to the specified bud site (CHANT 1999; PARK and BI 2007).

Despite the importance of the bud site selection regulatory module in specifying the budding pattern of *S. cerevisiae* yeast cells, it remains unclear whether it is used for a similar regulatory purpose in other fungi. *Ashbya gossypii* is a hemiascomycete fungus closely related to *S. cerevisiae* that is only capable of forming hyphae (PHILIPPSEN et al 2005). The *A. gossypii* Bud3 homologue, which can function in *S. cerevisiae*, appears to function as a landmark for septum formation and also controls the position of the contractile actin ring (WENDLAND 2003). In *A. gossypii* and *Candida albicans*, another hemiascomycete capable of forming true hyphae, Bud1/Rsr1 homologues appear to function at the hyphal tip to specify the direction of hyphal extension (BAUER et al 2004; HAUSAUER et al 2005). Although limited to hemiascomycetes, these studies suggest that the components of the bud site selection regulatory module may have broader functions within the fungal kingdom.

Here, we investigate the possibility that homologues of the bud site selection proteins may provide positional information that marks the hyphal tip and/or septation sites in *A. nidulans*. We characterize an apparent homologue of Bud3 and show that it is required for assembly of the CAR at septation sites. Our results provide new insight into

the regulation of septum formation by suggesting that AnBud3 functions downstream of the SIN as a GEF for Rho4.

MATERIALS AND METHODS

Strains, media, growth conditions and staining

Aspergillus nidulans strains used in this study are listed in Table 1. MNV (minimal + vitamins) media were made according to KAFER (1977). MNV-glycerol and MNV-threonine fructose media were made as described in PEARSON et al (2004). MAG (malt extract agar) and YGV (yeast extract glucose + vitamins) media were made as described previously (HARRIS et al 1994). 5-Fluoroorotic acid (5-FOA; US Biological, Swampscott, MA) was added to media at a concentration of 1mg/ml after autoclaving. For septation and hyphal growth studies, conidia from appropriate stains were grown at 28 °C for 12h on coverslips. Hyphae attached to the coverslip were fixed using a modified standard protocol (HARRIS et al 1994) [fixing solution contained 3.7% formaldehyde, 25 mM EGTA, 50 mM piperazine-N,N-bis(2 ethanesulfonic acid) (PIPES), and 0.5% dimethyl sulfoxide] for 20 min and then stained with staining solution containing both 273 nM fluorescent brightener 28 (Sigma-Aldrich Corporation, St. Louis, MI) and 160 nM Hoechst 33258 (Molecular Probes, Eugene, OR).

Construction of gene replacement strains

The *bud3*, *rho4*, and *msb1* genes from strains AHS3, AHS4, and AHS7, respectively, were replaced with the *pyroA*^{A.f.} marker from *A. fumigatus*. All gene replacements were generated using the gene targeting system developed by NAYAK et al (2006) and the gene replacement generation strategy developed by YANG et al (2004).

Oligonucleotides used in this study are listed in Suppl. Table 1. The *pyroA^{A.f.}* DNA marker fragment was PCR amplified from plasmid pTN1 (NAYAK et al 2006). DNA fragments upstream and downstream of *bud3* and *rho4* were amplified from the wild-type strain FGSC28 (available through the Fungal Genetics Stock Center, Kansas City, MO). High Fidelity and Long Template PCR systems (Roche Diagnostics Corporation, Indianapolis, IN) were used for amplifications of individual and fusion fragments, respectively, using a Px2 Hybaid or an Eppendorf Mastercycler gradient thermal cycler. The amplification conditions were according to the manufacturer's recommendations. PCR products were gel purified using the QIAquick gel extraction kit (QIAGEN Inc., Valencia, CA). The gene replacement constructs were transformed into strain TNO2A3, and plated on supplemented minimal medium with 0.6 M KCl. Transformations were performed according the protocol described by OSMANI et al. (2006). Transformation candidates were tested for homologous integration of the gene replacement construct and the absence of the wild-type gene by diagnostic PCR as described by YANG et al (2004). The same strategy was used to replace *bud3* with the *pyr-4* nutritional marker from *N. crassa*. The *pyr-4* DNA marker fragment was amplified from plasmid pRG3. The resulting constructs were transformed into TNO2A3. The *bud3* gene replacement construct with *pyroA^{A.f.}* marker was transformed to strain AAV123 to generate strain AHS30.

Genetic interaction experiments

The *cdc42* (ANID_07487.1), *racA* (ANID_04743.1) and *rho4* (ANID_02687.1) gene sequences, including upstream (~500bp) and downstream regions (~300bp), were retrieved from the *A. nidulans* genome at the Broad Institute

(<http://www.fgsc.net/aspergenome.htm>). These sequences were amplified (primers described in Suppl. Table 1) and cloned into the pCR2.1-TOPO vector (Invitrogen Corporation, Carlsbad, CA) to generate plasmids pHS11, pHS12 and pHS13 respectively. For overexpression experiments, strain AHS3 was cotransformed with pRG3-AMA1 and each of the plasmids pHS11, pHS12, pHS13.

Construction of GFP fusions to Anbud3 and Rho4

To localize AnBud3, we fused GFP to the N-terminus using the five piece fusion PCR approach recently described by TAHERI-TALESH et al. (2008). In addition to the retention of native promoter sequences, final constructs also contained a short linker of five glycines and alanines inserted between the GFP and AnBud3 coding sequences. In brief, the following five fragments were amplified (1) a 1.3-kb sequence upstream of *bud3*, (2) the GFP coding sequence (minus the stop codon) derived from plasmid pMCB17apx, (3) the *bud3* gene plus 400-bp of downstream sequence, (4) the *N. crassa pyr-4* selectable marker, also derived from pMCB17apx, and (5) a 1.3-kb sequence extending from 400 to 1700-bp downstream of *bud3*. Fragments (1), (3), and (5) were amplified by specific primers with 30bp tails that were reverse complements of the adjacent fragments. Finally, the forward primer used to amplify fragment (1) and the reverse primer used to amplify fragment (5) were used to fuse the entire five-fragment gene replacement construct. The High Fidelity and Long Template PCR systems (Roche Diagnostics Corporation, Indianapolis, IN) were employed to amplify individual and fusion fragments, respectively, on a Px2 Hybaid or an Eppendorf Mastercycler gradient thermal cycler. PCR products were gel purified using the QIAquick gel extraction kit

(QIAGEN Inc., Valencia, CA). The resulting *gfp::bud3::pyr-4* cassette was used to replace wildtype *bud3* in strain TNO2A3 using the approach described by NAYAK et al. (2006). The plasmid pHS31, containing *alcA(p)::gfp::rho4*, was constructed in two steps. An N-terminal sequence from *rho4* that corresponds to amino acids 1-261 was amplified from wildtype strain A28. Cloning sites for *AscI* and *PacI* were incorporated onto the ends of the amplified fragment. The PCR product was gel purified and cloned into pCR2.1-TOPO to generate pHS30. The resulting plasmid was digested with *AscI* and *PacI* (New England Biolabs, MA), and the liberated *rho4* fragment ligated into pMCB17apx (EFIMOV 2003) to generate pHS31. Thereby, the N-terminus of *rho4* was fused to GFP, which in turn is expressed under the control of *alcA(p)*. Upon transformation into strain TNO2A3, homologous integration of this construct generates a single full-length copy of *rho4* regulated by *alcA(p)*, plus a truncated version controlled by native promoter sequences.

AnBud3 *guanine nucleotide exchange assays*

MBP-tagged AnBud3 and Rho4 constructs were cloned by RT-PCR using the primers along with cDNA prepared from vegetative hyphae. Total RNA was obtained by TRIZOL extraction (Invitrogen) and cDNA prepared using RevertAid M-MuLV Reverse Transcriptase (Fermentas). cDNA was subcloned into pJet1.2/blunt vector (Fermentas). AnBud3 and Rho4 constructs were digested with either *NcoI* and *NotI* (*bud3*) or *NcoI* and *HindIII* (*rho4*) and inserted into a modified pMalc2x vector (VOGT and SEILER 2008), which was digested accordingly to generate plasmids pMal_AnBUD3 and pMal_AnRHO4. MBP-AnBud3 and MBP-Rho4 fusion proteins were expressed and

purified as previously described (VOGT and SEILER 2008).

Guanine nucleotide exchange assays were performed by fluorometric determination of mant-GDP (a fluorescently labeled GTP analog) incorporation as described (ABE et al 2000) using a Tecan Infinite 200 spectrophotometer at 21°C. The reaction was started by adding 0.1 mM mant-GDP and 1 mM MBP-Bud3 to 1 mM Rho4 in 30 mM Tris, pH 7.5, 5 mM MgCl₂, 10 mM NaH₂PO₄/K₂HPO₄, 3 mM DTT, which was pre-equilibrated for 5 min at 21°C. Fluorescence intensity ($\lambda_{exc}=356\text{nm}$, $\lambda_{em}=448\text{nm}$) was monitored over 16 min. The change of fluorescence over time was used to assess mant-GDP incorporation into Rho4 in the presence and absence of the GEF. Similar conditions were also used in recent publications by YEH et al (2007) and HLUBEK et al (2008). The latter authors also used equal amounts of GEF and GTPase. In the kinetics presented in Fig. 2-5B, the mixing of Bud3 and mant-GDP with Rho4-GDP is defined as time-point zero. After 16 min the measurement was stopped and the resulting emission curves were further analyzed. To allow comparison between independently prepared biological samples of each GEF and GTPase, we used the linear range of the slope from each individual experiment. The kinetics of two independent GEF and of two independent GTPase preparations each performed in duplicate measurements was determined and the background fluorescence of mant-GDP without added proteins was subtracted. The mean value of the slopes calculated for Rho4 in the absence of Bud3 represents the intrinsic activity of Rho4 and was set to 100%. To determine the exchange activity of Rho4 in the presence of the GEF relative to its intrinsic activity, the mean slope value calculated for emission curves of Rho4 in the presence of the GEF was divided by the mean slope value calculated for the intrinsic

activity of Rho4 and the resulting value was multiplied by 100 to obtain the relative value displayed in Fig. 2-5A (relative exchange activity of Rho4 in the presence of Bud3 = (mean value of slopeRho4+slopeBud3 /mean value of slopeRho4*100).

Conidiation experiments

Conidiophore development was monitored using the sandwich coverslip method described by LIN and MOMANY (2003). Briefly, 1ml of melted MAGUU media was placed on a coverslip that was then transferred to the surface of a 4% water agar plate. The coverslip was inoculated with spores once the media had solidified, whereupon a second coverslip was placed on top. After 3-4 days, conidiophores had formed and become attached to the top coverslip, which was then dipped into 100% ethanol and mounted for DIC microscopy. For Calcofluor staining, the coverslips were fixed and stained after ethanol treatment.

sepA1 and sepH1 experiments

The *sepA1* GFP-AnBud3 strain AHS51 was generated by crossing the GFP-AnBud3 strain AHS41 with the *sepA1* strain ASH630 and screening at restrictive temperature (42 °C) on selective media. The *sepH1* GFP-AnBud3 strain AHS62 was generated by transforming the *sepH1* strain AHS61 with the same GFP fusion construct used to generate AHS41. The DNA replication inhibitor hydroxyurea (HU) was used to arrest the nuclear division cycle. 50 mM HU was added to liquid cultures one hour prior to shiftdown, and cultures were maintained in the presence of HU for an additional two hours once returned to 28°C. The strain AHS53 (*sepA1 tpmA::gfp*) was used assess the effect of the *sepA1* mutation on the formation of contractile actin rings at the semi-permissive temperature of 37°C.

Microscopy

Digital images of plates were collected with an Olympus C-3020ZOOM digital camera. Differential interference contrast (DIC) and fluorescent images were collected with either an Olympus BX51 microscope with a reflected fluorescence system fitted with a Photometrics CoolSnap HQ camera or an Olympus Fluoview confocal laser-scanning microscope. Images were processed with IPLab Scientific Image Processing 3.5.5 (Scanalytics Inc., Fairfax, VA) and Adobe Photoshop 6.0 (Adobe Systems Incorporated, San Jose, CA).

Δ bud3 suppressor screen

A suspension of 10^6 conidia from the strain AHS3 was plated on MNUU plates and irradiated with UV to a survival rate of ~10%. Plates were incubated for 6 days at 28°C. The faint green colonies that emerged were patched in grids on master MNUU plates and for re-testing. In addition, retention of the *Δ bud3* mutation was verified by PCR. Candidates for further study were picked based on restoration of septum formation (as observed by Calcofluor staining). Standard genetic analysis was used to determine that suppressor mutations were not linked to *Bud3* and defined a single gene.

RESULTS

The *A. nidulans* homologue of Bud3 is required for septum formation

Our original annotation of the *A. nidulans* genome revealed the existence of potential homologues of the axial budding markers Bud4 and Ax12 (HARRIS and MOMANY 2004; GALAGAN et al., 2005). Subsequent annotation using the cognate proteins from *Ashbya gossypii* (AgBud3; WENDLAND 2003) and *Candida albicans*

(CaO19.7079) as additional queries for BLASTp and PSI-BLAST searches also uncovered a potential homologue of Bud3. AnBud3 (ANID_00113.1) is a predicted 1538 amino acid (AA) protein with a RhoGEF domain located between AAs 250 and 450 (Fig. 2-1). Homologues of AnBud3 (>40% identity over their entire lengths) exist in all sequenced eukaryotic genomes (e.g., Fig. 2-1). AnBud3 only possesses limited homology to *S. cerevisiae* and *A. gossypii* Bud3 (21% identity over the first ~550 AAs, which corresponds to the predicted RhoGEF domain). Our description and functional characterization of the Bud4 and Axl2 homologues will be presented elsewhere.

To determine the possible function of AnBud3 during hyphal morphogenesis, a mutant possessing a complete gene deletion was generated using recently described protocols (YANG et al 2004; NAYAK et al 2006). *Anbud3::pyroA*^{A.f.} deletion mutants (hereafter referred to as *bud3*) formed colonies that were slightly smaller than wildtype and were notably devoid of conidia (Fig. 2-2 A,B). On minimal media, Δ *Anbud3* mutants produced ~520-fold fewer conidia/ml compared to its parental strain TN02A3. A similar effect (i.e., ~75-fold reduction compared to TN02A3) was observed on rich media. To determine the possible basis of the conidiation defect, conidiophores from the mutant as well as wildtype controls were imaged using a previously described “sandwich slide” protocol (LIN and MOMANY 2003). A range of defects was noted, included elongated metulae and phialides, as well as conidiospores that apparently failed to undergo cytokinesis (Fig. 2-2 E,F). Because a stage-specific arrest was not observed, it seems likely that AnBud3 is required at multiple steps during conidiophore development.

Coverslip cultures were used to examine Δ *Anbud3* mutants for defects in hyphal morphogenesis. The timing and pattern of spore polarization was indistinguishable from wildtype, and the resulting hyphae displayed no obvious defects in polarized growth (Fig.

2-2 G,H). On the other hand, septum formation was completely abolished, as no septa were observed in $\Delta Anbud3$ mutants (Fig. 2-2 G,H; $n > 1000$ hyphae grown on YGVUU). To gain further insight into the nature of the septation defect in $\Delta Anbud3$ mutants, strains possessing a SepA-GFP fusion were analyzed. As noted previously (SHARPLESS and HARRIS, 2002), SepA is a component of the contractile actin ring (CAR) that forms at septation sites (Fig. 2-2 D). In $\Delta Anbud3$ *sepA::gfp* strains (AHS30), SepA-GFP exhibited normal localization at hyphal tips, but no rings were observed ($n > 1000$ hyphae grown on YGV; Fig. 2-2 C). Accordingly, AnBud3 appears to be required for an early step in septum formation that precedes the formation of the contractile actin ring.

These observations demonstrate that AnBud3 is not required for the establishment or maintenance of hyphal polarity, but is needed for normal septation. Notably, the defects in septum formation may account for the abnormal development observed in $\Delta Anbud3$ mutants, as reduced conidiation has previously been associated with defects in septum formation (HARRIS et al. 1994).

AnBud3 functions as a GEF for Rho4

The presence of a predicted Rho-GEF domain in AnBud3 suggested that its role in septation might be to locally activate a Rho GTPase by promoting GDP-GTP exchange. A genetic approach was used to identify candidate Rho GTPase targets for AnBud3. This approach is based on the premise that increased levels of a target GTPase can compensate for defects in its associated GEF. For example, in *S. cerevisiae*, the GTPases Cdc42 and Rho1 function as dosage suppressors of mutations affecting their cognate GEFs, Cdc24 and Rom1, respectively (BENDER and PRINGLE 1989; OZAKI

et al. 1996). Accordingly, we predicted that one of the six annotated Rho GTPases from *A. nidulans* (HARRIS et al, 2009) might function as a dosage suppressor of *Anbud3*. We were particularly interested in ANID_02687.1, a predicted homologue of *Neurospora crassa rho-4*, which is required for septum formation and assembly of the contractile actin ring (RASMUSSEN and GLASS 2005). Candidate GTPases were amplified and co-transformed into a $\Delta Anbud3$ *pyrG89* strain along with the autonomously replicating plasmid pRG3-AMA1. For each GTPase, multiple *Pyr*⁺ transformants were picked and tested for suppression of the conidiation defects caused by deletion of *Anbud3* and all small GTPases mentioned below are *A. nidulans* homologues without the “An” initial. Neither *cdc42* nor *racA* could suppress $\Delta Anbud3$; however multi-copy *rho4* was capable of restoring conidiation (Fig. 2-3 A-C). In addition, these transformants were also able to form septa (Fig. 2-3D,E). Two observations demonstrate that suppression was due to the presence of *rho4*. First, the entire *rho4* coding region could be amplified from pRG3-AMA1-based plasmids rescued from the original transformants. Second, re-transformation experiments showed that rescued plasmids containing *rho4* were able to suppress $\Delta Anbud3$.

Based on this genetic evidence, we conclude that AnBud3 likely functions as a GEF for the Rho GTPase Rho4. Because GEFs activate their target GTPase, mutational inactivation of the GTPase would typically be expected to cause the same phenotypes as loss of its GEF. Accordingly, we generated a $\Delta rho4$ deletion and tested for defects in septum formation and conidiation that resemble those observed in $\Delta Anbud3$ mutants. As shown in Fig. 2-4A and B, *rho4* mutants displayed similar colony morphology as $\Delta Anbud3$ mutants. Furthermore, *rho4* mutants were completely defective in septation and

formed aberrant conidiophores (Fig. 2-4C-G). These observations implicate Rho4 in the same morphological processes as AnBud3. To test this, we generated $\Delta Anbud3::pyrG^{A.f.}$ $\Delta rho4::pyroA^{A.f.}$ double mutants (AHS25) by a standard cross, and found that they exhibited the same phenotype as the two parent single mutants (Fig. 2-4H,I). This epistatic interaction provides additional support for the notion that AnBud3 and Rho4 function in the same pathway that regulates septum formation.

To provide further evidence for the relationship between AnBud3 and Rho4, we used *in vitro* assays to determine if AnBud3 exhibited GEF activity towards Rho4 (see Materials and Methods). As shown in Fig. 2-5, a fragment that encompasses the predicted GEF domain of AnBud3 specifically stimulated the GDP-GTP exchange activity of Rho4. Furthermore, the same fragment was also capable of promoting the exchange activity of the heterologous Rho4 from *N. crassa* (Fig. 2-6). Accordingly, when coupled with the genetic interactions and phenotypic similarities displayed by the respective mutants, these results strongly implicate AnBud3 as a Rho4 GEF in *A. nidulans*.

AnBud3 and Rho4 localization patterns at septa

As a further test for the function of AnBud3, we used a GFP fusion protein to characterize its localization pattern. We constructed strains in which the sole functional source of AnBud3 was supplied by a *GFP::AnBud3* fusion expressed under control of native promoter sequences. As expected, GFP-AnBud3 localized to septation sites, where it formed a constricting ring (FIG. 2-7A,B). Notably, GFP-AnBud3 first localized to incipient septation sites prior to the appearance of any detectable

Calcofluor-stained septum (i.e., 21/109 GFP-AnBud3 rings were not associated with a septum; FIG. 2-7C,D). GFP-AnBud3 localization at septation sites remained unchanged as septa first appeared (i.e., 22/109 rings co-localized with a thin septum; FIG. 2-7E,F) and then as they began to thicken (i.e., 54/109 rings co-localized with a thick septum; FIG. 2-7G,H). However, GFP-AnBud3 rings ultimately constricted (i.e., 12/109 rings were constricted and co-localized with a thick septum; FIG. 2-7I,J), suggesting that AnBud3 is a likely component of the contractile actin ring.

Because our genetic evidence implicates AnBud3 as a putative GEF for Rho4, we surmised that Rho4 would also localize to septa. Accordingly, we constructed a strain in which the sole functional copy of *rho4* was fused at its 5' end to GFP and was expressed under control of the inducible *alcA*(p) promoter. As expected, the *alcA*(p)::*gfp::rho4* strain displayed a growth defect on repressing glucose media, though not as severe as that caused by deletion of *rho4*. On the other hand, the strain grew no worse than wildtype on inducing threonine media. Under these conditions, GFP-Rho4 localized to septa and appeared to undergo constriction (FIG. 2-8). This observation suggests that like AnBud3, Rho4 is also a component of the contractile actin ring.

Our genetic analysis supports a model whereby AnBud3 acts as a GEF that locally activates Rho4, which in turn leads to localized recruitment of SepA and assembly of the CAR. According to this model, localization of AnBud3 to septation sites would precede formation of the CAR. To test this prediction, we took advantage of the temperature-sensitive *sepA1* mutation. At both restrictive (42°C) and semi-permissive temperatures (37-39°C), this mutation abolishes assembly of the CAR (SHARPLESS and HARRIS 2002; Fig. 2-9). We thus determined if AnBud3 localizes

to septation sites in *sepAI* mutants incubated under these conditions. As expected, GFP-AnBud3 localized to rings in wildtype hyphae at 37°C (FIG. 2-10A,B). Notably, in *sepAI* mutants, GFP-AnBud3 localization was also observed at septation sites (FIG. 2-10C-H). In most cases, GFP-AnBud3 accumulated at cortical sites or appeared to form incipient rings (FIG. 2-10E-H), though rare examples of a complete ring were occasionally observed (FIG. 2-10C-D). These results suggest that assembly of the CAR is not a pre-requisite for the recruitment of AnBud3 to septation sites.

Roles of nuclear division and the SIN in AnBud3 localization

We have previously demonstrated that the *sepAI* septation defect is reversible. In particular, a shift back to permissive temperature (i.e., 28°C) triggers rapid and synchronous formation of septa with appropriate spacing in a manner that is dependent upon nuclear division (HARRIS et al 1997; also see TRINCI and MORRIS 1979). We exploited the reversibility of the *sepAI* mutation to determine if nuclear division is required for the appearance of AnBud3 rings. In particular, *sepAI* hyphae that express GFP-AnBud3 were shifted to 28°C after incubation at 37°C. As expected, numerous AnBud3 rings appeared within 2 h, and in many cases, multiple rings formed in a single hypha (FIG. 2-10I-J). However, when shifted down in the presence of 50 mM hydroxyurea, which blocks DNA replication and subsequent nuclear division, the localized recruitment of AnBud3 and the formation of rings were abolished (Fig. 2-11). A similar treatment is known to prevent formation of septa upon shift-down of *sepAI* mutants (HARRIS et al 1997). Thus, nuclear division appears to be generally required for the localization of AnBud3 to septation sites and the subsequent formation of rings.

A potential pathway that might link nuclear division to AnBud3 localization is

the septation initiation network (SIN), which is required for assembly of the CAR in *A. nidulans* (BRUNO et al 2001; KIM et al 2006) and functions upstream of SepA (SHARPLESS and HARRIS 2002). To test this notion, we transformed our *GFP::bud3* construct into a strain possessing the temperature sensitive *sepHI* mutation. This mutation, which affects the *A. nidulans* homologue of the *S. pombe* Cdc7/*S. cerevisiae* Cdc15 protein kinase, abolishes CAR assembly and septation at restrictive and semi-permissive temperatures (BRUNO et al 2001; SHARPLESS and HARRIS 2002). At permissive temperature (28°C), AnBud3 localization and septum formation were indistinguishable from wildtype in the *sepHI* mutant (Fig. 2-12A,B). However, under semi-permissive conditions (39°C), no evidence for AnBud3 recruitment to septation sites was observed (Fig. 2-12C,D). Note that although the presence of AnBud3-GFP clearly altered the morphology of *sepHI* mutants, hyphae were large enough to form septa. These data suggest that the SIN could coordinate CAR assembly via recruitment of AnBud3 to septation sites. Nevertheless, if indeed this is the case, it is not the sole mechanism by the SIN acts, because *rho4* could not function as a dosage suppressor of the *sepHI* mutation in the same manner as it suppresses *Anbud3* (H. SI and S. D. HARRIS, unpublished observation).

The presumptive GAP Msb1 does not regulate septum formation

Annotation of the *A. nidulans* genome revealed almost all predicted Rho GTPase activating proteins (Rho GAPs) could be matched to a Rho GTPase by analogy to known modules in *S. cerevisiae* and *S. pombe* (Lab unpublished data). The sole

exception is ANID_02983.1, which is a presumptive homologue of *S. cerevisiae* Msb1. Both proteins are predicted to possess full-length Rho-GAP domains at their N-terminus. Furthermore, results from genetic analyses in budding yeast implicate Msb1 in both Cdc42 and Rho1 signaling pathways (BENDER and PRINGLE 1989; SEKIYA-KAWASAKI et al 2002), though it is not known if it possesses GAP activity. Accordingly, we reasoned that AnMsb1 might function as a GAP for Rho4, and tested this idea by deleting it in both wildtype and Δ An*bud3* strains. Our expectation was that loss of a Rho4 GAP would lead to a hyperactive Rho GTPase, which would result in increased septum formation in a wildtype background and would also be potentially capable of suppressing the loss of septation in An*bud3* mutants. However, deletion of *Anmsb1* only had minor effects on colony growth (i.e., reduced conidiation) and did not affect septum formation (Fig. 2-13). Furthermore, Δ An*msb1* did not restore septation to any extent to *bud3* mutants (data not shown). These observations suggest that AnMsb1 alone is not likely to function as a GAP for Rho4.

As an alternative approach to the identification of candidate GAPs for Rho4, we isolated a set of extragenic suppressors of Δ An*bud3* (Fig. 2-14), which were then tested to determine whether they harbored mutations in any of the annotated Rho GAPs (HARRIS et al 2009). However, no predicted GAP was capable of complementing the suppressor mutation (i.e., restoring the original Δ An*bud3* phenotype) when amplified and co-transformed with the pRG3-AMA1 plasmid. Thus, the nature, or even the existence, of the Rho4 GAP remains unresolved.

DISCUSSION

The formation of septa in *A. nidulans* hyphae requires the formin-dependent

assembly of a CAR (SHARPLESS and HARRIS 2002). Although Rho GTPases are known to activate formins (e.g., DONG et al 2003; MARTIN et al 2007), the identity of the relevant GTPase(s) that direct CAR assembly has remained unknown. Whereas our previous results show that Cdc42 has no detectable role in septation (VIRAG et al 2007), the results presented here demonstrate that a Bud3-Rho4 GTPase module is required for CAR assembly and formin recruitment to septation sites.

The Bud3-Rho4 GTPase module

Our observations demonstrate that AnBud3 and Rho4 are required for septum formation in *A. nidulans* hyphae. The loss of either protein abolishes septation; in the case of *bud3* mutants, this appears to be caused by the failure to recruit the formin SepA, which is required for CAR assembly, to septation sites. Furthermore, both proteins localize to septation sites, where they form constricting rings. Characterization of the AnBud3 localization pattern in particular reveals that it first appears prior to the formation of a detectable septum, then constricts in a manner consistent with the notion that it is a component of the CAR. Finally, our genetic and biochemical analyses clearly establish that AnBud3 serves as a GEF that promotes activation of Rho4. A similar relationship between Bud3 and Rho4 has recently been described for another filamentous ascomycete fungus, *N. crassa* (JUSTA-SCUCH et al 2010). In this case, Bud3 also acts as a GEF for Rho4, which in turn directs assembly of the CAR at septation sites (RASMUSSEN and GLASS 2005). Collectively, these results define Bud3 and Rho4 as essential components of the GTPase modules that direct CAR assembly during septation in those filamentous fungi that belong to the euascomycetes. Amongst the questions that still need to be addressed is the identity of the relevant Rho4 GAP. Although AnMsb1

appeared to be a reasonable candidate, our results suggest that even if it does have GAP activity, it is not the sole GAP for Rho4. Instead, it seems likely that multiple GAPs might act in a redundant manner to regulate Rho4.

In addition to *A. nidulans* and *N. crassa*, Bud3 and Rho4 homologues have been implicated in septum formation in filamentous fungi that belong to the hemiascomycetes. In *A. gossypii*, Bud3 serves as a landmark for future septation events and also functions to properly position the CAR (WENDLAND 2003). It remains unknown whether this Bud3 homologue, or for that matter the founding *S. cerevisiae* homologue, possess GEF activity. In *C. albicans*, Rho4 appears to regulate deposition of the septum during both yeast and hyphal phases of growth (DUNKLER and WENDLAND 2007). At this time, no relationship between Bud3 and Rho4 has been described for any hemiascomycete. We speculate that Bud3 activation of Rho4 may represent an ancestral interaction that was lost in the hemiascomycete lineage. This could presumably account for lack of pronounced sequence similarity between euascomycete Bud3 homologues and *S. cerevisiae* Bud3, and for the observation that the euascomycete Rho4 homologues form a distinct clade of fungal Rho GTPases that apparently lack hemiascomycete members (RASMUSSEN and GLASS 2005; though the relationship of *C. albicans* Rho4 to this clade is uncertain, DUNKLER and WENDLAND 2007). An investigation of the possible interaction between Bud3 and Rho4 homologues in archiascomycetes such as the yeast *Schizosaccharomyces pombe* might help to further clarify how the Bud3-Rho4 GTPase module has evolved in fungi.

The Bud3-Rho4 pathway

Our results show that the Bud3-Rho4 GTPase module controls assembly of the CAR during septation in *A. nidulans*. A likely effector of Rho4 that mediates this function is the formin SepA, which is no longer recruited to septation sites in *Anbud3* mutants even though its localization at hyphal tips is unaffected. Furthermore, our results show that AnBud3 still accumulates at septation sites in the absence of SepA, thereby implying that its function lies upstream of SepA. We envision the following scenario based upon our observations. In response to signals emanating from the nucleus (see below), AnBud3 localizes to presumptive septation sites, where it activates Rho4 to initiate the process of assembling the CAR. Activated Rho4 accomplishes this task by locally recruiting SepA and other regulators of actin filament dynamics. Moreover, AnBud3 and Rho4 remain associated with the assembled CAR during the process of constriction. By doing so, AnBud3, and by inference activated Rho4, may control additional steps beyond recruitment of SepA, such as maintenance of the CAR or coordination of septum deposition with ring constriction. (e.g., SANTOS et al. 2003; NAKANO et al. 2003).

One of the distinct features of septum formation in filamentous fungi such as *A. nidulans* is the uncoupling of cell division from nuclear division (CLUTTERBUCK 1970; HARRIS 2001; WALTHER and WENDLAND 2003), which implies the existence of unique regulatory mechanisms that coordinate CAR assembly with mitosis (i.e., not every dividing nucleus is capable of triggering formation of a CAR). Because Rho4 appears to serve as a pivotal regulator of CAR assembly during septation, it seems likely that it would be responsive to signals emanating from dividing nuclei. Moreover, by

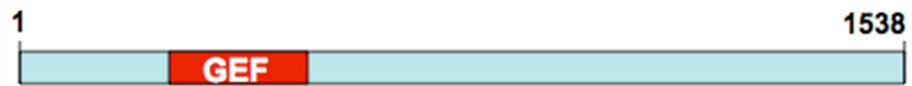
analogy to the well-characterized Rho/Cdc42 GTPase modules in *S. cerevisiae* (PARK and BI 2007), the GEFs and/or GAPs that regulate Rho4 are potential targets for these signals. Our observations that nuclear division and a functional SIN pathway are required for AnBud3 localization at septation sites are consistent with this idea. Future efforts will focus on determining whether the protein kinase constituents of the SIN (SepH, SepL, SidB; BRUNO et al 2001; KIM et al 2006; KIM et al 2009) interact directly with AnBud3 to control its localization and/or activity. Notably, in *S. pombe*, Orb6, which like SidB is a member of the NDR kinase family, spatially regulates polarized growth by restricting the localization of the Cdc42 GEF Gef1 (DAS et al 2009). Finally, it should also be noted that our data imply that the Bud3-Rho4 module is not the sole target of the SIN. Instead, we envision the SIN acting via multiple targets to coordinate CAR assembly and function with nuclear division.

Table 2-1

Strain	Genotype	
A28	<i>pabaA6 biA1</i>	FGSC (accession no. A28)
GR5	<i>pyrG89 wA3 pyroA4</i>	FGSC (accession no. A773)
TNO2A3	<i>pyrG89; argB2; pyroA4</i> <i>nkuA::argB</i>	
AHS2	<i>pyrG89; argB2; bud3::pry-4 pyroA4 nkuA::argB</i>	This study
AHS3	<i>pyrG89; argB2; bud3::pyroA pyroA4 nkuA::argB</i>	This study
AHS5	<i>pyrG89; argB2; rho4::pyroA pyroA4 nkuA::argB</i>	This study
AHS7	<i>pyrG89; argB2; msb1::pyroA pyroA4 nkuA::argB</i> <i>rho4::pyroA bud3::pyrG;</i>	This study
AHS25	<i>pyrG89; argB2; pyroA4</i>	This study
AHS30	<i>nkuA::argB</i> <i>sepA::gfp::pyr-4; pyrG89</i> <i>pabaA1; bud3::pyroA;</i>	This study
AHS252	<i>yA2</i> <i>yA2; argB2; pyroA4</i> <i>pyrG89 sepA::gfp::pyr-4; argB2; pyroA4</i>	This study
AAV123.1	<i>nkuA::argB</i>	Virag <i>et al</i> , 2007
ASH630	<i>sepA1; pyrG89; wA3</i> <i>tpmA::GFP::pyr-4; pyrG89;</i>	Lab stock
ACP115	<i>wA3</i>	Pearson <i>et al</i> , 2004 Sharpless and Harris, 2002
AKS70	<i>sepA::gfp::pyr-4; pyrG89 pabaA1; yA2</i> <i>pyrG89; argB2; gfp::bud3::pyr4; pyroA4;</i>	
AHS41	<i>nkuA::argB</i>	This study
AHS43	<i>pyrG89; argB2; alcA::gfp::rho4; pyr-4; nkuA::argB</i> <i>pyrG89; argB2; gfp::bud3::pyr4; pyroA4; sepA1</i>	This study This study
AHS51	<i>nkuA::argB</i> <i>sepA1;</i>	
AHS53	<i>tpmA::GFP::pyr4; pyrG89</i> <i>bud3</i>	This study
AHS3C2	<i>suppressor</i>	This study
AJM34	<i>sepH1; pabaA6; lysB5; chaA1</i>	
AHS61	<i>pyrG89; sepH1</i>	This study
AHS62	<i>pyrG89; gfp::bud3::pyr4; sepH1</i>	This study

Fig.2-1

A.



B.

Method: Neighbor Joining; Bootstrap (1000 reps); tie breaking = Systematic
 Distance: Poisson-correction
 Gaps distributed proportionally

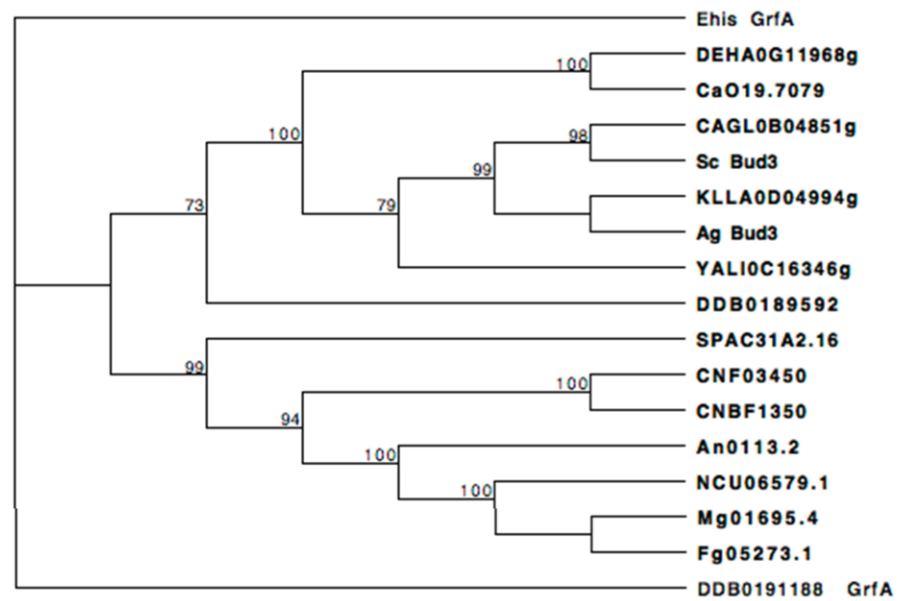


Figure 2-1. Organization and phylogenetic analysis of AnBud3. A. Schematic organization of AnBud3 depicting location of the GEF domain (red). B. Phylogenetic analysis of AnBud3. Predicted coding regions of putative Bud3 homologues were aligned using ClustalW (MacVector v7.0). The tree was constructed using the neighbor joining method with bootstrap support (1000 repetitions) and Poisson correction. All sequences are designated according to their annotation format or known protein name. Ehis = *Entamoeba histolytica*, DEHA = *Debaryomyces hansenii*, Ca = *Candida albicans*, CAGL = *C. glabrata*, Sc = *Saccharomyces cerevisiae*, KLLA = *Kluyveromyces lactis*, Ag = *Ashbya gossypii*, YALI = *Yarrowia lipolytica*, DD = *Dictyostelium discoideum*, SP = *Schizosaccharomyces pombe*, CN = *Cryptococcus neoformans*, An = *Aspergillus nidulans*, NC = *Neurospora crassa*, Mg = *Magnaporthe grisea*, and Fg = *Fusarium graminearum*.

Fig.2-2

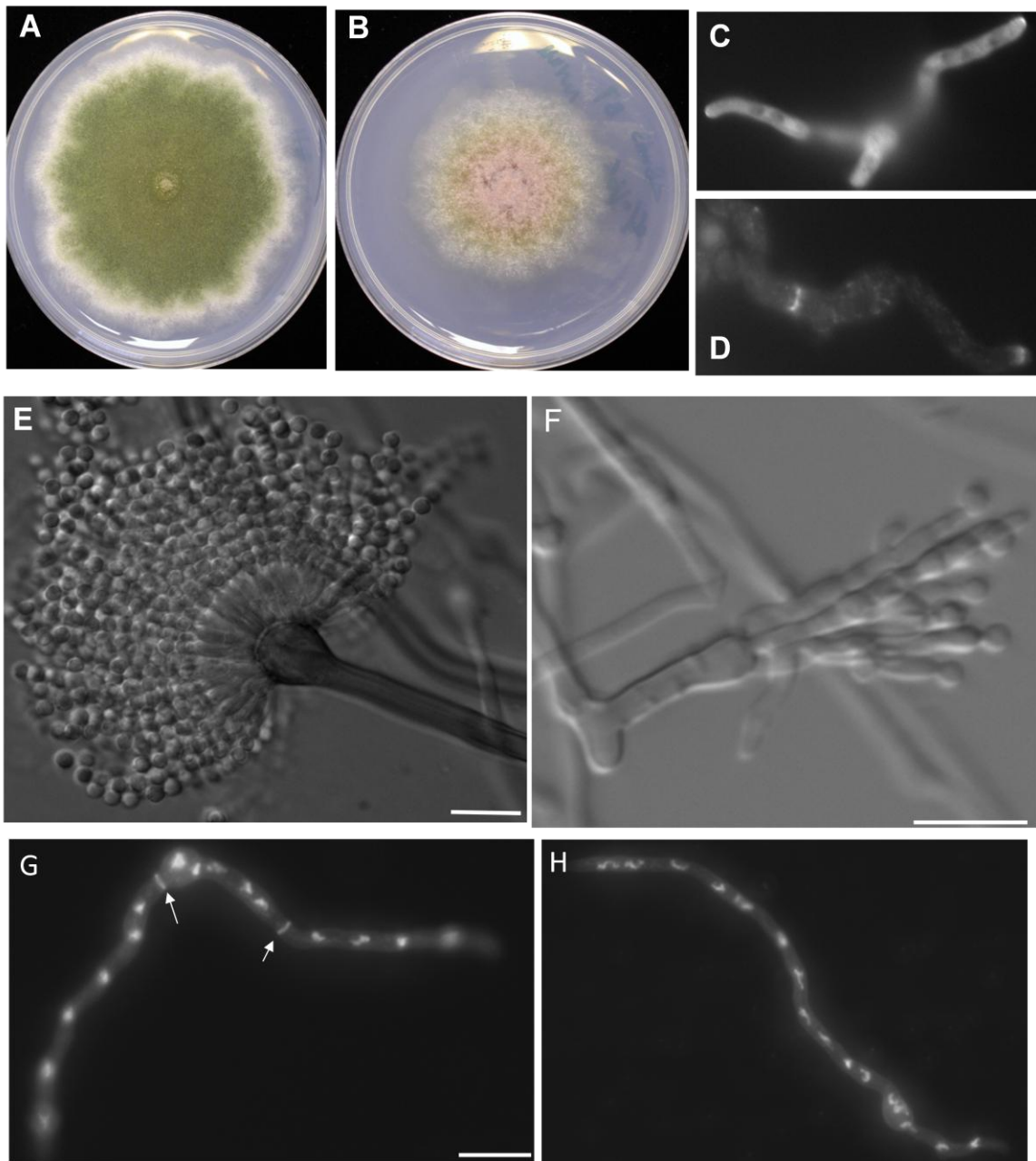


Figure 2-2. Effects of the *Anbud3* deletion on colony morphology, septum formation and conidiation. A-B. Colony morphologies of strains TNO2A3 (wildtype; A) and AHS3 ($\Delta Anbud3$; B) grown on minimal medium (MNUU) for nine days. C. SepA-GFP localizes to hyphal tips, but not septa, in $\Delta Anbud3$ mutants. D. SepA-GFP localization at septa in wildtype hyphae. For C and D, $\Delta Anbud3$ and wildtype strains possessing *sepA::gfp* (AHS30 and AKS70, respectively) were grown in YGV media for 12 hours prior to imaging. E. Wildtype conidiophore. F. $\Delta Anbud3$ conidiophore. Fused metulae and phialides bearing a few spores were observed. G and H. Wildtype (G) and $\Delta Anbud3$ (H) hyphae grown in YGVUU for 12 hours. Note the absence of septa in the $\Delta Anbud3$ mutant. Septa and nuclei were visualized in fixed hyphae using Calcofulor and Hoechst 33258, respectively. Arrows indicate septa. Bar=10 μm .

Fig.2-3

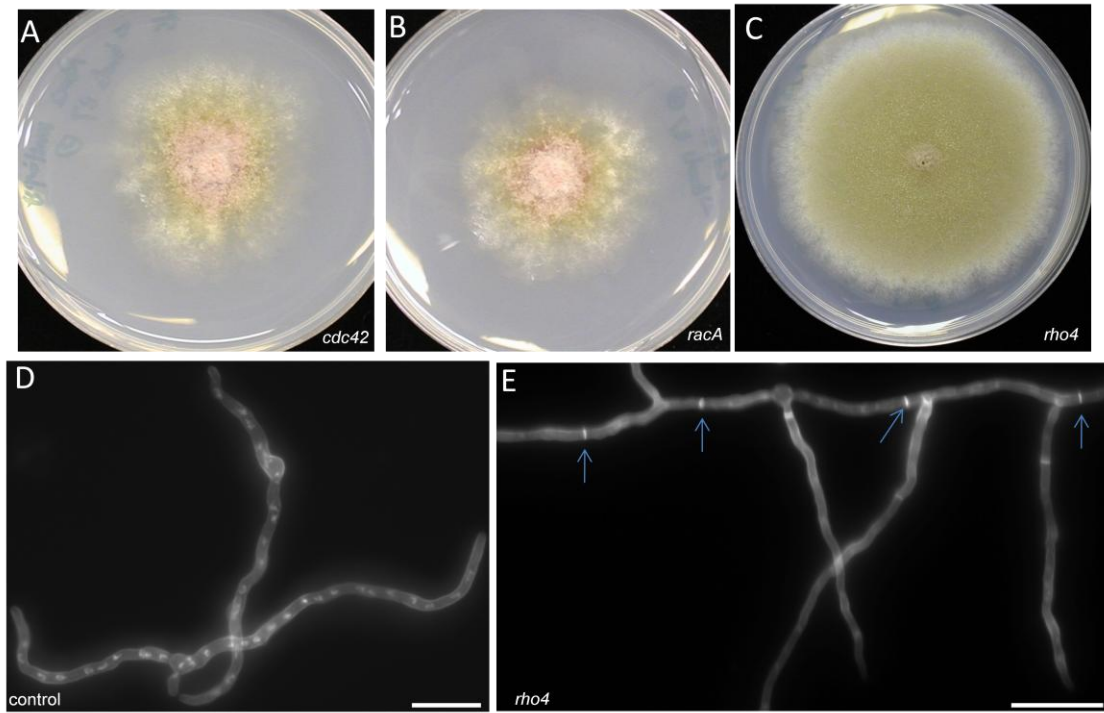


Figure 2-3. Dosage suppression of *bud3* growth and septation defects by *rho4*. A-C. Colony morphology of *bud3* strain AHS3 transformed with multiple copies of *cdc42* (A), *rac1* (B), or *rho4* (C) and grown on selective MN media. Only *rho4* functions as a dosage suppressor and restores conidiation. Hyphal morphology of $\Delta Anbud3$ strain AHS3 transformed with vector control (D) or *rho4* (E). Hyphae were grown on YGV medium for 14 hours and stained with Calcofluor and Hoechst 33258 to visualize septa and nuclei, respectively. The presence of $\Delta rho4$ restored septum formation (arrows) to the *Anbud3* mutant. Bar=10 μm .

Fig.2-4

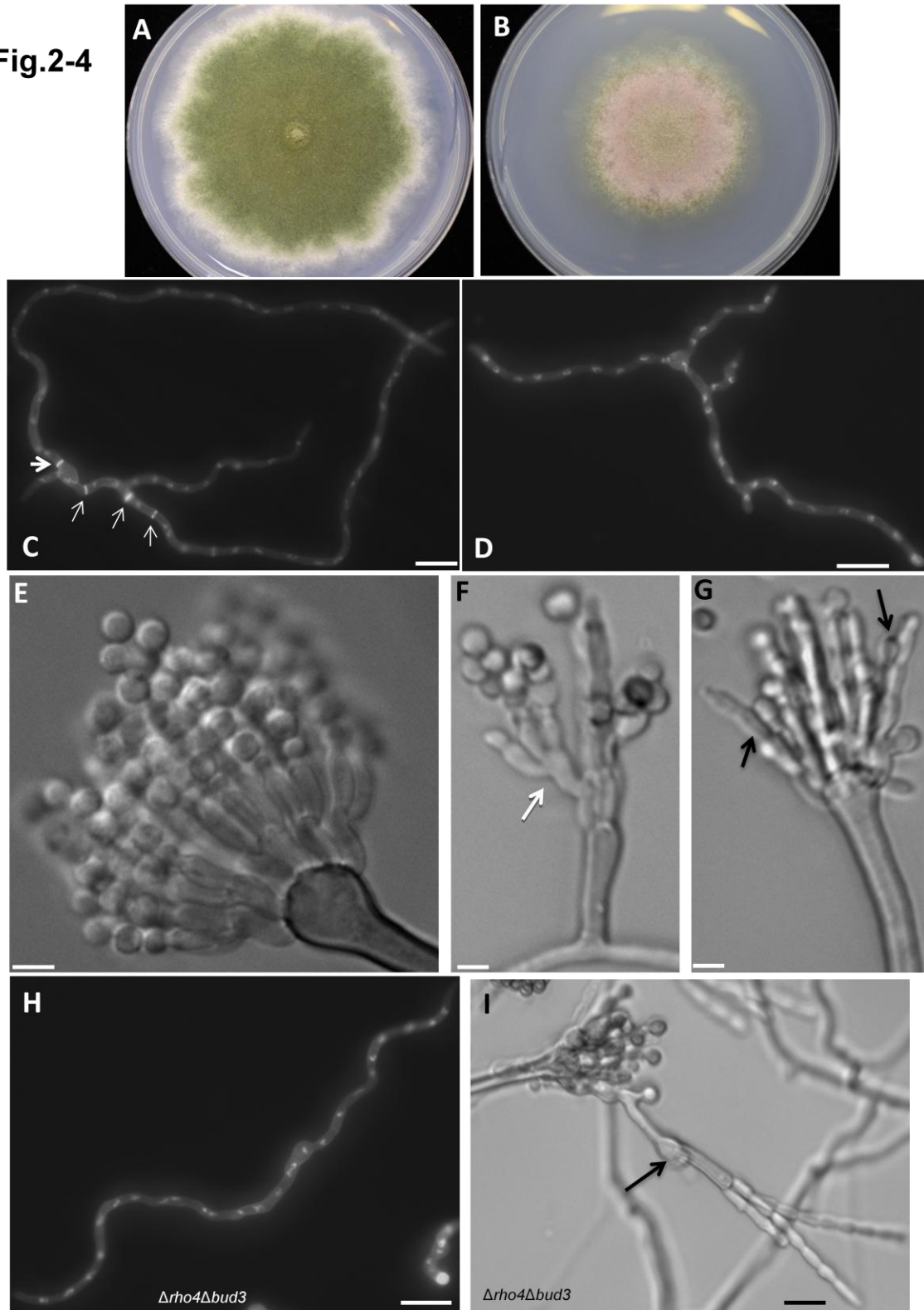
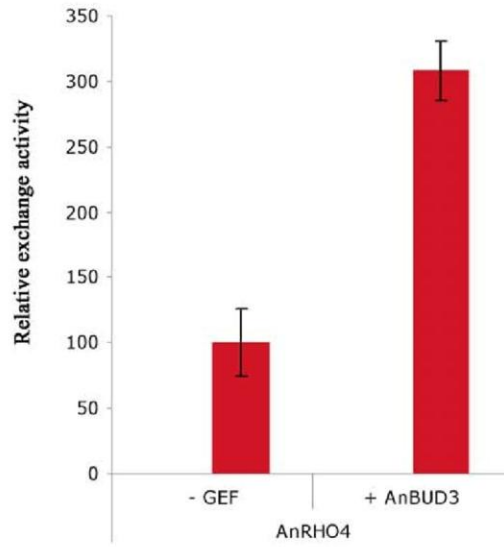


Figure 2-4. Effects of the $\Delta rho4$ mutation on growth, hyphal morphology, and development. A and B. Colony morphology of wildtype (TNO2A3; A) and $\Delta rho4$ (AHS5; B) strains following growth on MNUU medium for nine days. C and D. Hyphal morphology of wildtype (TNO2A3; C) and $\Delta rho4$ (AHS5; D) strains following growth for 14 hours on YGVUU at 28 °C. Arrows indicate septa. Bar=10 μ m. E-G. Conidiophore morphology of wildtype (TNO2A3; E) and $\rho ho4$ (AHS5; F-G) strains following growth for three days on MAGUU. Arrow in panel F indicates abnormal formation of a secondary conidiophore. Arrows in panel G indicate fused metulae and phialides. H. Hyphal morphology of $\Delta Anbud3 \Delta rho4$ double mutant strain (AHS25) after 14 hours of growth in YGVUU at 28 °C. I. Conidiophore morphology of $\Delta Anbud3 \Delta rho4$ double mutant strain (ASH25) following growth for three days on MAGUU. The arrow indicates abnormal formation of a secondary conidiophore generated from a phialide fused to its subtending metulae. Bars=10 μ m except for E-G, where bars=3 μ m.

Fig.2-5

A



B

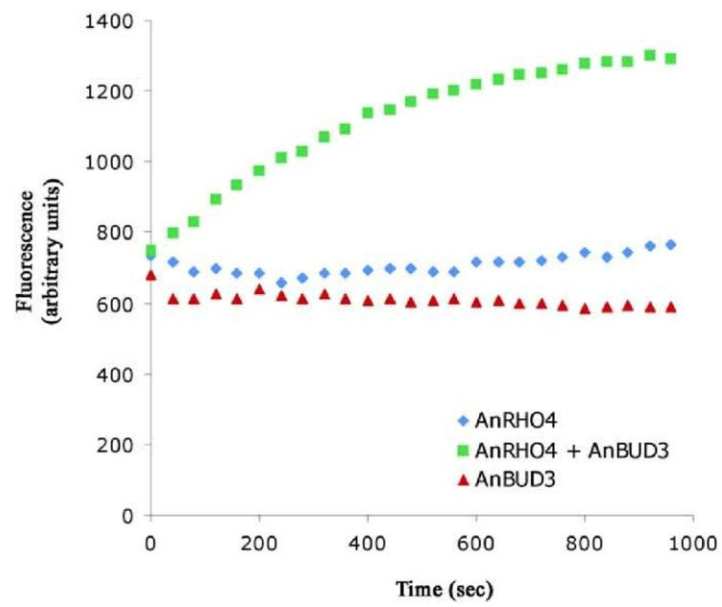


Figure 2-5. AnBud3 is a Rho4 exchange factor. *In vitro* guanine nucleotide exchange activity was determined by measuring binding of mant-GDP to purified Rho4 in the presence or absence of the putative GEF AnBud3 construct containing the GEF domain. The diagram indicates the mean values \pm SD of at least two independent Rho protein and two GEF purifications with each experiment performed in duplicate. The intrinsic Rho activity is set to 100% (**A**). An example of *in vitro* kinetics for mant-GDP binding to purified AnRho4, AnBud3 and both is shown. The exchange activity of AnRho4 is stimulated by AnBud3 (**B**).

Figure 2-6

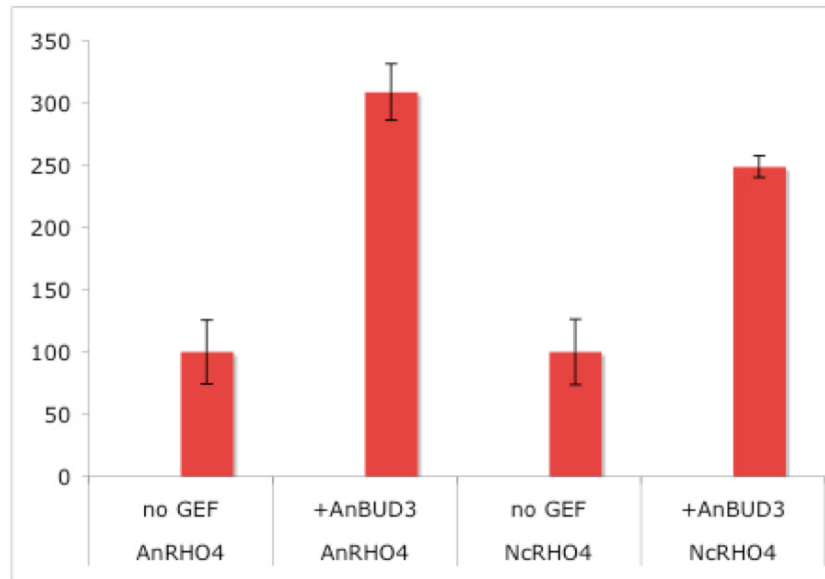


Figure 2-6. AnBud3 is able to stimulate the GDP-GTP exchange activity of *N. crassa* Rho4. The diagram indicates the mean values \pm SD of at least two independent Rho protein and two GEF purifications with each experiment performed in duplicate. The intrinsic Rho activity is set to 100%.

Fig.2-7

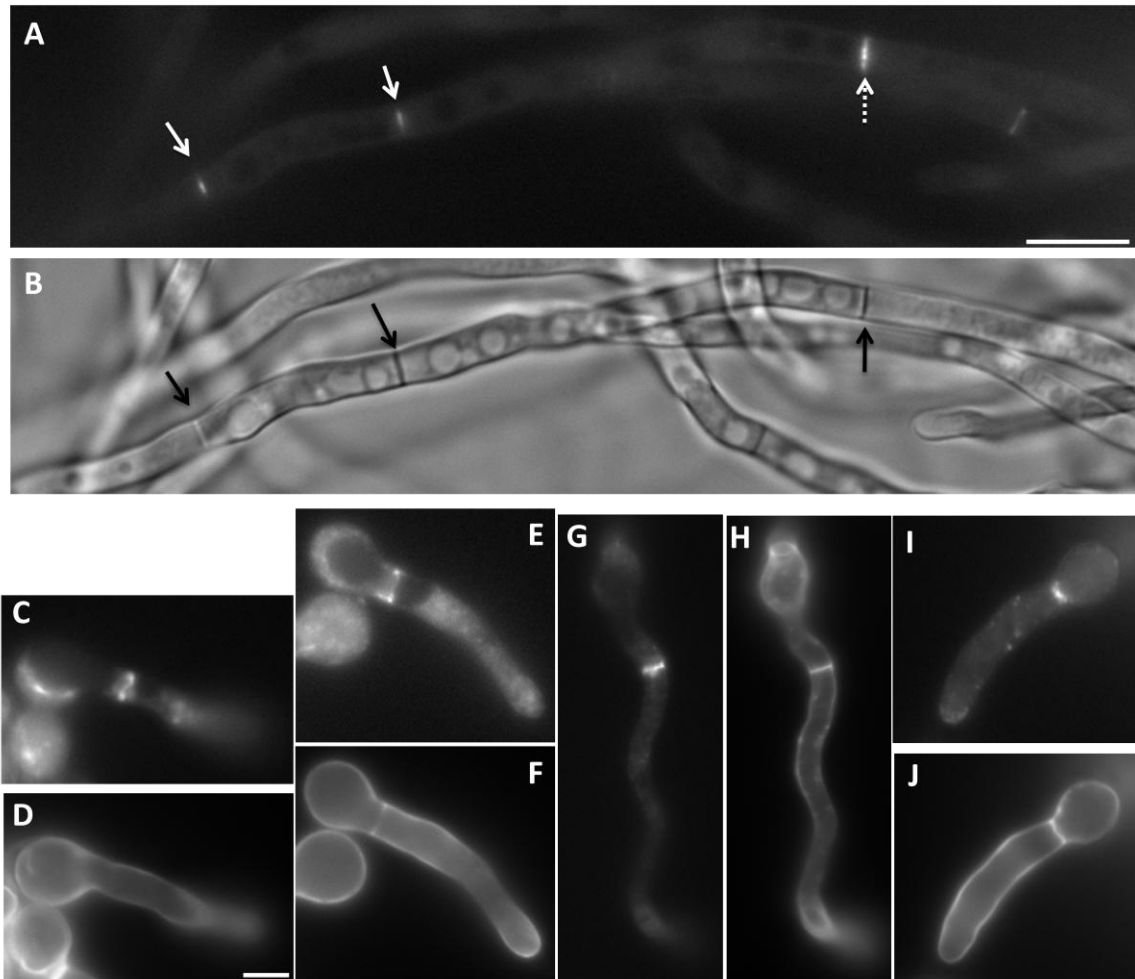


Figure 2-7. Localization of GFP-AnBud3. A and B. GFP-AnBud3 rings (A, white arrows) and corresponding septa (B, black arrows) following growth of strain AHS41 on YGVUU for 15 hours at 28°C. The dashed arrow indicates a thick ring in the process of constricting. C-J. Coordination of GFP-AnBud3 ring dynamics with septum deposition. C, E, G, and I. GFP-AnBud3 localization. D, F, H, and J. Calcofluor staining to visualize septa and cell walls. C and D. GFP-AnBud3 localization at septation site prior to appearance of visible septum. E and F. GFP-AnBud3 rings associated with thin septum. G and H. Thicker AnBud3 ring associated with more prominent septum. I and J. Constricting AnBud3 ring and associated septum. Bar=3 μm , except A and B, where bar=10 μm .

Fig.2-8

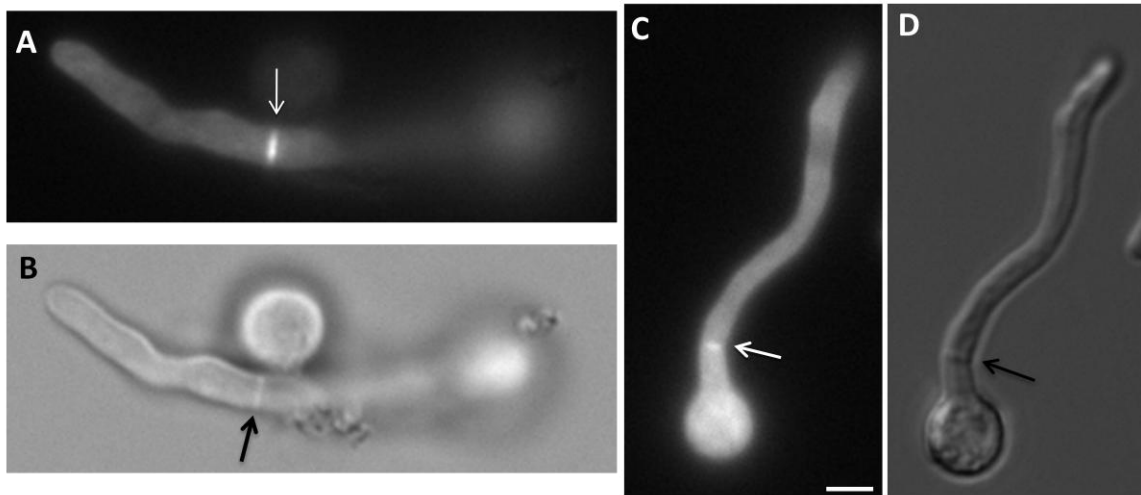


Figure 2-8. Localization of GFP-Rho4. A and B. GFP-Rho4 localization (A) and corresponding septum (B; observed using DIC optics) following 13 hours growth of strain AHS43 at 28°C on *alcA*(p) inducible threonine-MNV. Arrow indicates a GFP-Rho4 ring at the septation site. C and D. A constricting GFP-Rho4 ring (C; white arrow) and corresponding septum (D; black arrow). Bar=3 μ m.

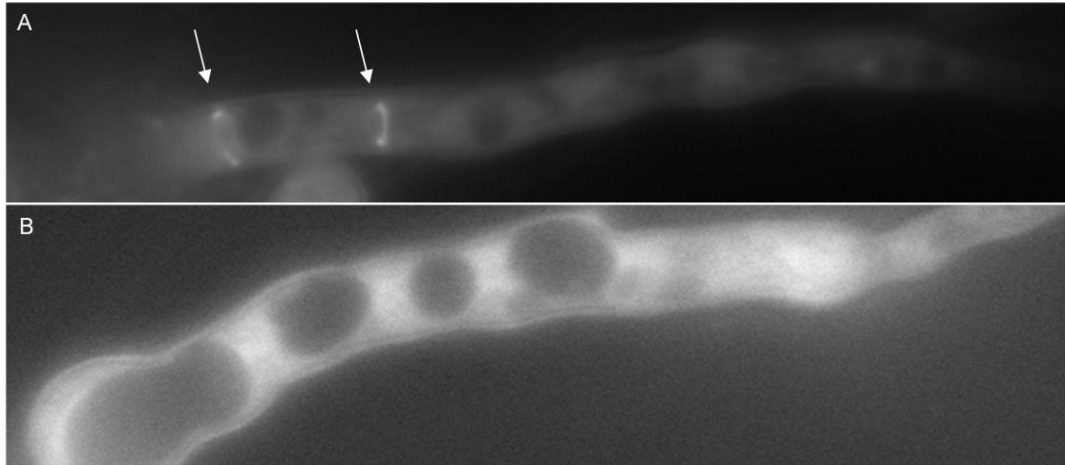
Fig.2-9

Figure 2-9. Absence of contractile actin rings in *sepA1* mutant hyphae grown at 37°C. Wildtype (ACP115; A) and *sepA1* (AHS53; B) hyphae were grown at 37°C for 11-13 h. Contractile actin rings were visualized using a TpmA-GFP fusion protein. Arrows indicate rings in wildtype hyphae. Note the absence of rings in *sepA1* hyphae despite the stronger background.

Fig.2-10

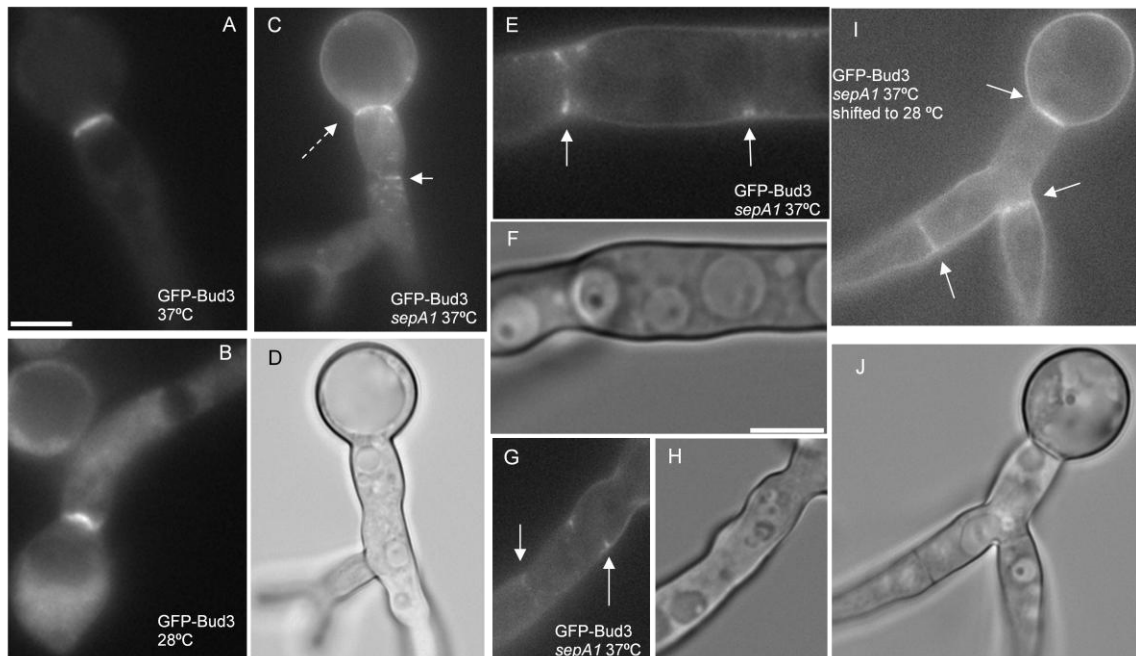


Figure 2-10. Recruitment of AnBud3 to septation sites does not require presence of the contractile actin ring. A and B. GFP-AnBud3 localization in wildtype hyphae (AHS41) grown at 37° (A) or 28°C (B). C-H. GFP-AnBud3 localization in the *sepA1* mutant (AHS51) at 37°C (C,E,G) and corresponding DIC images (D,F,H). Dashed arrow (C) indicates a rare example of an intact GFP-AnBud3 ring, whereas solid arrows mark the more prevalent examples of incomplete rings or cortical patches. I-J. GFP-AnBud3 localization (I) and corresponding DIC image (J) in *sepA1* mutant hyphae 2 h following a shift from 37 to 28°C. Solid arrows indicate GFP-AnBud3 rings. Bars=3 μm.

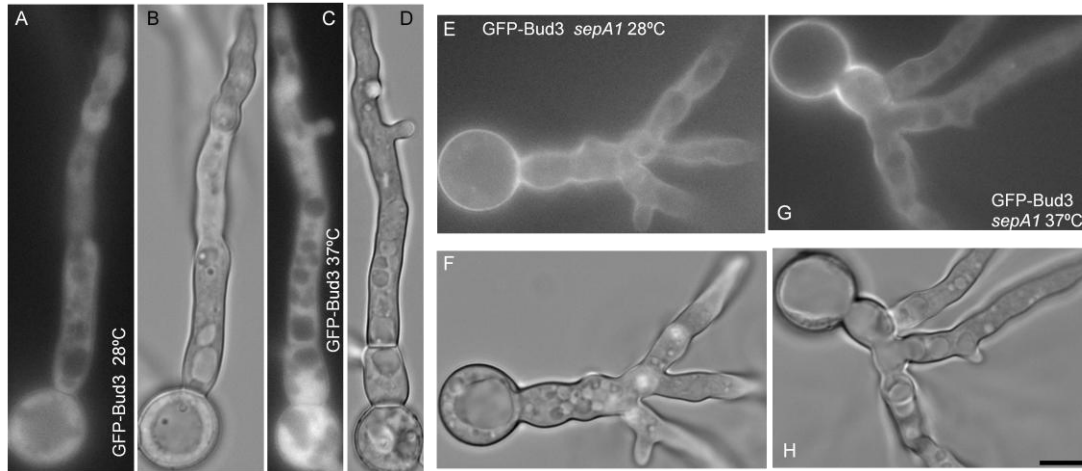
Fig.2-11

Figure 2-11 GFP-AnBud3 localization when nuclear division is blocked. Formation of GFP-AnBud3 rings does not occur in wildtype (A-D) or *sepA1* (E-H) hyphae when nuclear division is blocked by treatment with hydroxyurea (HU). Hyphae grown at 28°C (A,B,E,F) or 37°C (C,D,G,H) were treated with HU as described in the Materials and Methods. GFP (A,C,E,G) and corresponding DIC (B,D,F,H) images are shown.

Bars=3μm.

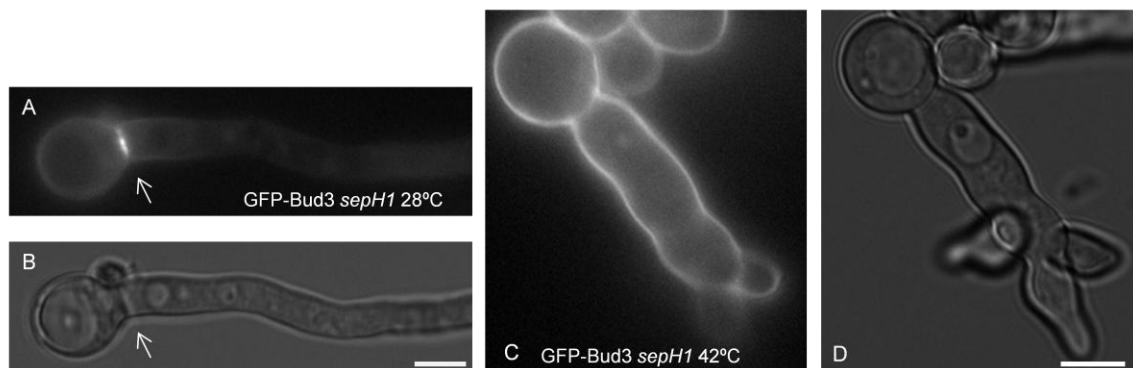
Fig.2-12

Figure 2-12. Localization of GFP-AnBud3 in the *sepH1* mutant. GFP-AnBud3 localization at 28°C (A) and 42°C (C) following 14 hours growth of strain AHS62 on YGV. GFP-AnBud3 localization to septation sites was not observed at 42°C. B and D are corresponding DIC images. Arrows indicate septation sites. Bar=5 μ m.

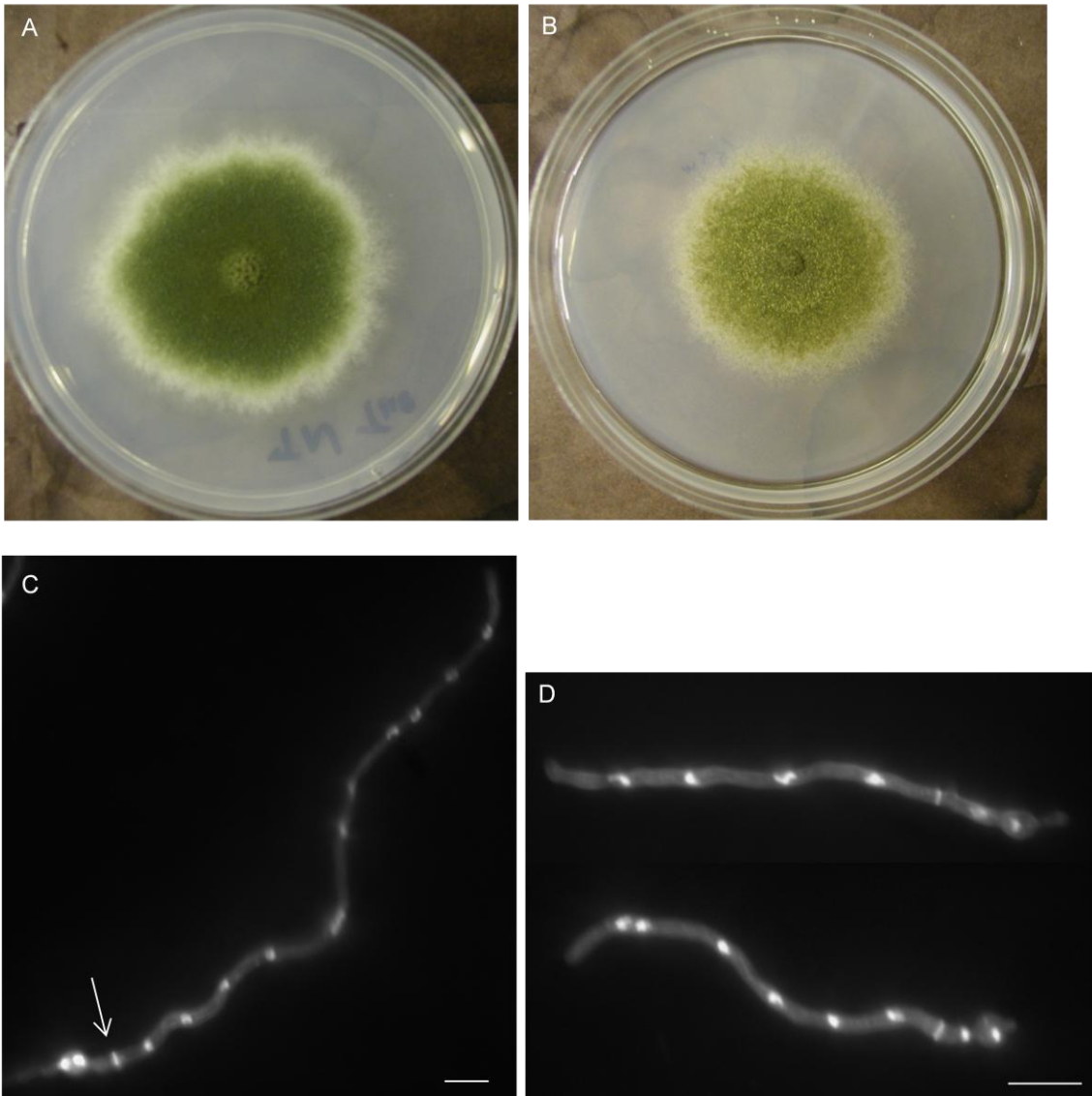
Fig.2-13

Figure 2-13. Effects of the *msb1* mutation on growth and hyphal morphology. A, B. Colony morphology of wildtype (TNO2A3; A) and *msb1* (AHS7; B) strains following growth on MNVUU medium for six days and seven days respectively. C, D. Hyphal morphology of wildtype (TNO2A3; C) and *msb1* (AHS7; D) strains following growth for 13 hours on MNVUU at 28°C. Arrows indicate septa. Bar=10 µm.

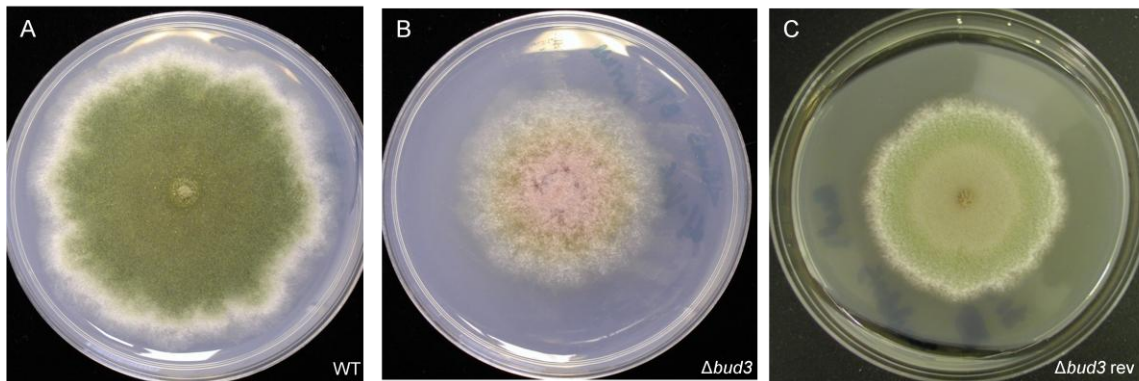
Fig.2-14

Figure 2-14. $\Delta bud3$ suppressors. A. Wild type TNO2A3; B. $\Delta bud3$ mutant AHS3; and C. $\Delta bud3$ suppressor AHS3C2.

REFERENCES

- ABE, K., K. L. ROSSMAN, B. LIU, K. D. RITOLA, D. CHIANG, et al., 2000 Vav2 is an activator of Cdc42, Rac1, and RhoA. *J. Biol. Chem.* **275**: 10141-10149.
- BALASUBRAMANIAN, M. K., E. BI, and M. GLOTZER, 2004 Comparative analysis of cytokinesis in budding yeast, fission yeast and animal cells. *Curr. Biol.* **14**: R806-818.
- BAUER, Y., P. KNECHTLE, J. WENDLAND, H. HELFER and P. PHILIPPSEN, 2004 A Ras-like GTPase is involved in hyphal growth guidance in the filamentous fungus *Ashbya gossypii*. *Mol. Biol. Cell.* **15**: 4622-4632.
- BENDER, A. and J. R. PRINGLE, 1989 Multicopy suppression of the *cdc24* budding defect in yeast by *CDC42* and three newly identified genes including the *ras*-related gene RSR1. *Proc. Natl. Acad. Sci. U.S.A.* **86**: 9976-9980.
- BRUNO, K. S., J. L. MORRELL, J. E. HAMER and C. J. STAIGER, 2001. SEPH, a Cdc7p orthologue from *Aspergillus nidulans*, functions upstream of actin ring formation during cytokinesis. *Mol. Microbiol.* **42**: 3-12.
- CHANT, J., 1999 Cell polarity in yeast. *Annu. Rev. Cell Dev. Biol.* **15**: 365-391.
- CHANT, J., and I. HERSKOWITZ, 1991. Genetic control of bud site selection in yeast by a set of gene products that constitute a morphogenetic pathway. *Cell.* **65**: 1203-1212.
- CHANT, J. and J. R. PRINGLE, 1995 Patterns of bud-site selection in the yeast *Saccharomyces cerevisiae*. *J. Cell Biol.* **129**: 751-765.
- CHANT, J., M. MISCHKE, E. MITCHELL, I. HERSKOWITZ and J. PRINGLE, 1995 Role of Bud3p in producing the axial budding pattern of yeast. *J. Cell Biol.* **129**: 767-778
- CLUTTERBUCK, A. J., 1970 Synchronous nuclear division and septation in *Aspergillus nidulans*. *J. Gen. Microbiol.* **60**: 133-135.
- DAS, M., D. J. WILEY, X. CHEN, K. SHAH, and F. VERDE, 2009 The conserved NDR kinase Orb6 controls polarized cell growth by spatial regulation of the small GTPase Cdc42. *Curr. Biol.* **19**: 1314-1319.
- DONG, Y., D. PRUYNE, and A. BRETSCHER, 2003 Formin-dependent actin assembly is regulated by distinct modes of Rho signaling in yeast. *J. Cell. Biol.* **161**: 1081-1092.
- DUNKLER, A., and J. WENDLAND, 2007 *Candida albicans* Rho-type GTPase-encoding genes required for polarized cell growth and cell separation. *Eukaryot. Cell.* **6**: 844-854.

- EFIMOV, V. P., 2003 Roles of NUDE and NUDF proteins of *Aspergillus nidulans*: insights from intracellular localization and overexpression effects. *Mol. Biol. Cell.* **14**: 871-888.
- FREIFELDER, D., 1960 Bud position in *Saccharomyces cerevisiae*. *J. Bacteriol.* **80**: 567-568.
- GALAGAN, J. E., S. E. CALVO, C. CUOMO, L. J. MA, J. R. WORTMAN, et al., 2005 Sequencing of *Aspergillus nidulans* and comparative analysis with *A. fumigatus* and *A. oryzae*. *Nature.* **438**: 1105-1115.
- GAO, X. D., L. M. SPERBER, S. A. KANE, Z. TONG, A. H. TONG, et al., 2007 Sequential and distinct roles of the cadherin domain-containing protein Axl2p in cell polarization in yeast cell cycle. *Mol. Biol. Cell.* **18**: 2542-2560.
- GULL, K., 1978 Form and function of septa in filamentous fungi, pp. 78-93 in *The Filamentous Fungi, Developmental Mycology*, edited by J. E. SMITH and D. R. BERRY. John Wiley and Sons, New York.
- HARKINS, H. A., N. PAGE, L. R. SCHENKMAN, C. DE VIRGILIO, S. SHAW, et al. 2001. Bud8p and Bud9p, proteins that may mark sites for bipolar budding in yeast. *Mol. Biol. Cell.* **12**: 2497-2518.
- HARRIS, S. D., 2001 Septum formation in *Aspergillus nidulans*. *Curr. Opin. Microbiol.* **4**: 736-739.
- HARRIS, S. D. and M. MOMANY, 2004 Polarity in filamentous fungi: Moving beyond the yeast paradigm. *Fungal Genet. Biol.* **41**: 391-400.
- HARRIS, S. D., J. L. MORRELL and J. E. HAMER, 1994 Identification and characterization of *Aspergillus nidulans* mutants defective in cytokinesis. *Genetics* **136**: 517-532.
- HARRIS, S. D., L. HAMER, K. E. SHARPLESS and J. E. HAMER, 1997 The *Aspergillus nidulans sepA* gene encodes an FH1/2 protein involved in cytokinesis and the maintenance of cellular polarity. *EMBO J.* **16**: 3474-3483.
- HARRIS, S. D., G. TURNER, V. MEYER, E. A. ESPESO, T. SPECHT, et al., 2009 Morphology and development in *Aspergillus nidulans*: a complex puzzle. *Fungal Genet. Biol.* **46**: S82-92.
- HAUSAUER, D. L., M. GERAMI-NEJAD, C. KISTLER-ANDERSON and C. A. GALE, 2005 Hyphal guidance and invasive growth in *Candida albicans* require the Ras-like GTPase Rsr1p and its GTPase-activating protein Bud2p. *Eukaryot. Cell.* **4**: 1273-1286.
- HLUBEK, A., K. O. SCHINK, M. MAHLERT, B. SANDROCK, and M. BOLKER, 2008 Selective activation by the guanine nucleotide exchange factor Don1 is a main determinant of Cdc42 signaling specificity in *Ustilago maydis*. *Mol. Microbiol.* **68**:

615-623.

JUSTA-SCUCH, D., Y. HEILIG, C. RICHTHAMMER, and S. SEILER, 2010 Septum formation is regulated by the RHO4-specific exchange factors BUD3 and RGF3 and by the landmark protein BUD4 in *Neurospora*. Mol. Microbiol., in press.

KAFER, E., 1977 Meiotic and mitotic recombination in *Aspergillus* and its chromosomal aberration. Adv. Genet. **19**: 33-131.

KANG, P. J., A. SANSON, B. LEE and H.-O. PARK, 2001 A GDP/GTP exchange factor involved in linking a spatial landmark to cell polarity. Science. **292**: 1376-1378.

KANG, P. J., E. ANGERMAN, K. NAKASHIMA, J. R. PRINGLE and H.-O. PARK, 2004 Interactions among Rax1p, Rax2p, Bud8p, and Bud9p in marking cortical sites for bipolar bud-site selection in yeast. Mol. Biol. Cell. **15**: 5145-5158.

KIM, J. M., L. LU, R. SHAO, J. CHIN and B. LIU, 2006 Isolation of mutations that bypass the requirement of the septation initiation network for septum formation and conidiation in *Aspergillus nidulans*. Genetics. **173**: 685-696.

KIM, J. M., C. J. ZENG, T. NAYAK, R. SHAO, A. C. HUANG, et al., 2009 Timely septation requires SNAD-dependent spindle pole body localization of the septation initiation network components in the filamentous fungus *Aspergillus nidulans*. Mol. Biol. Cell. **20**: 2874-2884.

KRAPP, A., and V. SIMANIS, 2008 An overview of the fission yeast septation initiation network (SIN). Biochem. Soc. Trans. **36**: 411-415.

KRAPPMANN, A. B., N. TAHERI, M. HEINRICH and H. U. MOSCH, 2007 Distinct domains of yeast cortical tag proteins Bud8p and Bud9p confer polar localization and functionality. Mol. Biol. Cell. **18**: 3323-3339. LIN, X. and M. MOMANY, 2003 The *Aspergillus nidulans* *swc1* mutants shows defects in growth and development. Genetics. **165**: 543-554.

LORD, M., F. INOSE, T. HIROKO, T. HATA, A. FUJITA, et al., 2002 Subcellular localization of Ax11, the cell type-specific regulator of polarity. Curr. Biol. **12**: 1347-1352.

MARTIN, S. G., S. A. RINCON, R. BASU, P. PEREZ, and F. CHANG, 2007 Regulation of the formin for3p by cdc42p and bud6p. Mol. Biol. Cell. **18**: 4155-4167.

MOMANY, M., and J. E. HAMER, 1997 Relationship of actin, microtubules, and crosswall synthesis during septation in *Aspergillus nidulans*. Cell Motil. Cytoskeleton. **38**: 373-384.

NAKANO, K., T. MUTOH, R. ARAI, and I. MABUCHI, 2003 The small GTPase

Rho4 is involved in controlling cell morphology and septation in fission yeast. *Genes Cells*. **8**: 357-370.

NAYAK, T., E. SZEWCZYK, C. E. OAKLEY, A. OSMANI, L. UKIL, et al., 2006 A versatile and efficient gene targeting system for *Aspergillus nidulans*. *Genetics*. **172**: 1557-1566.

OSMANI, A. H., B. R. OAKLEY and S. A. OSMANI, 2006 Identification and analysis of essential *Aspergillus nidulans* genes using the heterokaryon rescue technique. *Nat. Protocols*. **1**: 2517-2526. OZAKI, K., K. TANAKA, H. IMAMURA, T. HIHARA, T. KAMEYAMA, et al., 1996 Rom1p and Rom2p are GDP/GTP exchange proteins (GEPs) for the Rho1p small GTP binding protein in *Saccharomyces cerevisiae*. *EMBO J*. **15**: 2196-2207.

PARK, H.-O. and E. BI, 2007 Central roles of small GTPases in the development of cell polarity and beyond. *Microbiol. Mol. Biol. Rev.* **71**: 48-96.

PEARSON, C. L., K. XU, K. E. SHARPLESS and S. D. HARRIS, 2004 MesA, a novel fungal protein required for the stabilization of polarity axes in *Aspergillus nidulans*. *Mol. Biol. Cell* **15**: 3658-3672.

PHILIPPSEN, P., A. KAUFMANN and H. P. SCHMITZ, 2005 Homologues of yeast polarity genes control the development of multinucleated hyphae in *Ashbya gossypii*. *Curr. Opin. Microbiol.* **8**: 370-377.

RASMUSSEN, C. G. and N. L. GLASS, 2005 A Rho-type GTPase, *rho-4*, is required for septation in *Neurospora crassa*. *Eukaryot. Cell*. **4**: 1913-1925.

SANTOS, B., J. GUTIERREZ, T. M. CALONGE, and P. PEREZ, 2003 Novel Rho GTPase involved in cytokinesis and cell wall integrity in the fission yeast *Schizosaccharomyces pombe*. *Eukaryot. Cell*. **2**: 521-533.

SEKIYA-KAWASAKI, M., M. ABE, A. SAKA, D. WATANABE, K. KONO, et al., 2002 Dissection of upstream regulatory components of the Rho1p effector, 1,3-beta-glucan synthase, in *Saccharomyces cerevisiae*. *Genetics*. **162**: 663-676. SHARPLESS, K. E. and S. D. HARRIS, 2002 Functional characterization and localization of the *Aspergillus nidulans* formin SEPA. *Mol. Biol. Cell*. **13**: 469-479.

TAHERI-TALESH, N., T. HORIO, L. ARAUJO-BAZAN, X. DOU, E. A. ESPESO, et al., 2008 The tip growth apparatus of *Aspergillus nidulans*. *Mol. Biol. Cell*. **19**: 1439-1449.

TRINCI, A. P.J. and N. R. MORRIS, 1979 Morphology and growth of a temperature-sensitive mutant of *Aspergillus nidulans* which forms aseptate mycelia at non-permissive temperatures. *J. Gen. Microbiol.* **114**: 53-59.

VIRAG, A., M. P. LEE, H. SI, and S. D. HARRIS, 2007 Regulation of hyphal morphogenesis by *cdc42* and *rac1* homologues in *Aspergillus nidulans*. *Mol. Microbiol.* **66**: 1579-1596.

VOGT, N., and S. SEILER, 2008 The RHO1-specific GTPase-activating protein LRG1 regulates polar tip growth in parallel to Ndr kinase signaling in *Neurospora*. *Mol. Biol. Cell.* **19**: 4554-4569.

WALTHER, A., and J. WENDLAND, 2003 Septation and cytokinesis in fungi. *Fungal Genet. Biol.* **40**: 187-196.

WENDLAND, J., 2003 Analysis of the landmark protein Bud3 of *Ashbya gossypii* reveals a novel role in septum construction. *EMBO Rep.* **4**: 200-204.

WESTFALL, P. J. and M. MOMANY, 2002 *Aspergillus nidulans* septin AspB plays pre- and postmitotic roles in septum, branch, and conidiophore development. *Mol. Biol. Cell.* **13**: 110-118.

WOLKOW, T. D., S. D. HARRIS, and J. E. HAMER, 1996 Cytokinesis in *Aspergillus nidulans* is controlled by cell size, nuclear positioning and mitosis. *J. Cell Sci.* **109**: 2179-2188.

YANG, L., L. UKIL, A. OSMANI, F. NAHM, J. DAVIES, et al., 2004 Rapid production of gene replacement constructs and generation of a green fluorescent protein-tagged centromeric marker in *Aspergillus nidulans*. *Eukaryot. Cell.* **3**: 1359-1362.

YEH, B. J., R. J. RUTIGLIANO, A. DEB, D. BAR-SAGI, and W. A. LIM, 2007 Rewiring cellular morphology pathways with synthetic guanine nucleotide exchange factors. *Nature.* **447**: 596-600.

Chapter III Characterization of yeast bud site selection homologues

Axl2 and Bud4

ABSTRACT

The bud site selection system of *Saccharomyces cerevisiae* represents the best-understood example of budding morphogenetic regulatory system. Axl2 and bud4 are two of factors that are required for the axial budding pattern. How conservative the function of the two proteins in *Aspergillus nidulans* is still unclear since the low similarity in protein sequence to their related budding pattern proteins. Here, we describe the functional characterization and localization of *A. nidulans* homologues of the axial bud site markers Axl2 and Bud4. Both AnBud4 and AnAxl2 are not required for polarized hyphal growth, but AnBud4 is involved in septum formation. Interestingly, AnAxl2 only functions at the tip of phialides and has a unique function in sexual development. Additional promoter swap experiments suggest that proper expression of both genes is essential for their localization. On the other hand, AnBud4 and AnAxl2 are predicted to play a role in septin organization.

INTRODUCTION

Cell morphology is a critical feature for proper cellular function in many eukaryotic cells. For *A. nidulans*, the mechanisms involved in septum formation, conidiophore development and fruiting body formation are still far from clear. During vegetative growth, the partitioning of hyphae into cellular units by cross-walls known as septa permit compartmentalization of functions and is thought to play a key role in

supporting the development of reproductive structures that bear spores. Spore chain formation on the top of phialides can be considered as multi-nuclear divisions from stem cell and they are precisely regulated by proper expression and re-localization of landmarks. During sexual development, function of landmarks may also affect the timing of hülle cell (nursing cell) and cleistocium formation. In this chapter, my work focused on the functional characterization and localization of homologues of the yeast axial bud site markers Bud4 and Axl2 for morphological function in *A. nidulans*

Summary of bud4 and axl2 in Saccharomyces cerevisiae

Bud4 and Axl2 are two axial budding pattern factors in *S. cerevisiae*. Like $\Delta bud3$, both $\Delta axl2$ and $\Delta bud4$ can switch from axial budding to bipolar pattern in haploid cells of budding yeast. For the axial pattern, the cell wall protein Axl2 serves as a landmark whose function is facilitated by its association with Axl1 and the septin-interacting proteins Bud3 and Bud4 (CHANT 1999; LORD et al 2002; GAO et al. 2007; PARK and BI 2007). In *S. cerevisiae*, Bud4 forms rings encircling the mother-bud neck in a septin-dependent manner (Sanders and Herskowiz, 1996). Axl2 was first found to be a multicopy suppressor of the $\Delta spa2 cdc10-10$ double mutants (Roemer, Madden et al. 1996) to rescue the lethality of *S. cerevisiae*. Spa2 (spindle pole associated) is a scaffold protein that interacts with other yeast polarisome components and bud selection. Spa2 deletion mutants significantly reduced the capacity of cells to generate pheromone-induced shmoos (Sheu, Santos et al. 1998; van Drogen and Peter 2002). Cdc10 is the one of the seven septins found in budding yeast (Longtine, DeMarini et al. 1996). In addition,

Axl2p is a membrane protein and expressed throughout the cell cycle (Halme, Michelitch et al. 1996; Roemer, Madden et al. 1996).

Axl2-GFP localization is determined by the cell cycle in yeast.

Axl2 expression peaks at G1 and changing the timing of expression by promoter exchange resulted in uniform membrane localization of Axl2p. Artificially induced pulses of Axl2 around late G1 corrected localization of Axl2p to the incipient bud site and to the bud neck (Roemer, Madden et al. 1996; Lord, Yang et al. 2000). When *Axl2* was placed under either constitutive MET3 promoter or periodic *BUD3* promoter (S/G2), Axl2-GFP lost its precise localization to the bud necks, and instead it had uniformly distributed throughout the plasma membrane. However, pulsed expression of BUD10 (*Axl2*) in late G1 phase restores the correct localization of Bud10p (Lord, Yang et al. 2000). Because of distinct differences in the organization and regulation of cell division in budding yeast versus filamentous fungi, the bud site selective markers will have their unique function on morphology of the latter regulating cell division.

Secondary development in Aspergillus nidulans

A.nidulans differentiates by two morphologically distinct stages: vegetative and secondary structures (Casselton and Zolan 2002). It propagates efficiently by producing asexual spores called conidia and sexual spores called ascospores during secondary development. Conidia are formed on specialized structures called conidiophores. Conidiophore formation is initiated from a thick-walled foot cell forming a stalk. The tip of the stalk swells and forms a vesicle where elongated cells called sterigmata develop

(Fig. 3-1). Sterigmata include two types of distinct cells: metulae and phialides. Metulae are generated from vesicles in 3-4 hours and each metula produces two phialides in optimal growth condition. On the top of phialides, multiple cycles of mitosis occur and long chains of airborne conidia are produced. In this process, since phialides undergo repeated divisions to produce chains of spores and compel the older spores upwards, a shuttle of landmark localization and re-localization happens by an unclear mechanism to ensure the correct polarity of new spores.

During sexual development, vegetative hyphae coil and fuse to form the ascogenous hyphae. Reproductive ascogenous hyphae then proliferate to generate ascospore-containing asci within the cleistothecia. In addition, large thick-walled cells called Hülle cells nurse the cleistothecial primordia contributing to the formation of the cleistothecium wall (Alexopoulos, 1962; Yager, 1992; Alexopoulos et al., 1996).

Transcriptional factors on conidiophore development

BrlA and AbaA are two key transcriptional factors which regulate the conidiophore development. BrlA is a transcriptional factor which is required for the expression of a series of proteins in all developmental steps (Prade and Timberlake 1993). Null *BrlA* mutant can start stalk formation but only fail to vesiculate. When inducing *BrlA* expression in the conditional mutant during induction, differentiating hyphal tips can be transformed into reduced conidiophores that produced spores in submerged cultures (Chang and Timberlake 1993). AbaA is upregulated by BrlA and acts as a positive feedback regulator of BrlA during conidiation. AbaA is required for phialide differentiation and its null mutant will reiterate metular development, which

will generate a chain of abnormal metulae to form abacus structures (Sewall, Mims et al. 1990). Without BrlA, *abaA* mutants fail to accumulate numerous developmentally regulated transcripts (Boylan, Mirabito et al. 1987), and also make abnormal reduced conidiophores in submerged culture.

Septins in S. cerevisiae and A. nidulans

Septins are GTPase that form filaments and rings in fungi and animal and were first found in cell cycle defect mutants of *S. cerevisiae*. They play key roles in cellular organization process ranging from cytokinesis to surface growth (Fares, Goetsch et al. 1996; Longtine, DeMarini et al. 1996). Members of the septin family have been found in all eukaryotic model system including yeast, fruit fly, worm and human. In *S. cerevisiae*, there are seven septins, including Cdc3, Cdc10, Cdc11, Cdc12, Spr3, Sep7 and SPR28. The core septin proteins (Cdc3, Cdc10, Cdc11, and Cdc12) localize to the mother/bud neck, where they assemble into heteropolymers that organize proteins necessary to complete cytokinesis and ensure proper coordination between bud formation and nuclear division (Cid, Adamikova et al. 2001; Gladfelder, Bose et al. 2002).

AspA, AspB, AspC, AspD and AspE are five septins found in *Aspergillus nidulans*. They localize in three basic patterns in fungi including projects at tips or branches, septa and septin filaments (Momany, Zhao et al. 2001). AspA and AspC are orthologs of CDC11 and CDC12 respectively and their localization appears to be mutually dependent (Lindsey and Momany 2006). AspB has the higher expression level to the others and is required for viability. AspD is classified in Cdc10 group and AspE may participate in a more specialized, non-essential function (Momany, Zhao et al. 2001)

because deletion of AspE results in a slightly defect in development (Momany, unpublished data).

Axl2 and Vac8 belongs to Cadherin and catenin families respectively.

In *S. cerevisiae*, Vac8p is a phosphorylated and palmitoylated vacuolar membrane protein with armadillo catenin repeats, which are super-helix of helices proposed to mediate interaction of β -catenin with its ligands. Vac8p is required for the cytoplasm-to-vacuole targeting (Cvt) pathway in budding yeast (Scott, Nice et al. 2000). Interestingly, when analyzing the AnAxl2 protein sequence in NCBI by BLASTp, two tandem cadherin domains were found at the N-terminus.

Cadherins and catenins were first found to form cytoplasmic complexes at cell-cell junction in mammalian cells. Cadherins (Calcium dependent adhesion molecules) are a class of type-1 transmembrane proteins and dependent on Ca^{2+} to function. In structure, they share cadherin repeats, which are the extracellular Ca^{2+} -binding domains. Cadherins play important roles in cell adhesion by associating with catenins, ensuring that cells within tissues are bound together (Burford, Baloch et al. 2009; Hage, Meinel et al. 2009).

Catenins have to form complexes through physical connection (Weis and Nelson 2006). The first two catenins identified (Peyrieras, Louvard et al. 1985) were α -catenin and β -catenin. α -catenin can bind to β -catenin and actin filaments. β -catenin binds to the cytoplasmic domain of some cadherins. Additional catenins such as gamma- and delta-catenin have also been identified. In addition to adhere to junctions, catenins also function at desmosomes, which are cell structures specialized for cell-to-cell adhesion, to intermediate filaments and stress fibers (Garrod and Kimura 2008). Catenin-cadherin

complexes also function in the modulation of cadherin endocytosis and small GTPases (McCrea and Gu 2010). Catenin Armadillo regions engage in protein-protein interactions and promote the association of β -catenin with cadherins (Nelson and Nusse 2004). Even though some proteins contain Armadillo domains but do not associate with cadherins, they cannot be classified as catenins by definition. We believe the cadherin (AnAxl2) and the catenin (AnVac) proteins will have some parallel morphogenetic functions through their hypothetical interaction.

MATERIALS and METHODS

Strains, media, growth conditions and staining

Aspergillus nidulans strains used in this study are listed in Table 2-1. MNV (minimal + vitamins) media were made according to Kafer (1977). MNV-glycerol and MNV-threonine fructose media were made as described in PEARSON et al (2004). MAG (malt extract agar) and YGV (yeast extract glucose + vitamins) media were made as described previously (Harris et al 1994). 5-Fluoroorotic acid (5-FOA; US Biological, Swampscott, MA) was added to media at a concentration of 1mg/ml after autoclaving.

For septation and hyphal growth studies, conidia from appropriate stains were grown at 28 °C for 12h on coverslips. Hyphae attached to the coverslip were fixed using a modified standard protocol (HARRIS et al 1994) [fixing solution contained 3.7% formaldehyde, 25 mM EGTA, 50 mM piperazine-N,N-bis(2 ethanesulfonic acid) (PIPES), and 0.5% dimethyl sulfoxide] for 20 min and then stained with staining solution containing both 273 nM fluorescent brightener 28 (Sigma-Aldrich Corporation, St. Louis, MI) and 160 nM Hoechst 33258 (Molecular Probes, Eugene, OR).

Construction of gene replacement strains

The Bud4 and Axl2 genes from strains AHS4, AHS6 were replaced with the *pyroA*^{A.f.} marker from *A. fumigates* and the *pyroA*^{A.n.} marker from *A. nidulans* respectively. All gene replacements were generated using the gene targeting system developed by NAYAK et al (2006) and the gene replacement generation strategy developed by YANG et al (2004). Oligonucleotides used in this study are listed in Table2- 3. *PyroA*^{A.n.} DNA marker, the DNA fragments upstream and downstream of Axl2 were amplified from wild-type FGSC strain GR5 (available through the Fungal Genetics Stock Center, Kansas City, MO). *PyroA*^{A.f.} DNA marker fragment was PCR amplified from plasmid pTN1 (available through the Fungal Genetics Stock Center, Kansas City, MO) and the DNA fragments upstream and downstream of Bud4 were amplified from the wild-type strain FGSC28. High Fidelity and Long Template PCR systems (Roche Diagnostics Corporation, Indianapolis, IN) were used for amplifications of individual and fusion fragments, respectively, using a Px2 Hybaid or an Eppendorf Mastercycler gradient thermal cycler. The amplification conditions were according to the manufacturer's recommendations. PCR products were gel purified using the QIAquick gel extraction kit (QIAGEN Inc., Valencia, CA). The gene replacement constructs were transformed into strain TNO2A3 or GR5, and plated on supplemented minimal medium with 0.6 M KCl. Transformations were performed according the protocol described by OSMANI et al. (2006). Transformation candidates were tested for homologous integration of the gene replacement construct and the absence of the wild-type gene by diagnostic PCR as described by YANG et al (2004).

Construction of GFP fusions to Axl2 and Bud4

To localize Axl2, a GFP-pyr4 fragment was amplified from plasmid pFNO3 (available through the Fungal Genetics Stock Center, Kansas City, MO). A 1.5kb Axl2 fragment and a 1.5kb Axl2 downstream fragment were amplified from strain TNO2A3. The same approach described by NAYAK et al. (2006) was used to make the gene targeting system. The fusion PCR construct was transformed to strain TNO2A3 and the transformants were verified by PCR to ensure the homologous gene insertion.

To localize Bud4, we fused GFP to the N-terminus using the five piece fusion PCR approach recently described by Taheri-Talesh et al. (2008). In addition to the retention of native promoter sequences, final constructs also contained a short linker of five glycines and alanines inserted between the GFP and Bud4 coding sequences. In brief, the following five fragments were amplified (primers described in Table 2-2); (1) a 1.3-kb sequence upstream of the target gene, (2) the GFP coding sequence (minus the stop codon) derived from plasmid pMCB17apx, (Scott, Nice et al.) (3) the target gene plus 400-bp of downstream sequence, (4) the *N. crassa* pyr-4 selectable marker, also derived from pMCB17apx, and (5) a 1.3-kb sequence extending from 400 to 1700-bp downstream of target gene. Fragments (1), (Scott, Nice et al.), and (5) were amplified by specific primers with 30bp tails that were reverse complements of the adjacent fragments. Finally, the forward primer used to amplify fragment (1) and the reverse primer used to amplify fragment (5) were used to fuse the entire five-fragment gene replacement construct. The High Fidelity and Long Template PCR systems (Roche Diagnostics Corporation, Indianapolis, IN) were employed to amplify individual and fusion fragments, respectively, on a Px2 Hybaid or an Eppendorf Mastercycler gradient thermal cycler. PCR products were gel purified using the QIAquick gel extraction kit (QIAGEN Inc.,

Valencia, CA). The resulting *gfp::Bud4::pyr-4* cassettes was used to replace its respective wildtype gene in strain TNO2A3 using the approach described by NAYAK et al. (2006).

The Axl2 and Bud4 promoter swap and alcA::Axl2 construct

The promoter regions of both Axl2 and Bud4 were approximately determined by the adjacent upstream gene sequence acquired from *Aspergillus* genome database

(http://www.broadinstitute.org/annotation/genome/Aspergillus_group/multihome.html).

For making *pbud4::Axl2-GFP* strain, four fragments were amplified: (1) A 1.5Kb sequence upstream of Axl2 from TNO2A3, (2) *pyroA^{A.f.}* marker from pTN1 (Nyak et al., 2006), (3) a 1043bp sequence upstream of Bud4 from TNO2A3, (4) a 1.5kb sequence from the start codon of Axl2 from TNO2A3. Fragments (1), and (4) were amplified by specific primers (listed in table 2-2) with 30bp tails that were reverse complements of the adjacent fragments. Finally, the forward primer used to amplify fragment (1) and the reverse primer used to amplify fragment (4) were used to fuse the entire four-fragment gene replacement construct. The amplification system is the same with N-terminal GFP fusion protocols described above. The construct was transformed to AHS65 to achieve pBud4-Axl2-GFP and verified by both PCR and sequencing through the promoter region. Two strains (AHS657 and AHS659) were finally chosen out of 10 sequenced strains since there are only two nuclei changes from wild type on the pbud4 sequence. The same method was used to make alcA-Axl2-GFP, except for the fragment alcA promoter amplified from pMCB17apx (Efimov 2003). The similar strategy was used to make the *pAxl2-Bud4* construct with (1) a 1.5kb sequence upstream of Bud4, (2) *pyroA^{A.f.}*

marker from pTN1, (3) a 907bp sequence upstream of Ax12 and the fragment (4) was amplified from strain AHS41 through start codon of GFP sequence to 1.5kb inside of Bud4. The fusion PCR construct was transformed to TNO2A3 to achieve pAx12-GFP-Bud4.

Conidiophore observation

Conidiophore development was monitored by using the sandwich coverslip method described by LIN and MOMANY (2003). Briefly, 1ml of melted MAGUU media was placed on a coverslip that was transferred to the surface of a 4% water agar plate. The coverslip was inoculated with spores once the media had solidified, whereupon a second coverslip was placed on top. After 3-4 days, conidiophores had formed and become attached to the top coverslip, which was then dipped into 100% ethanol and mounted for DIC microscopy. For Calcoflour staining, the coverslips were fixed and stained after ethanol treatment.

Spore counting for sexual development

100 μ l conidium suspension was spread to minimal media with the concentration around 10^4 /ml. After incubated for 8 days at 28 $^{\circ}$ C (dark) and 24 $^{\circ}$ C (light), agar squares with spore lawn on the top were sampled every day with a borer of 1 cm diameter until 19 days. The agar squares were crushed in 1.5ml eppendoff tubes, mixed with 1ml 0.5% Tween20 and vortex at mid-speed for one hour to shake off conidia and hülle cell and break cleistothecia. The spore suspension is diluted 100 times and counted with hemocytometer (Fisher Scientific).

Examining GFP localization on conidiophores

To localize GFP-Bud4 and Ax12-GFP, cellophane stripes were used to synchronize and helped to handle conidiation from plates. Briefly, sterilized cellophane stripes (~1cm *7cm) were placed on MAG plates, and then diluted spore suspension (10^4 /ml) was spread on the top of stripes (~100 spores). After 24 hrs incubated at 28 °C, stalks start to form on the surface of cellophane stripes. Every one to two hours, a stripe a time can be peeled from the plates and mounted with YGV liquid media for fluorescent screening for Ax12 localization at each developmental stage.

RT-PCR from RNA extracted from normal and induced culture

All strains were grown in glucose media for biomass overnight as non-induced condition. Mycelia was collected by vacuum-filtering on Whatman filter paper and washed with 1x PBS buffer. Half of the biomass was transferred to minimal media using threonine as solo carbon source as induced condition. For monitoring gene expression during conidiation, filter papers with biomass on top were cut in half and placed on glucose and threonine plates for 1day and 4 days respectively to inducing conidiation. We grew TPM1 and TTA1 in MNV-glucose overnight for normal expression of BrlA and AbaA for biomass. The biomass then was transferred to MNV-threonine for induction of both genes. Samples were taken at 0, 2, 4, 6 hours respectively. The cultures with conidiophores were then harvested and ground in liquid nitrogen. RNA was extracted by using Trizol (Invitrogen) and purified by RNAeasy Clean Kit (Qiagen) as described in lab protocol. RT-PCR was performed using the Ambion RETROscript Kit with the 3' primer oligoDT.

Microscopy

Digital images of plates were collected with an Olympus C-3020ZOOM digital camera.

Differential interference contrast (DIC) and fluorescent images were collected with either an Olympus BX51 microscope with a reflected fluorescence system fitted with a Photometrics CoolSnap HQ camera or an Olympus Fluoview confocal laser-scanning microscope. Images were processed with IPLab Scientific Image Processing 3.5.5 (Scanalytics Inc., Fairfax, VA) and Adobe Photoshop 6.0 (Adobe Systems Incorporated, San Jose, CA).

RESULTS

Identification of A. nidulans Axl2 and Bud4

The original annotation of the *A. nidulans* genome revealed the existence of potential homologues of the axial budding markers Bud4 and Axl2 (Harris and Momany 2004; Galagan et al., 2005). AnBud4 (AN6150.3) is a predicted 1433 AA protein that contains a C-terminal anillin-like (DUF1709) domain followed by a single pleckstrin-homology (PH) domain (**Fig. 3-2A**). Homologues of AnBud4 (>38% identity over their entire length) exist in all sequenced euscomycete genomes. Similarity between AnBud4 and its hemiascomycete homologues is solely confined to the DUF1709 and PH domains, and ranges from 41 to 51%. AnAxl2 (AN1359.3) is a predicted 929 AA protein that contains two Dystroglycan-type cadherin-like domains (CADG) close to its N-terminus (**Fig. 3-2B**). These two cadherin-homologous domains are suspected to bind calcium. It has 29% similarity with its *S. cerevisiae* homologue and is relatively highly conserved at the N-terminus.

Role of Axl2 in A. nidulans morphogenesis

To determine possible function of AnAxl2, Δ Anaxl2 mutants were made by PCR mediated gene replacement from the wild type GR5 strain. After 7 days of growth on minimal plates, colonies of AHS6 (Δ Anaxl2::pyroA^{A.n}, hereafter referred to as Δ Anaxl2), appeared restricted growth compared to wild type GR5 which produced about 5 times less conidia than GR5 on MNUU (**Fig. 3-3** and **Table 3-3**). On MAGUU, the colony size was similar between Δ Anaxl2 mutants and GR5. Notably, Δ Anaxl2 mutants had an early entry into sexual cycle as yellowish color (hülle cells) and black dots (fruiting bodies) are visible compared with GR5 on both minimal and rich media. Coverslip cultures were used to examine Δ axl2 mutants for defects in hyphal morphogenesis. No significant morphological defect was found during vegetative growth.

To determine the possible basis of the conidiation defects, conidiophores from Δ Anaxl2 mutants as well as wildtype controls were imaged using a previously described “sandwich slide” protocol (LIN and MOMANY 2003). Matulae and phialides of Δ Anaxl2 are normal but only bear one layer of spores on the tops of phialides (**Fig. 3-4**). This is in contrast with wildtype conidiophores with long chains of spores.

Axl2 localizes to the top of phialides.

To localize AnAxl2, a C-terminal AnAxl2-GFP strain (AHS65) was generated with the same strategy as gene replacement. In this strain, the sole functional source of AnAxl2 was supplied by the AnAxl2::GFP fusion protein expressed under the control of native promoter sequences (**Fig. 3-5A**). For localization of AnAxl2-GFP in vegetative growth, spores were inoculated on coverslips in liquid MNUU for 12h and the coverlip

was mounted and examined under the fluorescent microscope. AnAx12-GFP could not be localized on hyphal surface, hyphal tips and septation site during vegetative growth. To further examine the localization on conidiophores, conidia of AnAx12-GFP strain were inoculated on cellophane stripes placed on MAG plates to synchronize conidiophore growth. After 20 hours, conidiophore stalks started to form from cellophane stripes and one stripe at a time was peeled and mounted with YGV and examined for Ax12-GFP localization every hour. The timing of conidiation on cellophane stripes was also dependent on inoculum density. AnAx12-GFP localization was neither found in hyphae nor on the top of vesicles and metulae during the early stages of conidiophore development. After about 30 hours, conidiophores were fully developed and bright AnAx12-GFP rings were solely localized between phialides and the nascent conidia on mature conidiophores but not the top of phialides before generating conidia (**Fig. 3-6**). The results suggest that AnAx12 does not function in vegetative growth but only in the last step of conidiation and its expression is regulated during cytokinesis.

Roles of Bud4 in A.nidulans morphogenesis

To determine the possible of function AnBud4 during hyphal morphogenesis, mutants possessing complete gene deletions were generated using protocols discussed above (YANG et al 2004; NAYAK et al 2006). The *Bud4::pryoA*^{A.f.} deletion mutants (AHS4, hereafter referred to as Δ Anbud4) formed colonies that were slightly smaller than wild type and were notably devoid of conidia (**Fig. 3-7A.C**). On minimal media, Δ Anbud4 mutants produced ~1850-fold fewer conidia/mL compared to their parental strain TN02A3. A similar effect (i.e., ~710-fold reduction for Δ bud4 compared

to TN02A3) was observed on rich media. “Sandwich slide” protocol was also used to determine the possible defect of conidiophore. A range of defects was noted, including elongated metulae and phialides, as well as conidiopores that apparently failed to undergo cytokinesis (**Fig 3-7E, F, G.**). Because a stage-specific arrest was not observed, it seems likely that AnBud4 is required at multiple steps during conidiophore development.

Coverslip cultures were used to examine $\Delta Anbud4$ mutants for defects in hyphal morphogenesis. The timing and pattern of spore polarization in $\Delta Anbud4$ mutants were indistinguishable from wildtype, and the resulting hyphae displayed no obvious defects in polarized growth (**Fig. 3-8**). On the other hand, septum formation was compromised. Although $\Delta Anbud4$ mutants were capable of forming septa (**Fig.3-8B the small panel**), they did so only after a pronounced delay (**Table 3-4**).

In *S. cerevisiae*, genetic analysis demonstrated that Bud3 and Bud4 function together to specify the axial budding pattern (Marston, Chen et al. 2001). To determine if a similar epistatic relationship underlies the roles of AnBud3 and AnBud4 in septum formation, we generated $\Delta bud3::pyrG^{A.f.}; \Delta bud4::pyroA^{A.f.}$ double mutants (AHS24) by a standard cross. Because these mutants displayed a synthetic slow growth phenotype (**Fig. 3-7B, C, and D**), we conclude that AnBud3 and AnBud4 have at least one distinct function and are thus not obligate partners.

Localization of Bud4 in A. nidulans

To localize AnBud4, we generated strains in which the sole functional source of AnBud4 was supplied by a *GFP::bud4* fusion gene expressed under the control of native

promoter sequences. AnBud4 formed constricting rings that localize to septation sites (**Fig 3-9. A and B**). Furthermore, AnBud4 rings appeared at incipient septation sites prior to the formation of any detectable septum (i.e., 40/200 GFP-AnBud4 rings were not associated with a septum; **FIG 3-9 C-E.**). However, unlike AnBud3, AnBud4 rings split in two as septum formation progressed. For those cases where we observed a double AnBud4 ring, the Calcofluor-stained septum overlay one of the rings (**FIG 3-9 F-H.**), though there was no obvious preference as to which ring it co-localized with. We also observed that one of the double AnBud4 rings was subsequently lost. As shown in **FIG. 3-10**, we followed four double AnBud4 rings, two of which were associated with a detectable septum (observed using DIC). In each case, one of the two rings had disappeared within 20 minutes, and all the remaining rings were now associated with a septum. Because of photo bleaching, we could not follow the fate of these remaining rings. Nevertheless, they presumably constrict, since all constricting AnBud4 rings that we observed were single rings that co-localized with a septum.

To examine the localization of GFP-Anbud4 on developmental structure, cellophane strip have been used to synchronize conidiophore development. Anbud4 formed bright rings between nascent metular buds and vesicles, then it localized between metulae and phialides. Finally, it formed relative weak rings between phialides and nascent spores like AnAxl2 (**Fig. 3-11**). These results suggest that Anbud4 has a ubiquitous function during conidiophore development.

Axl2 was upregulated when AbaA and BlrA expression were induced

As the key transcription factor that regulates conidiophore development, BlrA binds to C/A-G/A-AGGG-G/A on the promoter sequence to initiate vesicle formation and

further regulate all stages of conidiation. The later transcription factor AbaA binds to CATTCC/T to initiate phialide formation. According to distance from the upstream gene (An1358.3), we scanned 867nt upstream of AnAxl2 as the promoter region; two AbaA and one BrlA binding sites were found in this region (*pAxl2*). Combining the result with the sole localization on top of phialides during conidiation, expression of *Axl2* might be regulated in a BrlA and AbaA dependent manner. To induce the expression of *AbaA* and *BrlA*, strains TPM1 (*alcA::BrlA; BrlA*) and TTA1 (*alcA::AbaA; AbaA*) strains were used to examine the expression of *Axl2* at induced conditions. Both strains have two copies of *BrlA* or *AbaA* respectively: one copy under its endogenous promoter and the other under *alcA* promoter control. Total RNA was extracted from A28, TPM1 and TTA1, and then half quantified RTPCR was used to determine AnAxl2 expression in induction conditions (**Fig 3-12**). AnAxl2 expression started to increase after two hours of induction and reached a maximum at 4 hours. These results indicate that *Axl2* expression is regulated by BrlA and AbaA at the transcriptional level.

Axl2 localization under Bud4 and alcA promoter control

Cell cycle-dependent transcription is prevalent in yeast and the periodic transcription serves as a general mechanism of regulation within the cell cycle. In *S. cerevisiae*, Bud4 expression occurred at M phase (Cho, Campbell et al. 1998; Spellman, Sherlock et al. 1998) and Bud10 (*Axl2*) is expressed at late G1 (Lord, Yang et al. 2000). As shown above, *Axl2*-GFP localization has solely been found between phialides and nascent spores but GFP-Bud4 was found prevalent on conidiophores. If *bud4* and *axl2* were solely transcriptional controlled, promoter swap experiment would change their protein

localization pattern. The length of *pAxl2* and *pBud4* were decided by the distance between the upstream genes and *AnAxl2* or *AnBud4* from the database of the *Aspergillus* Genome at the Broad Institute. Sequences of *pAxl2* and *pBud4* are 994bp and 1019 respectively. The four ways PCR, which was similar to the five way PCR used for N-terminal GFP construction, was used to synthesize the constructs for transforming the *Axl2*-GFP strain and TNO2A3 strain. The *pBud4-Axl2-GFP* (AHS651) and *pAxl2-GFP-Bud4* (AHS451) strains were achieved by inserting *pyroA-pbud4* and *pyroA-paxl2* constructs to replace the endogenous promoters of *Axl2* and *Bud4* respectively (**Fig. 3-13**). For better controlling the expression of *AnAxl2*, the inducible *alcA* promoter was used to replace endogenous promoter of *AnAxl2* in *AnAxl2*-GFP strains in the same way (Stain AHS652).

The RNA expression under normal (glucose) and induced (threonine) condition was shown on figure (**Fig. 3-14**). RNA level increased in both *pBud4::Axl2* and *aclA(p)::Axl2* strains, which were expected, after 12 hours of induction during vegetative growth in threonine media. The same results have been found during conidiophore development on threonine plates.

Coverslip culture and cellophane stripes were used to examine *pBud4::Axl2*-GFP localization in hyphae and conidiophores. Surprisingly, *pbud4::Axl2*-GFP localized to vacuoles or other organelles (**Fig. 3-15A,B**) inside of cells during vegetative growth, which was not found in the wildtype. During asexual development, *pBud4::Axl2*-GFP could not properly localized between phialides and nascent spores, and on the contrary, it formed bright dots inside of conidophore cells (**Fig. 3-15C, D**), which was similar in hyphae. These results suggested that earlier expression of *Axl2* (in hyphae) and

improper expression timing (early stage of conidiation) were not required and that the excessive Ax12 was dumped into vacuoles for degradation. Moreover, we used the submerged culture to examine AnAx12-GFP on reduced conidiophores of *pBud4::Ax12-GFP* strain for better views. In most cases, Ax12-GFP accumulated as patches at cortical sites between phialides and spores or uniformly distributed throughout spore surface (**Fig 3-15E, F**), though rare examples of a complete ring were occasionally observed (**Fig 3-15G, H**).

We also used *alcA* promoter for better control of AnAx12 expression. *alcA::Ax12* expression was shut down in glucose media and increases in threonine media as sole carbon source. *alcA::Ax12-GFP* stains formed colonies slightly smaller than wildtype but had dramatically decreased conidiophore density on MN-threonine (**Fig 3-16A, B**). A sandwich method was used to examine conidiophore structure. The organization of metulae and phialides on vesicles was close to normal with long spore chains. This showed that excessive expression of AnAx12 did affect the density of asexual development but had little effect on conidiophore structure.

Both cellophane strips and submerged culture were used to determine the *alcA::Ax12-GFP* localization during induction in MN-Thr media. By both methods, Ax12-GFP could not localize anywhere on the cortical of conidiophores but formed bright localizations inside vegetative cells (**Fig 3-16C, D**). Accordingly, expression of AnAx12 is regulated by both spatial and timing during asexual development. Excessive copies of AnAx12 may disrupt its subtle interaction with partner proteins for proper localization between phialides and nascent spores.

Bud4 localization under AnAxl2 promoter control

We failed to identify the *pAxl2*-GFP-Bud4 mutants from transformation plates since the transformants appeared dramatically sick and they formed tiny colonies notably devoid of conidia. Interestingly, this phenotype was not consistent with the Δ An*bud4* mutants. This suggested that proper expression of AnBud4 might have essential function for the viability of *A. nidulans*. I suspected that *paxl2*-Bud4 strains could conidiate better on rich media. Thus, fourteen transformants were transferred to MAGUU by dissecting colony chunks from original transformation plates and the spores could be harvested for further morphological examination.

Interaction between septins and Axl2 in A. nidulans

Axl2 was first found to suppress the double mutation of *Spa2* and *Cdc10-10* in budding yeast. Cdc10p is one of the septin ring components (Longtine, DeMarini et al. 1996; Roemer, Madden et al. 1996). In *S. cerevisiae*, overexpression of Axl2p can induce elongated bud morphology and mislocalization of septins to the bud-tip region and disorganization at the bud neck. In addition, multicopy *Axl2* can suppress *cdc42*^{V36G} cells which have pronounced defects in septin organization (Gao, Sperber et al. 2007). Other reports showed that Bud4 co-localized with septins in a septin dependent manner in *S. cerevisiae* (Sanders and Herskowitz 1996; Gladfelter, Kozubowski et al. 2005). In *A. nidulans*, septin AspD is classified to the Cdc10 group (Momany, Zhao et al. 2001).

We wanted to determine the interaction between both Axl2/Bud4 and septins by making double mutants through a normal sexual cross. ARL144, ARL146, ARL148 and ARL150 were null mutants of AspA, AspC, AspD, AspE (provided by Dr. Momany's lab,

AspD and AspE are unpublished strains). $\Delta axl2 \Delta septins$ double mutants were achieved by crossing AHS6 ($\Delta axl2$) to septin null mutants. After growth on minimal media for 3 days, colony phenotypes of double mutants showed the following variations to wildtype. $\Delta axl2 \Delta aspE$ mutants and $\Delta axl2 \Delta aspC$ mutants indicated a single septin deletion phenotype (both $\Delta aspC$ and $\Delta aspE$ are epistatic to $\Delta axl2$). Only $\Delta axl2 \Delta aspD$ showed a $\Delta axl2$ phenotype, indicating that $\Delta axl2$ was epistatic to $\Delta aspD$ (**Fig 3-17**). These results suggest that Axl2 may directly interact with AspD during conidiophore development.

Vec8 and Axl2 are involved in sexual development.

Vac8 is a phosphorylated and palmitoylated vacuolar membrane protein that interacts with Atg13p and is required for the cytoplasm-to-vacuole targeting (Cvt) pathway in autophages. When using yeast Vac8p sequence to do BLASTp search in the *Aspergillus* genome database, *AnVac8* was sequenced on two different contigs (1.114 and 1.237). After aligning the two sequences into one large 6065bp sequence, the *AnVac8* locus was deleted from the genome by gene replacement with the *pyroA^{A.f.}* marker. Notably, $\Delta Anvac8$ had no conidiation defect on MAG but decreased spore production on minimal media, which was consistent with its possible function on nitrogen source utilization during autophages (Kikuma, Ohneda et al. 2006). Using BLASTp in the NCBI database, we noticed that *AnVac8* had three ARM domains which stand for Armadillo/beta-catenin-like repeats. Moreover, we found that *AnAxl2* was the only protein with two cadherin domains on its N-terminus in *A. nidulans*. Interestingly, asexual cycles (golden hulle cells and black fruiting bodies) were observed early on $\Delta Anvac8$ and $\Delta Anaxl2$ colonies compared to wild type (**Fig. 3-18**). Thus, in order to

determine the function of AnVac8 and AnAxl2 during the sexual cycle, conidia, hülle cells and ascospores were counted from 9 to 19 days grown both in dark and light. The countings were repeated twice and averaged. The findings were three fold (**Table 3-3**):

First, both $\Delta Anaxl2$ and $\Delta Anvac8$ mutants produced more sexual spores than wildtype in dark and light. In dark at 28 °C, the number of hülle cells peaked at the tenth day in $\Delta Anaxl2$ mutants and $\Delta Anvac8$ mutants. Whereas the peak of hülle cells in wildtype was half that of $\Delta Anaxl2$ and 1/5 that of $\Delta Anvac8$ and peaked at the twelfth day. Notably, $\Delta Anvac8$ mutants produced about 3 times the number of hülle cells as the $\Delta Anaxl2$ mutants.

Second, the number of ascospores in $\Delta Anaxl2$ mutants kept increasing up to 19 days but stabilized after 14 days. One explanation for this result was that $\Delta Anaxl2$ mutants produced more cleistothecia than wildtype and would reach a much higher peak after all the cleistothecia mature. Notably, the ascospore production was blocked or at least severely delayed in $\Delta Anvac8$ mutant strains.

Third, all three strains have a wildtype *VeA* gene (a gene whose product activates the sexual cycle in dark) but early entry into the sexual cycle was not affected by light in both $\Delta Anaxl2$ and $\Delta Anvac8$ mutant strains, even though light did increase conidium production in $\Delta Anaxl2$ and $\Delta Anvac8$ mutant strains and decreased the generation of hülle cells and ascospores.

Accordingly, these results suggest that AnAxl2 and AnVac8 can suppress sexual development in a both light and *VeA* independent manner.

Discussion

The purpose of this chapter is to characterize the function of the *A. nidulans* homologues of the yeast axial bud site selection markers Axl2 and Bud4. Our observations implicate AnAxl2 and AnBud4 in septum formation and secondary development. In particular, AnBud4 appears to function in septum formation and might facilitate septin organization at septation sites. During secondary development, AnAxl2 functions solely at the late stage of conidiophore development, whereas AnBud4 is active at the whole conidiophore structure. Both AnAxl2 and AnBud4 are regulated by transcription factors (BrlA and AbaA), but the timing of proper expression is required for their right localization and function. Our results also suggest that Axl2 may be involved in sexual development through the cadherin domain interaction with the catenin domain of AnVac8.

The roles of Bud4 in septum formation

Our analysis of AnBud4 is consistent with the notion that it associates with the septins and facilitates their function during septum formation. In particular, the AnBud4 localization pattern during septum formation is almost identical to that of AspB. Both proteins initially form a single ring that converts to a double ring, followed by the loss of one of the two rings. Because of the proximity of the remaining AnBud4 ring to the septum in living hyphae, we could not determine if the basal ring was preferentially lost as is the case for AspB. (note that AspB was localized following fixation, which tends to spread the contractile actin ring; SHARPLESS and HARRIS, 2002). In addition to *S. cerevisiae*, Bud4 homologues in *Candida albicans* (Int1) and *Schizosaccharomyces pombe* (Mid2) also associate with septins and have been implicated in the organization of

septin rings (GALE et al. 2001; BERLIN et al. 2003; TASTO et al. 2003). Thus, it seems likely that septin organization is a conserved function of Bud4 homologues. Indeed, based on their domain organization, these proteins may represent the fungal analogues of the animal septin organizing protein anillin (HICKSON and O'FARRELL 2008). Nevertheless, the observation that loss of AnBud4 did not prevent, but only delayed, septum formation suggests that *A. nidulans* septins are capable of organizing a ring in the absence of Bud4. Alternatively, as noted in *S. pombe*, septins may be dispensable for septation in *A. nidulans*.

Although AnBud3 and AnBud4 both function in septum formation, our results show that they do not have an epistatic relationship. The synthetic slow growth phenotype observed in $\Delta bud3 \Delta bud4$ double mutant strains implies that at least one of these proteins has an additional function that is not shared with the other (BOONE et al. 2007). The nature of this function is not known but, assuming that AnBud4 does promote septin organization, it might be related to the roles of *A. nidulans* septins in additional functions beyond their involvement in septum formation (WESTFALL and MOMANY 2002). Nevertheless, this observation does not eliminate the possibility that AnBud3 and AnBud4 directly interact during the process of septation. Indeed, we strongly suspect that AnBud4 and the septins serve as a scaffold that enables the Bud3-Rho4 GTPase module to direct assembly of the CAR, and are currently undertaking experiments to test this idea.

Collectively, these observations imply that neither AnBud3 nor AnBud4 are required for the establishment or maintenance of hyphal polarity, but do show that they are needed for normal septation. Notably, the defects in septum formation may account

for the abnormal development observed in $\Delta bud3$ and $\Delta bud4$ mutant strains, as reduced conidiation has previously been associated with defects in septum formation (HARRIS et al. 1994). Finally, these results suggest that AnBud3 and AnBud4 may not regulate septation via the same mechanism.

The role of Bud4 and Axl2 in conidiophore development

According to their localization patterns, AnAxl2 solely localizes between phialides and nascent spores, whereas AnBud4 localizes to all developmental stages of the conidiophore (**Fig 3-19**). These localizations have been proved by observing conidiophore structures in the corresponding deletion mutant strains. Because of the yeast Axl2 homologue is the suppressor of $\Delta Spa2$ and $Cdc10-10$ double mutant strains, by analogy, AnAxl2 may function at the top of phialides through interaction with AspD, the CDC10 ortholog. The reasoning is as follows. First, in *S. cerevisiae*, one third yeast Axl2 sequence close to the C-terminus can partially restore the septin organization defect, which sequence is conservative in AnAxl2. Second, Axl2 may directly interact with AspD because $\Delta Anaxl2 \Delta aspD$ double mutant strains suggest a $\Delta Anaxl2$ phenotype which is different with other AnAxl2 and septin double deletion mutants. This suggests that AnAxl2 may directly organize AspD to the sporulation neck. An *in vivo* protein-protein can be done to test this hypothesis in the future.

Proper expression of Axl2 and Bud4 is required for their localization

Axl2-GFP cannot localize to the right position after promoter swap with Bud4. This result is consistent with disruption of Axl2 localization to the neck in budding yeast when Axl2 was under bud3 promoter control (Gao, Sperber et al. 2007). Thus, timing of Axl2

expression is critical for its proper localization and is not solely transcriptional determined. *pBud4-Axl2-GFP* can localize to vacuoles or Golgi during vegetative growth, which is not found in wildtype. This indicates that excessive *axl2* is not required and is therefore dumped for degradation. Similar to the *Axl2-GFP* localization in budding yeast with promoter swap, *pBud4-Axl2-GFP* is uniformly distributed to surface of spores and formed thick deposition to the neck walls in reduced conidiophores. This suggests a pulse of exotic *Axl2* at a proper mitotic stage will restore the correct localization between phialides and spores. Interestingly, high expression of *Axl2* under the *alcA* promoter will decrease the number of conidiophores, but not affect the conidiophore structure.

The role of *Axl2* and *Vac8* in sexual development

We have observed that both $\Delta Anaxl2$ and $\Delta Anvac8$ mutant strains have early entry into the sexual cycle, and have the higher ratio of sexual spores to conidia compared to wildtype. The suppression of asexual development shows difference between the two mutants. Compared with wildtype, $\Delta Anaxl2$ mutant strains demonstrate a high production of ascospores with two fold the number of hülle cells compared to wildtype. Interestingly, $\Delta Anvac8$ mutant strains produce much higher (around 5-10 times) number of hülle cells but almost was blocked in ascospore generation. The *VeA* gene is proposed to be a negative regulator of asexual development and its function can be inhibited by light (Mooney and Yager 1990; Timberlake 1990; Kim, Han et al. 2002). When grown in light, $\Delta Anaxl2$ mutant strains produce four fold more conidia in the dark compared to wildtype, which can be expected since *VeA* is inhibited. However, early entry into the sexual stage is observed 5-7 days early, even though production of both sexual cells is

reduced. Thus AnAxl2 represses sexual development in a light and VeA independent manner.

As the possible mechanism, cadherin and beta-catenin interaction may be involved in this process through Cdc42 and RacA. Cdc42 and Rac1 have been well characterized as key player for polarity establishment in *A.nidulans* (Virag, Lee et al. 2007). A recent report shows that the Rho-family GTPase Cdc42 may play a critical role by controlling cadherin-based intercellular junctions and cell polarity in many species (Chen, Ha et al. 2006). In addition, E-cadherin can negatively regulate cell proliferation and migration by reducing the level of the predominant GTP bound form of Rho family protein RhoA or Cdc42 in mammal cells (Asnaghi, Vass et al. 2010). Since both AnAxl2 and AnVac8 have common function in sexual development, AnAxl2 could interact with AnVac8 (catenin) as a cadherin through Cdc42 and RacA to repress sexual development.

Figure 3-1

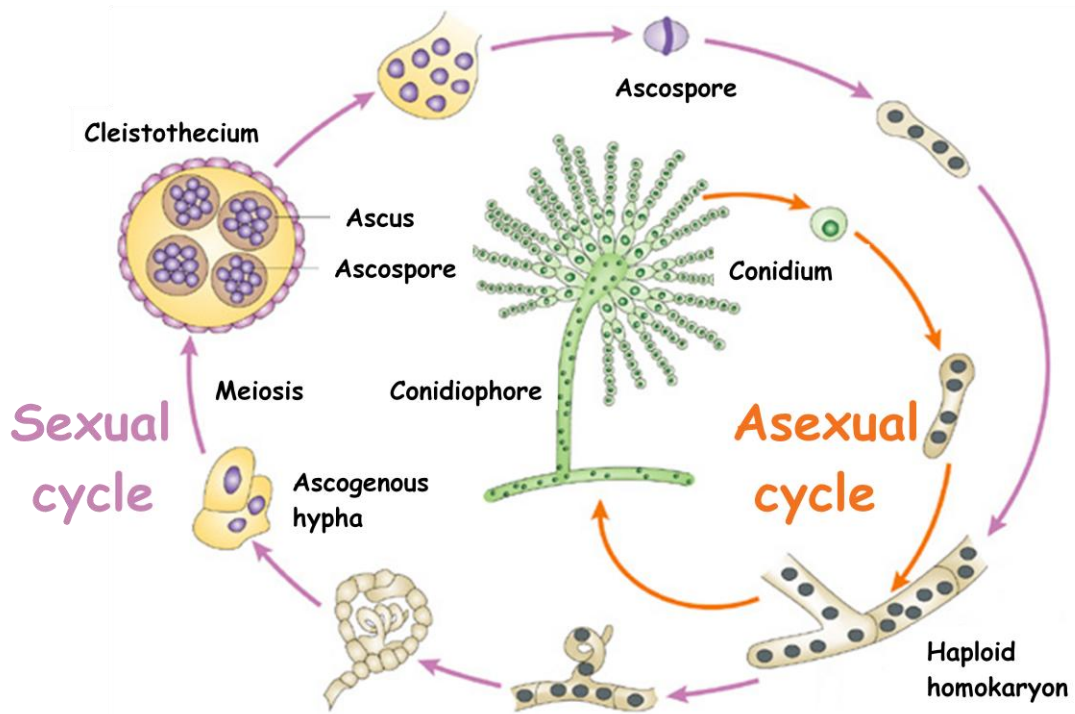


Figure 3-1. The life cycle of *Aspergillus nidulans*

Figure 3-2

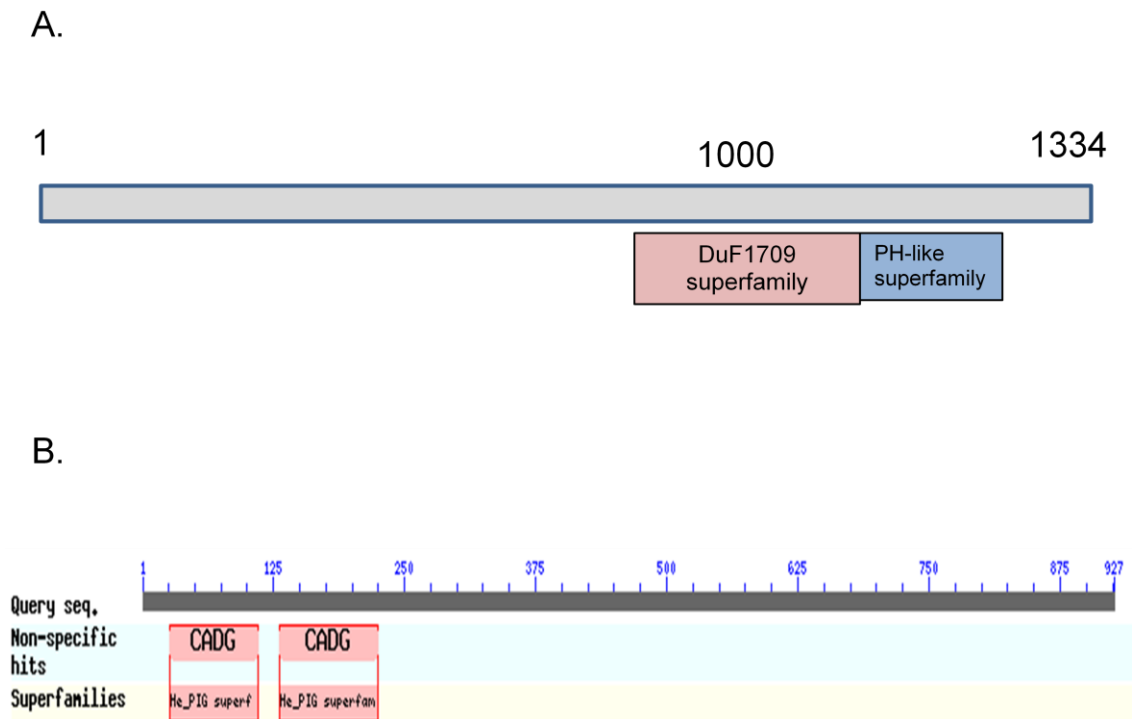


Figure 3-2. Amino acid (AA) sequence and domains of AnBud4 and AnAxl2. A. AA sequence of AnBud4 sequence, DuFdomain (pink) span from ~800-1100 and PH domain (blue) is adjacent to the DuFdomain. B. AA sequence of AnAxl2, the two cadherin domains are in the C-terminus.

Figure 3-3

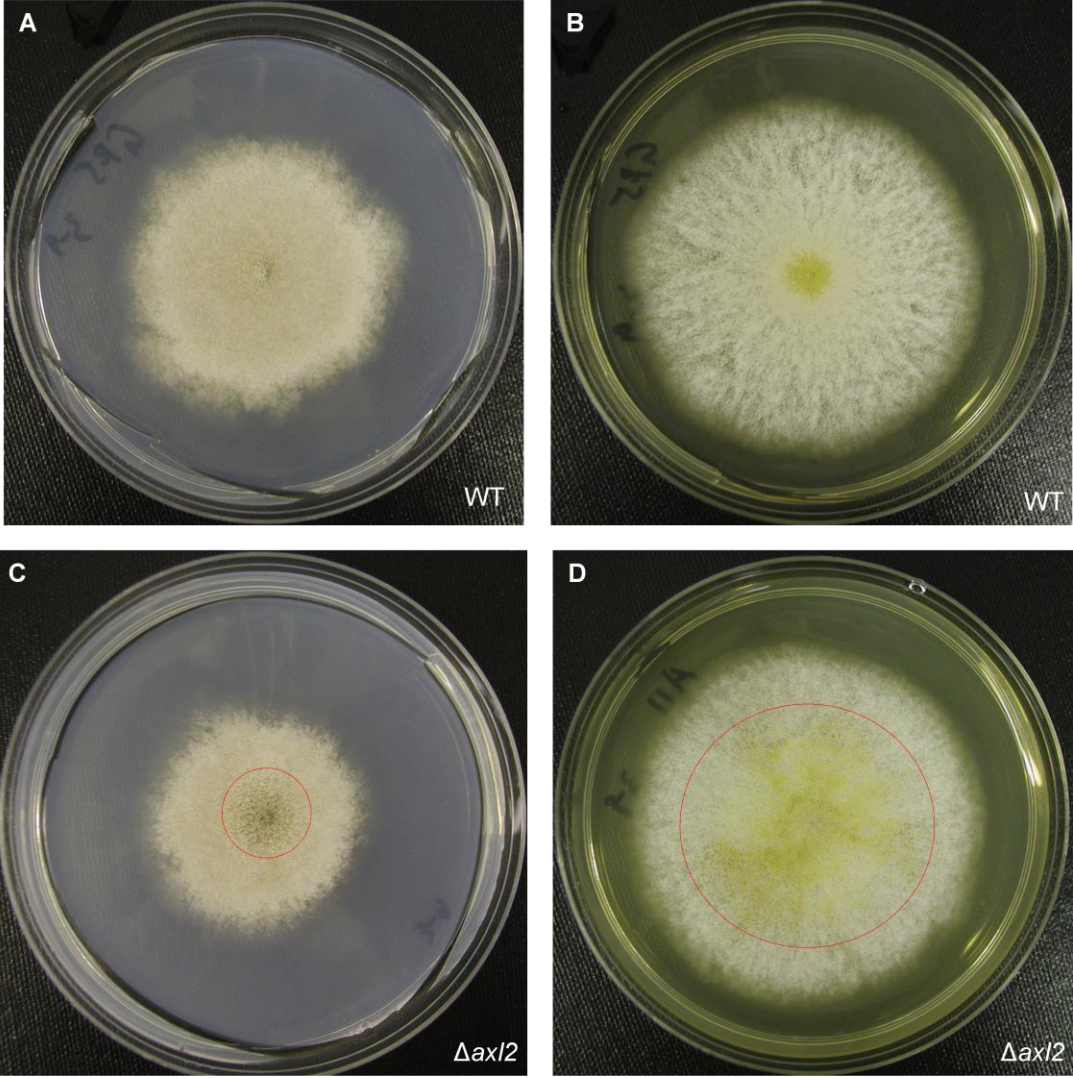


Figure 3-3. Effects of the $\Delta Anax12$ deletion on colony morphology. A and B. Colony morphologies of strain TNO2A3 grown on MNUU (A) minimal media and MAGUU (B) rich media for 7 days. C and D. Colony morphologies of strain AHS6 ($\Delta Anax12$) grown on MNUU (C) and MAGUU (D) for 7 days. Notice the black dots (cleistothecia) on C and yellow patches (hülle cells) on D in the red circles.

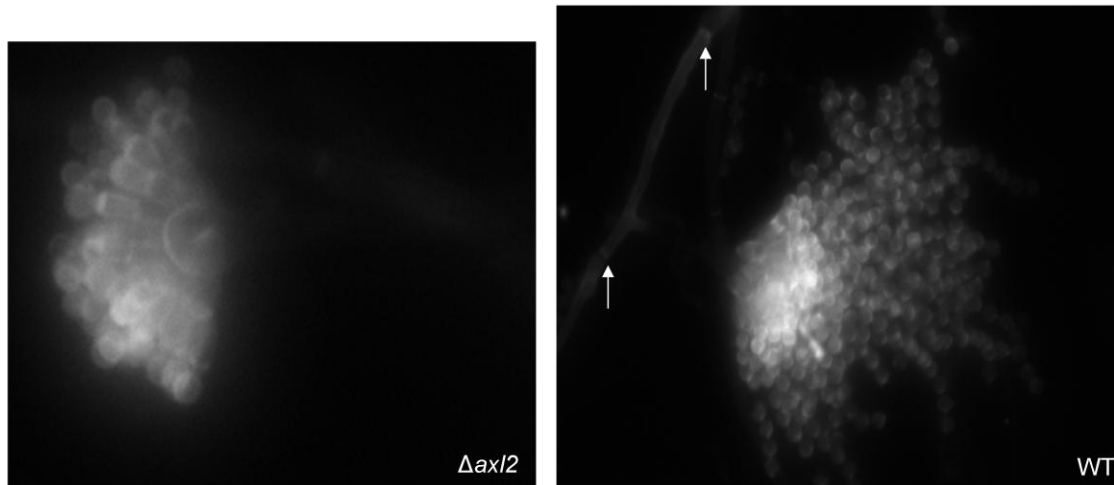
Figure 3-4

Figure 3-4. Effect of $\Delta Anaxl2$ on conidiophore morphology. Both $\Delta Anaxl2$ and TNO2A3 (wildtype) were stained with calcofluor and photos were taken at 60X and 40X respectively. Arrows indicate septa of foot cells on wild type. Notice only one layer of spores from conidiophore of $\Delta Anaxl2$.

Fig 3-5

GFP fusion

A



B

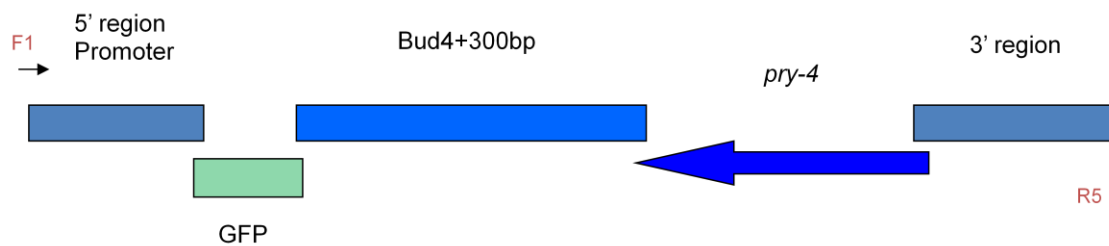


Figure 3-5. Drawing for AnAx12::GFP C-terminal fusion (A) and GFP::AnBud4 N-terminal fusion (B).

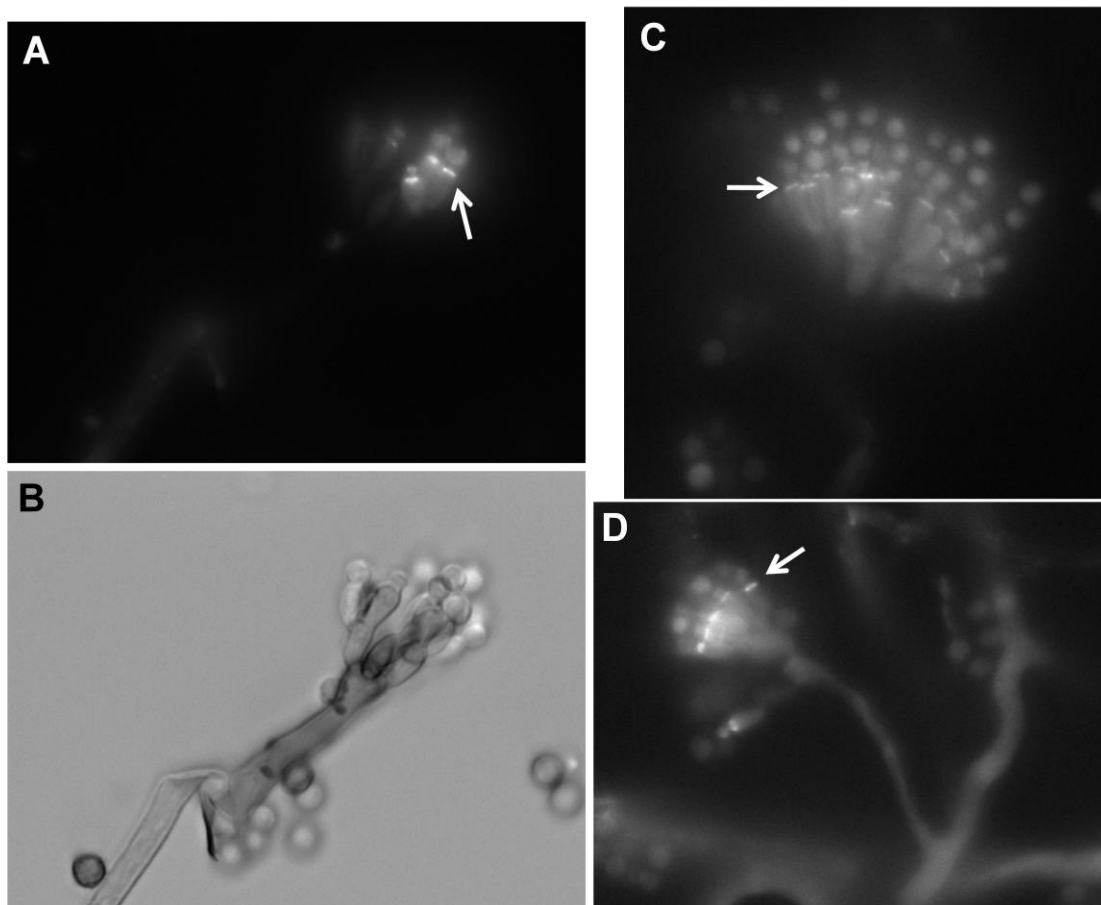
Fig 3-6

Figure 3-6. Localization of AnAxl2-GFP. A, C and D. AnAxl2-GFP rings (white arrows) following growth of strain AHS65 on YGVUU (top with cellophane) for 27 hours at 28 °C. B. DIC photo corresponding to A.

Fig 3-7

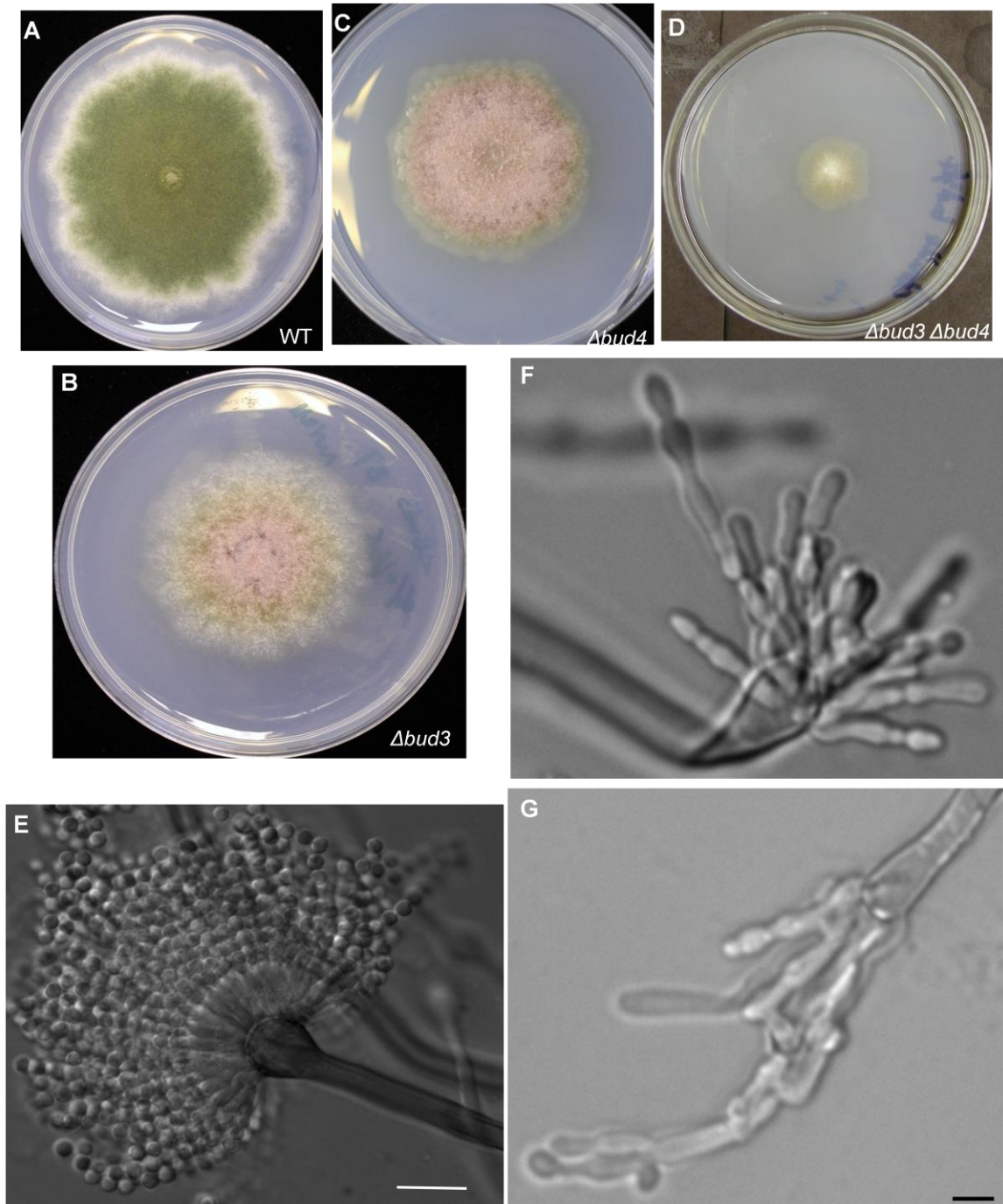


Figure 3-7. Effects of the $\Delta Anbud4$ deletion on colony morphology and conidiation. A-C. Colony morphologies of strains TNO2A3 (wild type; A), AHS3 ($\Delta Anbud3$; B), and AHS4 ($\Delta Anbud4$; C) grown on minimal medium (MNUU) for 9 days. D. $\Delta Anbud3::pyrG^{A.f.} \Delta Anbud4::pyroA^{A.f.}$ double mutants (AHS24) exhibit a synthetic slow growth phenotype. E. Wildtype conidiophore. F and G. $\Delta Anbud4$ conidiophores. Fused metulae and phialides (F), as well as an abnormal secondary conidiophore (G) were observed. Bar=10 μ m.

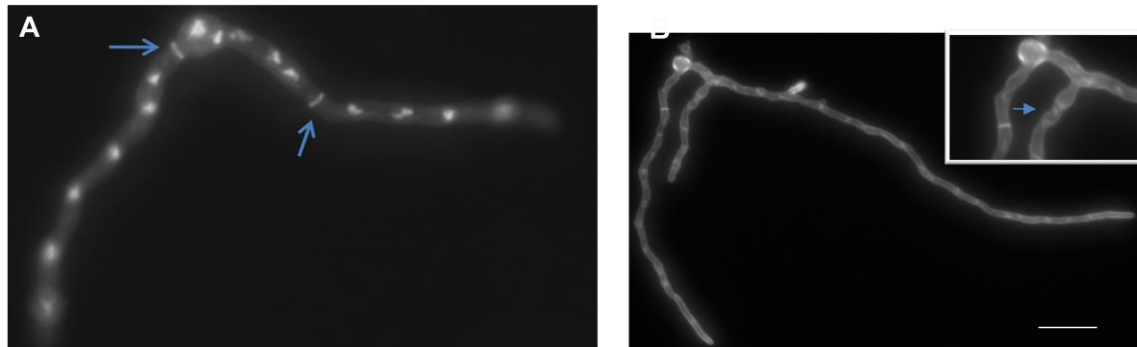
Fig 3-8

Figure 3-8. AnBud4 is involved in septum formation. A. Wildtype. B. $\Delta Anbud4$. Both hyphae were grown in YGVUU for 12 hours. Note the absence of septa in the $\Delta Anbud4$ mutants. Anbud4 hyphae grown on YGVUU for 16 hours, at which time septa are now present. A close-up of a septation site is shown in the inset. Septa and nuclei were visualized in fixed hyphae using Calcofulor and Hoechst 33258, respectively. Arrows indicate septa.

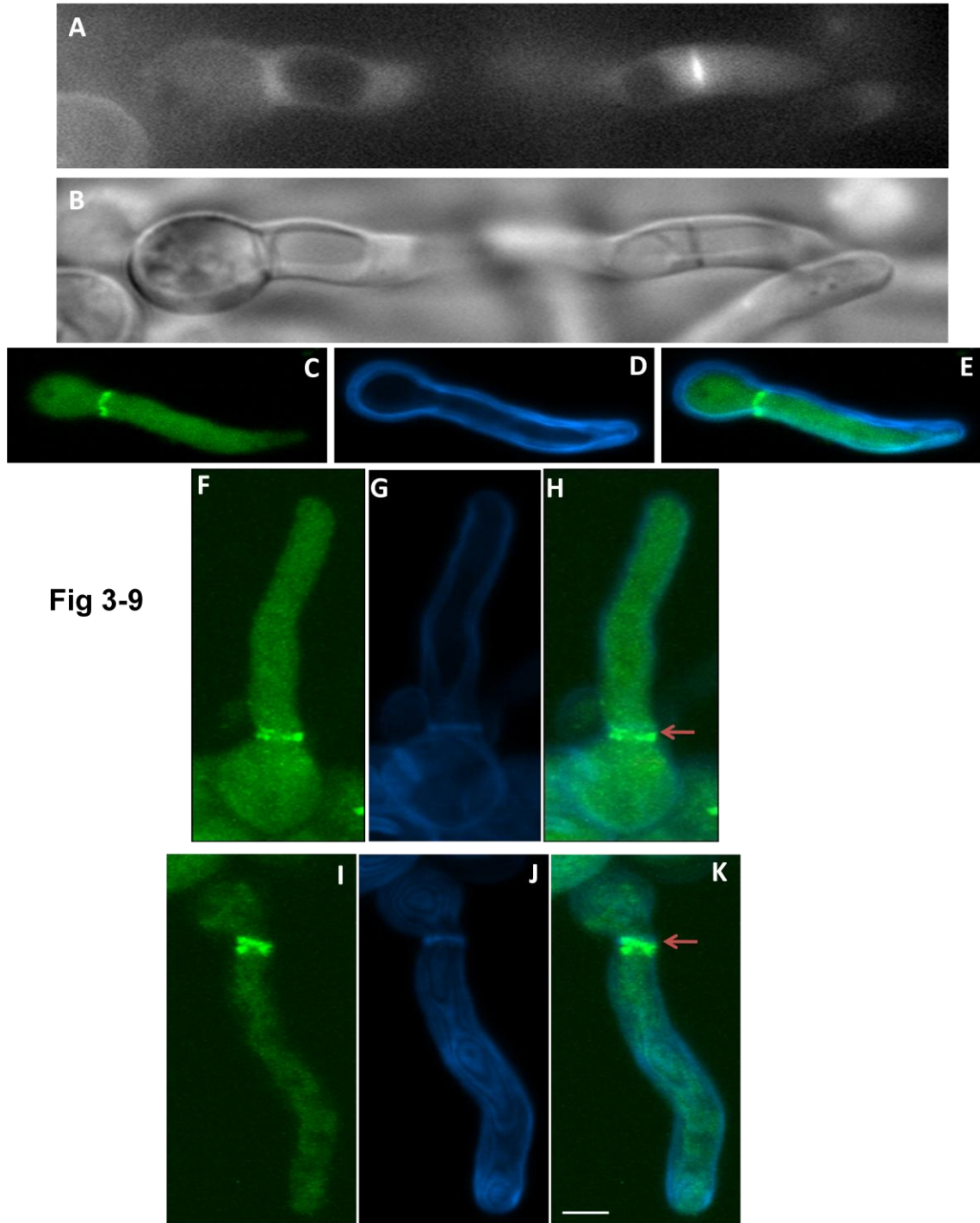


Fig 3-9

Figure 3-9. Localization of GFP-AnBud4 in hyphae. Constricting GFP-AnBud4 ring (A) and corresponding septum (B) following growth of strain AHS42 on YGV for 15 hours at 28 °C. C-K. Coordination of GFP-AnBud4 ring dynamics with septum deposition. C, F, and I. GFP-AnBud4 localization. D, G, and J. Calcofluor staining to visualize septa and cell walls. E, H, and K. Merged images. C-E. GFP-AnBud4 localization at septation site prior to appearance of the visible septum. F-H. Double GFP-AnBud4 rings. Co-localization of associated septum with the apical ring. I-K. Double GFP-AnBud4 rings. Co-localization of associated septum with the basal ring. Red arrows indicate the co-localization of septum and rings. Bars=3 μ m.

Fig 3-10

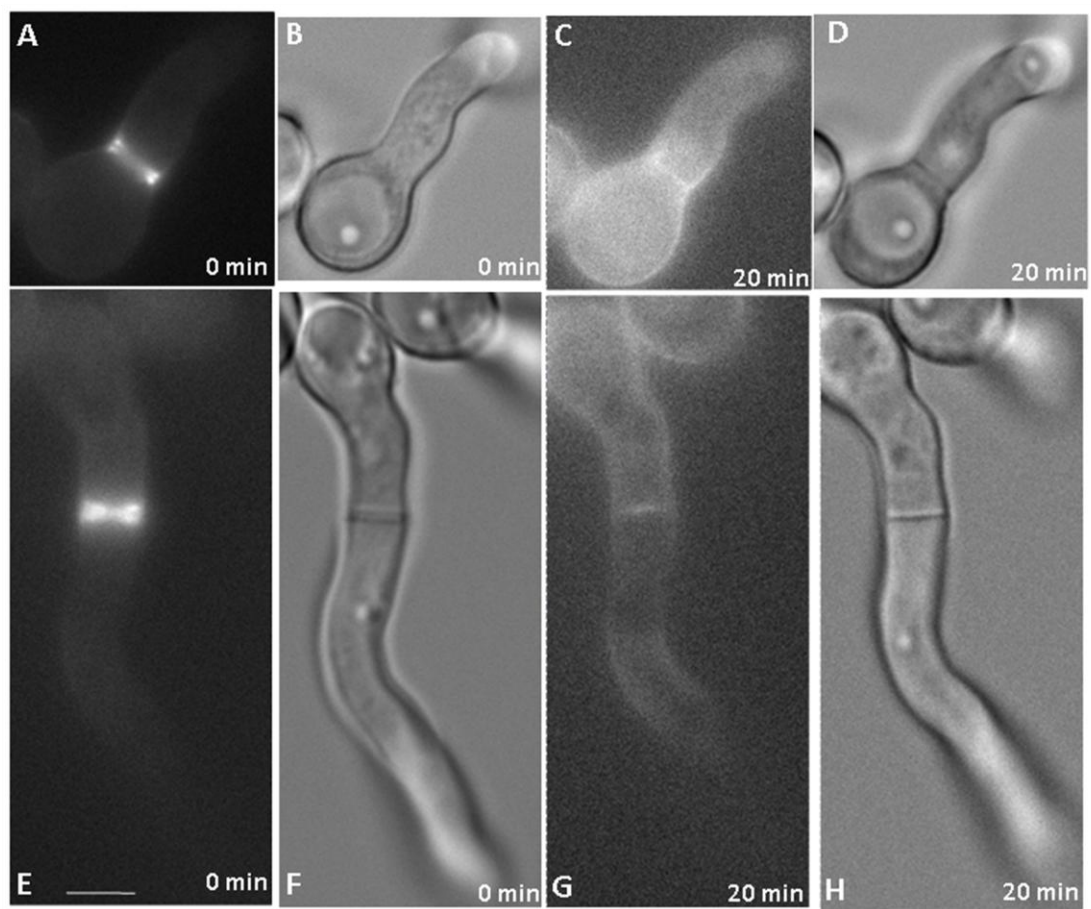


Figure 3-10. GFP-AnBud4 ring dynamics. Double GFP-AnBud4 rings were identified and images captured at times zero (A,B,E,F) and 20 mins. (C,D,G,H). A-D. The double GFP-AnBud4 rings were not associated with a septum. Following 20 min, one of the rings had disappeared and a septum was now visible (black arrows). E-H. The double GFP-AnBud4 rings were associated with a septum. Following 20 min, one of the rings had disappeared and a septum was now visible (black arrow). Bar=3 μ m.

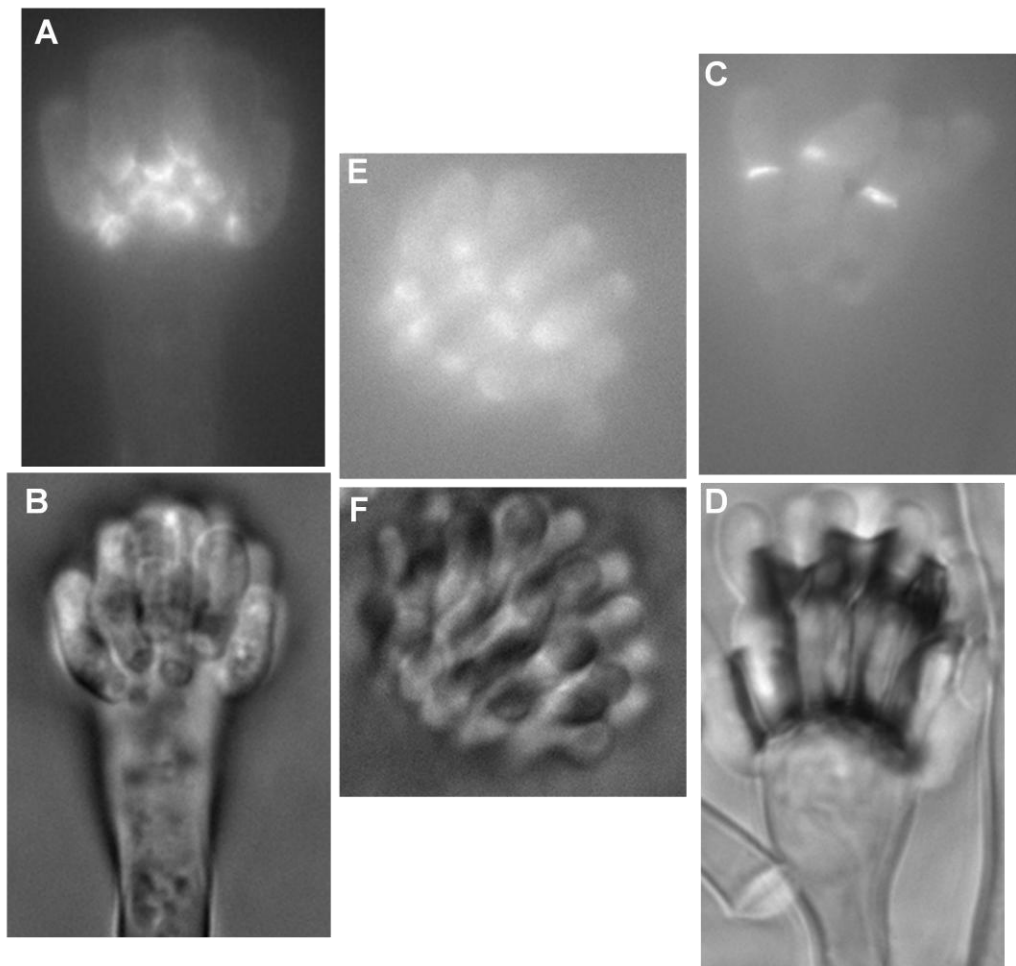
Fig 3-11

Figure 3-11. Localization of GFP-AnBud4 during asexual development. GFP-AnBud4 rings localized between vesicle and nascent metulae (A.), then between metulae and nascent phialides (C.) finally, the rings appeared between phialides and nascent spores (E.). B.D.F. DIC images correspond to A, C, E respectively.

Fig 3-12

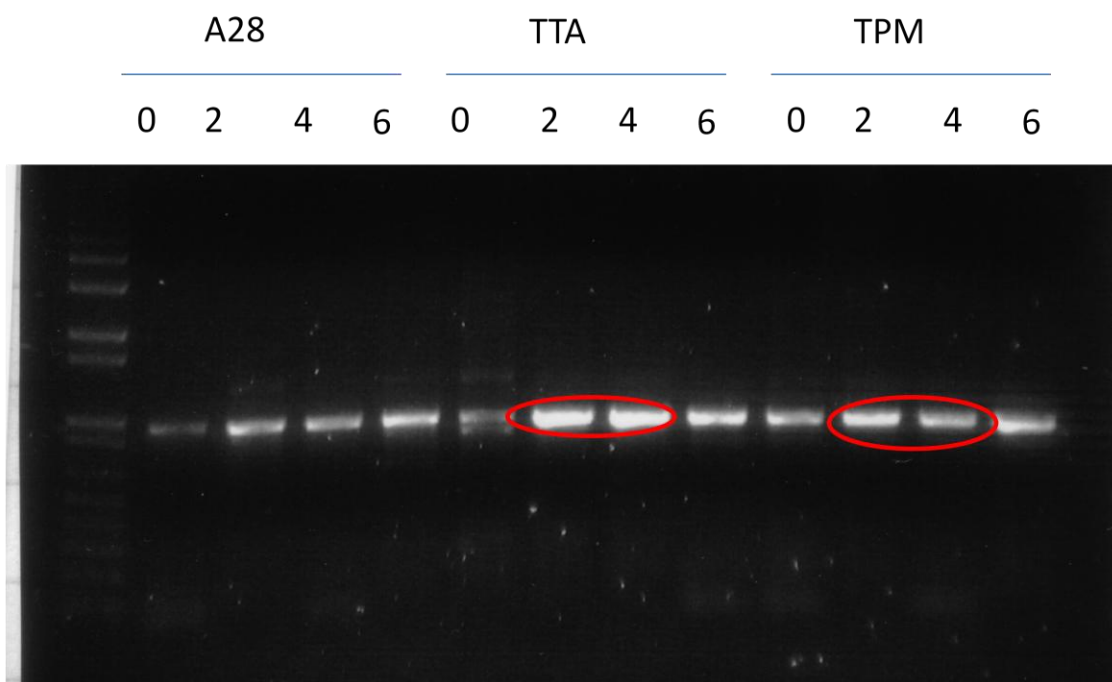


Figure 3-12. RT-PCR of *AnAx12* expression During *BrlA* (TTA1) and *AbaA* (TPM1) induction compared with A28 (Wildtype). The red cycles indicates the high level of *AnAx12* expression at 2 and 4 hours in both TTA1 and TPM1 compared with wildtype.

Fig 3-13

Promoter Swap

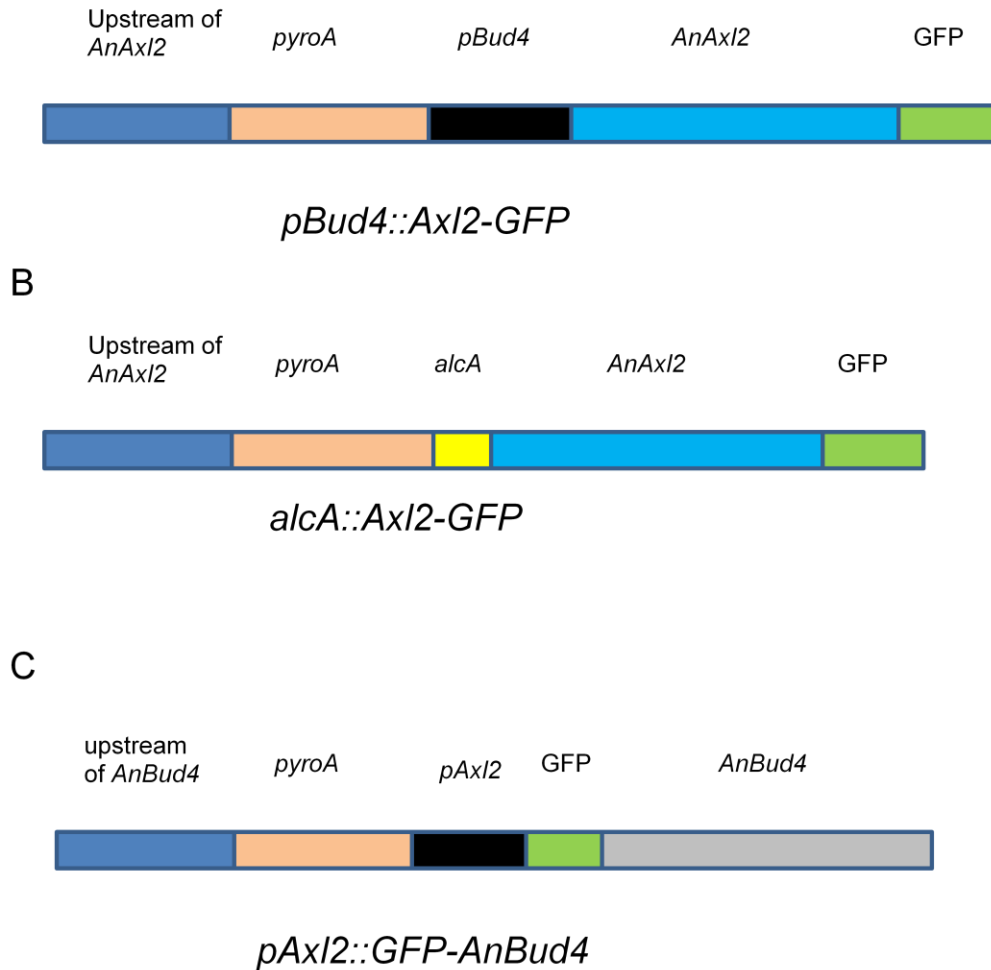


Figure 3-13. Constructs for *AnAx12* and *AnBud4* promoter swap and *AnAx12* under *alcA* promoter

Fig 3-14

Expression of Axl2 in hyphae

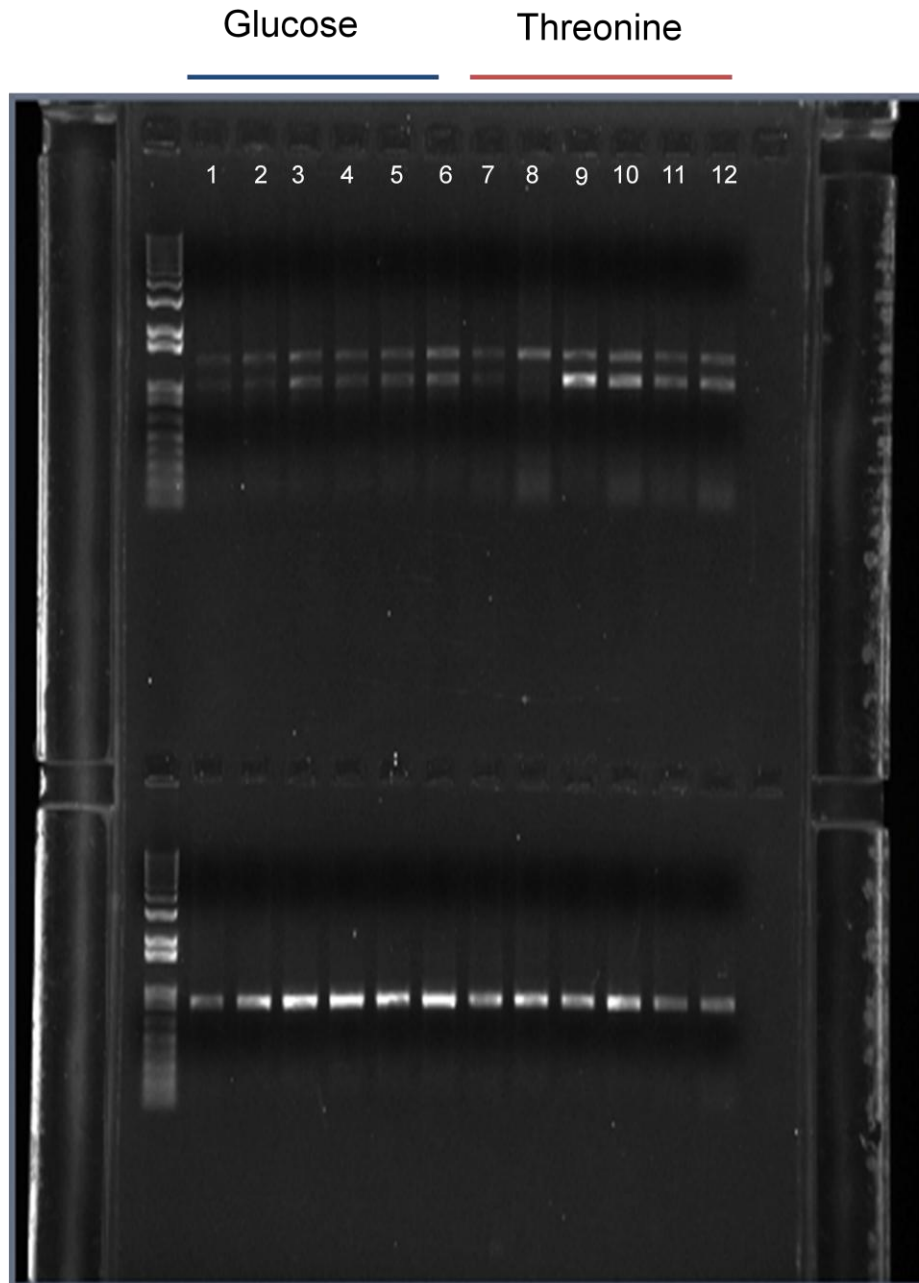


Figure 3-14. *AnAxl2* expression under different promoters during hyphal growth.

Upper gel indicates RT-PCR of *AnAxl2* expression in glucose (lane 1-6) and in threonine (lan7-12). The lower gel is RT-PCR of tubulin C (tubC) expression as input control.

AnAxl2 has a high level expression under *alcA* promoter (lane 9, 10) and under *pBud4* promoter (lane 11, 12) compared to wild type (lane 7, 8).

Fig 3-15

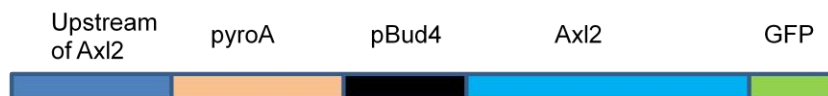
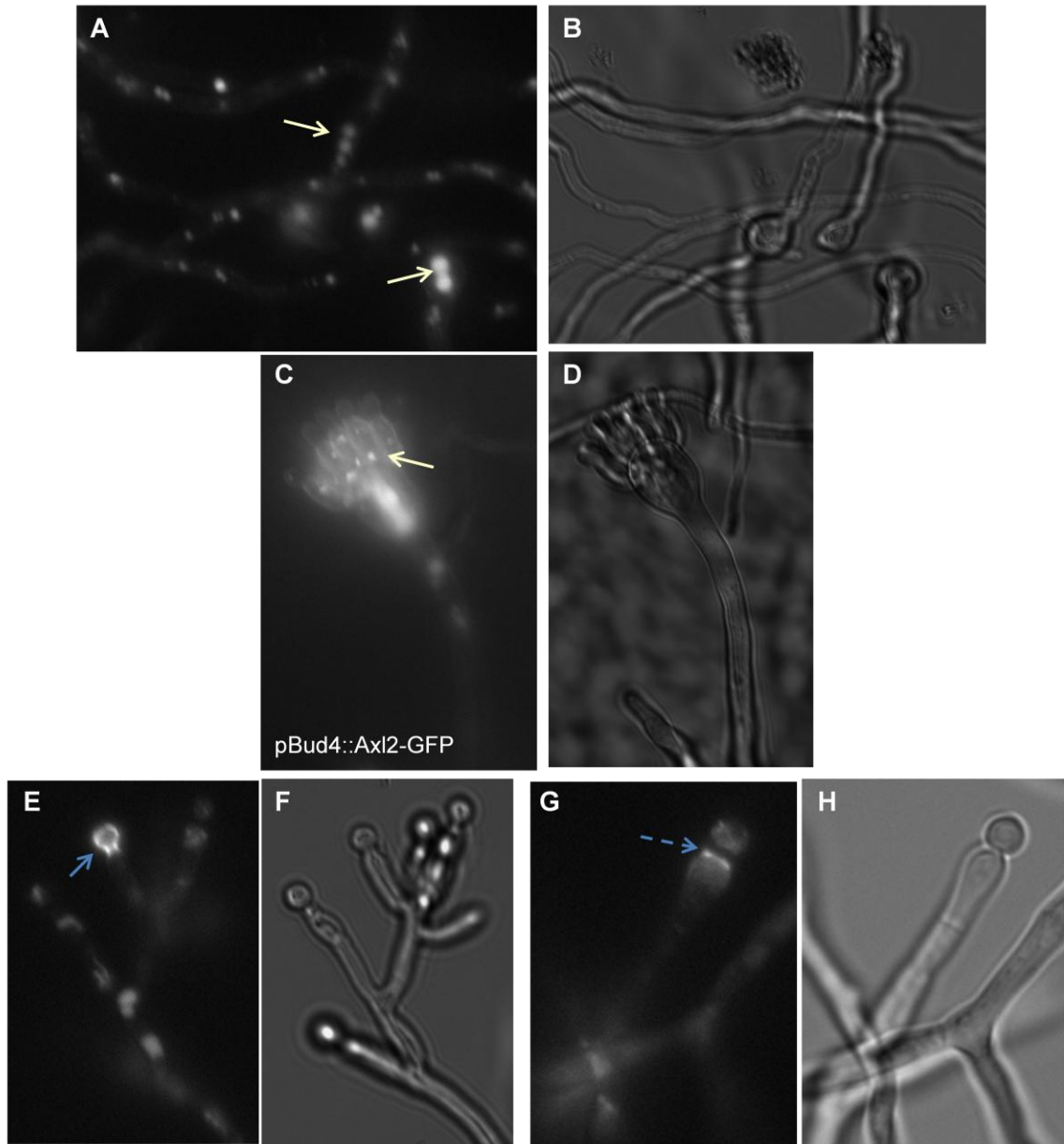


Figure 3-15. Localization of AnAxl2-GFP under *pAnbud4* promoter control. A and C. localized into vacuoles in hyphae(A, white arrows) and conidiophores (C, white arrows). B and D. DIC images corresponding to A and C respectively. E and G. localization of AnAxl2-GFP in reduced conidiophores grown in MN-Thr for 4 days. Dashed arrow (G) indicates a rare example of an intact AnAxl2-GFP ring, whereas solid arrows mark the more prevalent examples of uniform distribution on spore surface and cortical patches at neck (E). F and H. DIC images corresponding to E and G respectively.

Fig 3-16

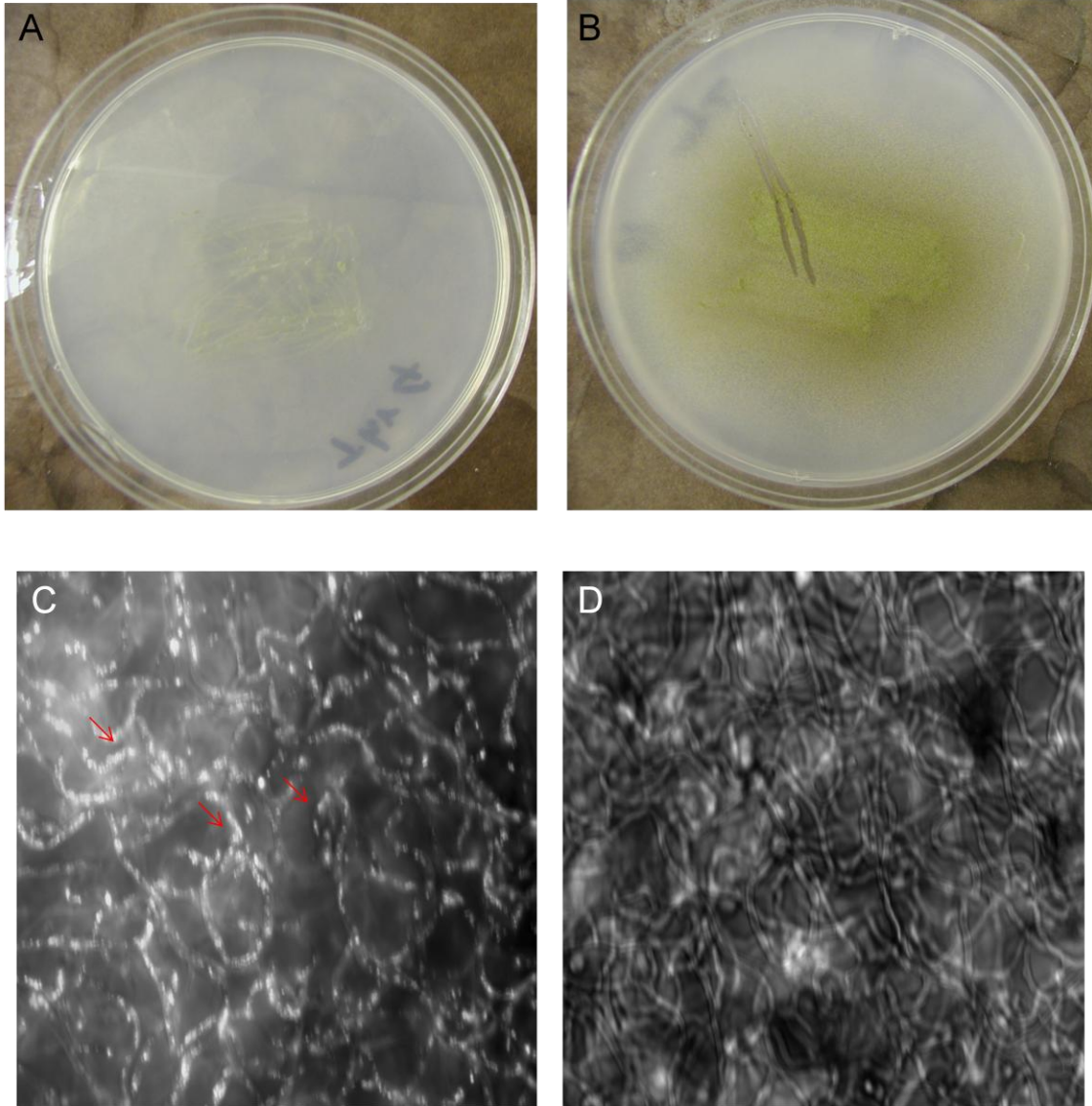
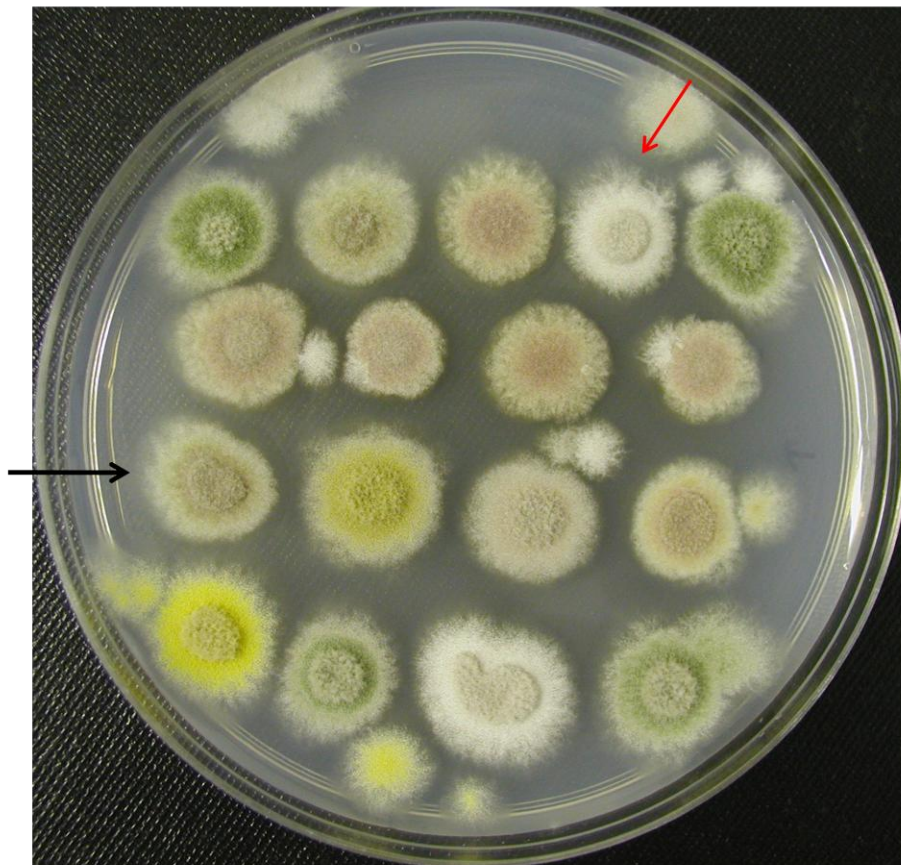


Figure 3-16. Effects of hyper-expression of AnAxl2 on colony morphology. A. *alcA::Axl2* grown on MN-Thr for 9 days compared with wildtype (B). Notice the low density of conidiation on (A). Hyper induced AnAxl2 formed bright localization (dots) in hyphae (C, red arrows) after growth in MN-Thr for 15 hours. D. DIC image corresponding to C.

Fig 3-17



$\Delta aspE$	$\Delta aspD$	$\Delta aspC$	$\Delta axl2$	TN
$\Delta axl2 \Delta aspC$	Strain1	Strain2	Strain3	Strain4
$\Delta axl2 \Delta aspD$	Strain1	Strain2	Strain3	Strain4
$\Delta axl2 \Delta aspE$	Strain1	Strain2	Strain3	Strain4

Figure 3-17. Colony morphology of septin mutants, $\Delta Anax12$ deletion mutants and their crossed double mutants. The arrange of patched colonies is in the table below. Colonies were grown on minimal media for 3 days. $\Delta AnAx12 AspD$ double mutants (the row indicated by the black arrow) has a similar phenotype to $\Delta AnAx12$ (the red arrow).

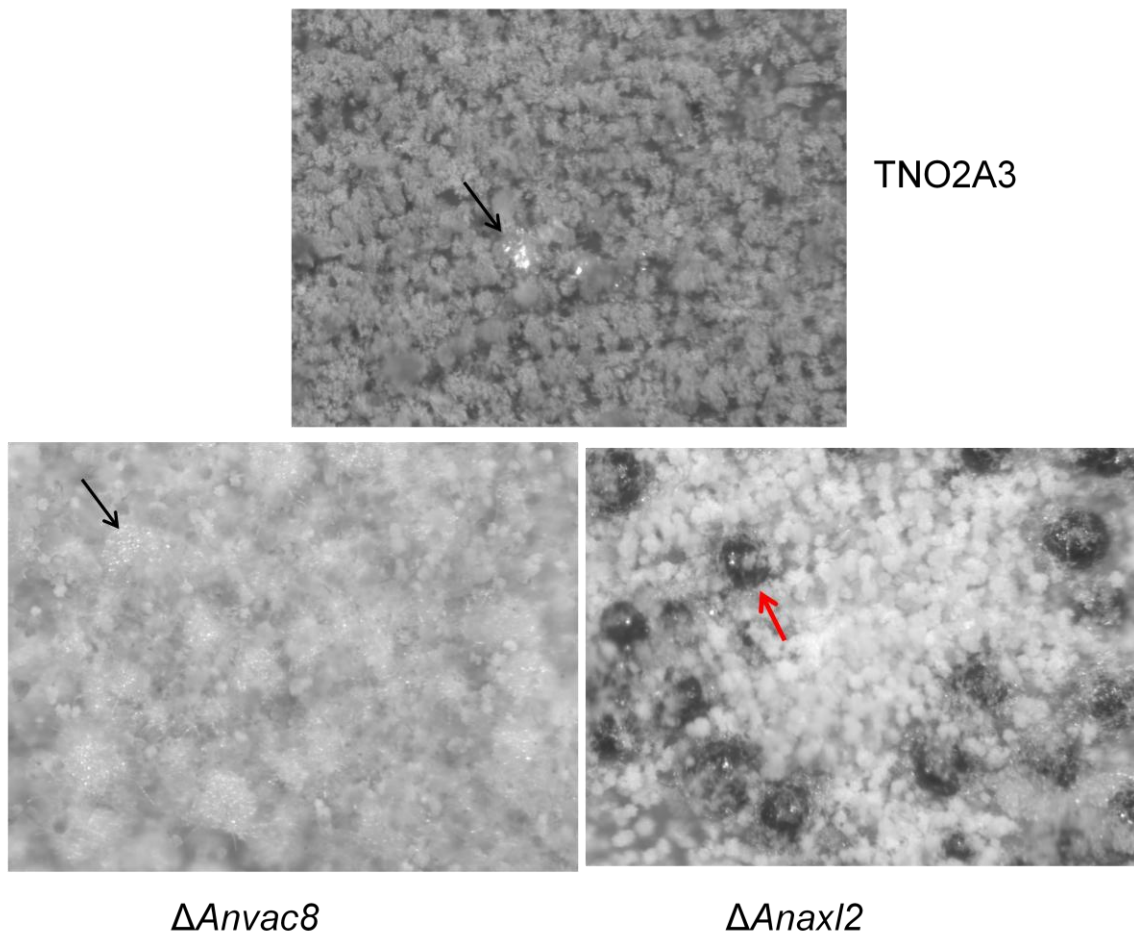
Fig 3-18

Figure 3-18. Sexual spore production of WT, $\Delta Anvac8$ and $\Delta AnAxl2$ grown on minimal media for 9 days in dark. Black arrows indicate hülle cells prevalent on $\Delta Anvac8$ and sporadic on WT. The red arrow indicates a mature cleistothecium (fruiting body) on $\Delta AnAxl2$.

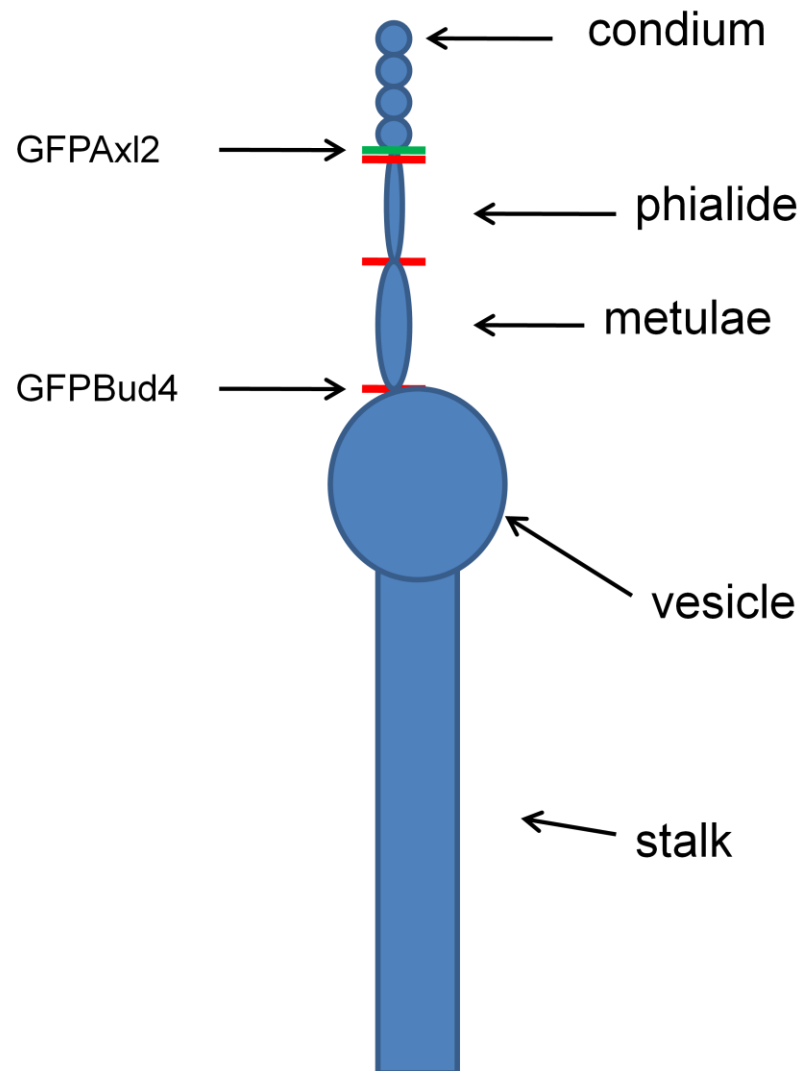
Fig 3-19

Figure 3-19. Schematic illustration of AnAxl2-GFP and GFP-AnBud4 localization. Red arrows indicate GFP-AnBud4 and the green arrow indicates AnAxl2-GFP.

Table 3-1

Strain	Genotype	Source or reference
A28	<i>pabaA6 biA1</i>	FGSC (accession no. A28)
GR5	<i>pyrG89 wA3 pyroA4</i>	FGSC (accession no. A773)
TNO2A3	<i>pyrG89; argB2; pyroA4 nkuA::argB</i>	
AHS4	<i>pyrG89; argB2; Δbud4::pyroA; pyroA4; nkuA::argB</i>	This study
AHS41	<i>pyrG89; argB2; gfp::bud4::pyr4; pyroA4; nkuA::argB</i>	This study
AHS6	<i>pyrG89; Δaxl2::pyroA; pyroA4; wA3</i>	This study
AHS65	<i>pyrG89; argB2; Axl2::GFP; pyroA4; nkuA::argB</i>	This study
AHS61	<i>pyrG89; argB2; pyroA4; Axl2::GFP::pyr4; nkuA::argB</i>	This study
AHS651	<i>pyrG89; argB2; pBud4::Axl2::GFP; pyroA4; nkuA::argB</i>	This study
AHS652	<i>pyrG89; argB2; pryOA; alcA(p)::Axl2::GFP; pyroA4; nkuA::argB</i>	This study
AHS252	<i>yA2; argB2; pyroA4</i>	This study
AAV123.1	<i>pyrG89 sepA::gfp::pyr-4; argB2; pyroA4 ΔnkuA::argB</i>	Virag et al, 2007
ACP115	<i>tpmA::GFP::pyr-4; pyrG89; wA3</i>	Pearson et al, 2004
AHS52	<i>pyrG89; argB2; gfp::Bud4::pyr4; pyroA4; sepA1 nkuA::argB</i>	This study
AHS53	<i>sepA1; tpmA::GFP::pyr4; pyrG89</i>	This study
AHS7	<i>pyrG89; argB2; Δmsb2::pyroA; pyroA4; nkuA::argB</i>	This study
AHS8	<i>pyrG89; argB2; Δrgal1::pyroA; pyroA4; nkuA::argB</i>	This study
AHS81	<i>pyrG89; argB2; Rgal1::GFP::pyr4; pyroA4; nkuA::argB</i>	This study

Table 3-4

septa	13h					16h				
	0	1	2	3	>4	0	1	2	3	>4
TN02A3	103	92	5	0	0	21	69	60	24	26
	100	96	4	0	0	24	72	57	24	25
	106	91	3	0	0	24	82	59	14	22
average	103	93	4	0	0	23	74	59	21	24
Δ Bud3	200	0	0	0	0	200	0	0	0	0
	200	0	0	0	0	200	0	0	0	0
	200	0	0	0	0	200	0	0	0	0
average	200	0	0	0	0	200	0	0	0	0
Δ Rho4	200	0	0	0	0	190	10	0	0	0
	200	0	0	0	0	192	8	0	0	0
	199	1	0	0	0	188	12	0	0	0
average	200	<1	0	0	0	190	10	0	0	0
Δ Bud4	185	15	0	0	0	81	69	38	11	1
	188	11	1	0	0	98	58	33	10	1
	188	12	0	0	0	98	69	24	8	1
average	187	13	<1	0	0	92	65	32	10	1

All strains are grown in YGVUU media. At each time course, septa have been counted in 200 hyphae with similar length. All hyphae counted grew directly from spore, no branches were counted.

References

- Asnaghi, L., W. C. Vass, et al. (2010). "E-cadherin negatively regulates neoplastic growth in non-small cell lung cancer: role of Rho GTPases." Oncogene.
- Burford, H., Z. Baloch, et al. (2009). "E-cadherin/beta-catenin and CD10: a limited immunohistochemical panel to distinguish pancreatic endocrine neoplasm from solid pseudopapillary neoplasm of the pancreas on endoscopic ultrasound-guided fine-needle aspirates of the pancreas." Am J Clin Pathol **132**(6): 831-839.
- Casselton, L. and M. Zolan (2002). "The art and design of genetic screens: filamentous fungi." Nat Rev Genet **3**(9): 683-697.
- Chen, C., Y. S. Ha, et al. (2006). "Cdc42 is required for proper growth and development in the fungal pathogen *Colletotrichum trifolii*." Eukaryot Cell **5**(1): 155-166.
- Cho, R. J., M. J. Campbell, et al. (1998). "A genome-wide transcriptional analysis of the mitotic cell cycle." Mol Cell **2**(1): 65-73.
- Cid, V. J., L. Adamikova, et al. (2001). "Cell cycle control of septin ring dynamics in the budding yeast." Microbiology **147**(Pt 6): 1437-1450.
- Efimov, V. P. (2003). "Roles of NUDE and NUDF proteins of *Aspergillus nidulans*: insights from intracellular localization and overexpression effects." Mol Biol Cell **14**(3): 871-888.
- Fares, H., L. Goetsch, et al. (1996). "Identification of a developmentally regulated septin and involvement of the septins in spore formation in *Saccharomyces cerevisiae*." J Cell Biol **132**(3): 399-411.
- Gao, X. D., L. M. Sperber, et al. (2007). "Sequential and distinct roles of the cadherin domain-containing protein Axl2p in cell polarization in yeast cell cycle." Mol Biol Cell **18**(7): 2542-2560.
- Garrod, D. and T. E. Kimura (2008). "Hyper-adhesion: a new concept in cell-cell adhesion." Biochem Soc Trans **36**(Pt 2): 195-201.
- Gladfelter, A. S., I. Bose, et al. (2002). "Septin ring assembly involves cycles of GTP loading and hydrolysis by Cdc42p." J Cell Biol **156**(2): 315-326.
- Gladfelter, A. S., L. Kozubowski, et al. (2005). "Interplay between septin organization, cell cycle and cell shape in yeast." J Cell Sci **118**(Pt 8): 1617-1628.
- Hage, B., K. Meinel, et al. (2009). "Rac1 activation inhibits E-cadherin-mediated adherens junctions via binding to IQGAP1 in pancreatic carcinoma cells." Cell Commun Signal **7**: 23.

- Halme, A., M. Michelitch, et al. (1996). "Bud10p directs axial cell polarization in budding yeast and resembles a transmembrane receptor." Curr Biol **6**(5): 570-579.
- Kikuma, T., M. Ohneda, et al. (2006). "Functional analysis of the ATG8 homologue Aogat8 and role of autophagy in differentiation and germination in *Aspergillus oryzae*." Eukaryot Cell **5**(8): 1328-1336.
- Kim, H., K. Han, et al. (2002). "The *veA* gene activates sexual development in *Aspergillus nidulans*." Fungal Genet Biol **37**(1): 72-80.
- Lindsey, R. and M. Momany (2006). "Septin localization across kingdoms: three themes with variations." Curr Opin Microbiol **9**(6): 559-565.
- Longtine, M. S., D. J. DeMarini, et al. (1996). "The septins: roles in cytokinesis and other processes." Curr Opin Cell Biol **8**(1): 106-119.
- Lord, M., M. C. Yang, et al. (2000). "Cell cycle programs of gene expression control morphogenetic protein localization." J Cell Biol **151**(7): 1501-1512.
- Marston, A. L., T. Chen, et al. (2001). "A localized GTPase exchange factor, Bud5, determines the orientation of division axes in yeast." Curr Biol **11**(10): 803-807.
- McCrea, P. D. and D. Gu (2010). "The catenin family at a glance." J Cell Sci **123**(Pt 5): 637-642.
- Momany, M., J. Zhao, et al. (2001). "Characterization of the *Aspergillus nidulans* septin (*asp*) gene family." Genetics **157**(3): 969-977.
- Mooney, J. L. and L. N. Yager (1990). "Light is required for conidiation in *Aspergillus nidulans*." Genes Dev **4**(9): 1473-1482.
- Nelson, W. J. and R. Nusse (2004). "Convergence of Wnt, beta-catenin, and cadherin pathways." Science **303**(5663): 1483-1487.
- Peyrieras, N., D. Louvard, et al. (1985). "Characterization of antigens recognized by monoclonal and polyclonal antibodies directed against uvomorulin." Proc Natl Acad Sci U S A **82**(23): 8067-8071.
- Roemer, T., K. Madden, et al. (1996). "Selection of axial growth sites in yeast requires Axl2p, a novel plasma membrane glycoprotein." Genes Dev **10**(7): 777-793.
- Sanders, S. L. and I. Herskowitz (1996). "The BUD4 protein of yeast, required for axial budding, is localized to the mother/BUD neck in a cell cycle-dependent manner." J Cell Biol **134**(2): 413-427.

- Sewall, T. C., C. W. Mims, et al. (1990). "abaA controls phialide differentiation in *Aspergillus nidulans*." Plant Cell **2**(8): 731-739.
- Scott, S. V., D. C. Nice, 3rd, et al. (2000). "Apg13p and Vac8p are part of a complex of phosphoproteins that are required for cytoplasm to vacuole targeting." J Biol Chem **275**(33): 25840-25849.
- Sheu, Y. J., B. Santos, et al. (1998). "Spa2p interacts with cell polarity proteins and signaling components involved in yeast cell morphogenesis." Mol Cell Biol **18**(7): 4053-4069.
- Spellman, P. T., G. Sherlock, et al. (1998). "Comprehensive identification of cell cycle-regulated genes of the yeast *Saccharomyces cerevisiae* by microarray hybridization." Mol Biol Cell **9**(12): 3273-3297.
- Timberlake, W. E. (1990). "Molecular genetics of *Aspergillus* development." Annu Rev Genet **24**: 5-36.
- van Drogen, F. and M. Peter (2002). "Spa2p functions as a scaffold-like protein to recruit the Mpk1p MAP kinase module to sites of polarized growth." Curr Biol **12**(19): 1698-1703.
- Virag, A., M. P. Lee, et al. (2007). "Regulation of hyphal morphogenesis by cdc42 and rac1 homologues in *Aspergillus nidulans*." Mol Microbiol **66**(6): 1579-1596.
- Weis, W. I. and W. J. Nelson (2006). "Re-solving the cadherin-catenin-actin conundrum." J Biol Chem **281**(47): 35593-35597.

Chapter IV Functional characterization of Cdc42 regulators in *Aspergillus nidulans*

The Cdc42 GTPase plays a central role in signal transduction pathways that controls multiple aspects of cellular behavior, including global changes to the cell wall integrity, cell polarity, and stress response. Upstream transmembrane landmark proteins guide the subsequent signal to Cdc42 to organize and establishment a polarity axis. The Locally activated Cdc42 then promotes recruitment of the morphogenetic machinery localization during cell surface expansion and cell wall deposition. For its important roles in multiple signaling pathways, Cdc42 activity is precisely regulated by Cdc24 (GEF, Guanine exchange factors) and GAPs (GTPase activating proteins) including Bem3, Rga1 and Rga2. In addition, MSb2 was first found as multicopy suppressor of Cdc24 in yeast. In this chapter, some pilot experiments have been performed to examine functions of the Cdc42 regulators AnMsb2 and AnRga1 in hyphal and conidiophore morphogenesis.

Introduction

Cdc42 GTPase signaling and the GTPase activating protein Rga1

CDC42 is a small GTPase of the Rho-subfamily, which regulates signaling pathways that control diverse cellular functions including cell morphology, migration, endocytosis and cell cycle progression in many fungi such as *Saccharomyces cerevisiae*, *Ashbya gossypii*, *Penicillium marneffei* and *Aspergillus nidulans* (Johnson 1999; Wendland and Philippsen 2001; Momany 2002; Virag, Lee et al. 2007). In yeast *S. cerevisiae*, Cdc42 and its related proteins act as molecular switches and regulate many

cellular processes by mediating the transfer of positional information to the morphogenetic machinery. The active form of yeast Cdc42p (GTP-Cdc42p) and inactive form (GDP-Cdc42p) have to reach a dynamic balance regulated by its GEF(s) and GAP(s) respectively. In its active GTP-bound form, Cdc42p functions via multiple effectors to recruit components of the morphogenetic machinery. In *S. cerevisiae*, Cdc42p localizes to sites of growth, including the bud tip, bud, and mother-bud neck. In *A. nidulans*, the *cdc42* homologue has first been reported as *ModA* (Harris and Momany 2004). To establish polarity, Cdc42p needs to be recruited to the cell cortex and activated (Chant 1999; Virag, et al. 2007). In filamentous fungi, Cdc42 is required for the establishment of hyphal polarity in *Ashbya gossypii* and *Candida albicans*, however, it is only required for the maintenance of hyphal polarity in *A. nidulans* and *Penicillium marneffeii* (Boyce, Hynes et al. 2001; Virag, Lee et al. 2007). Moreover, proper regulation of Cdc42 activity is required to form a stable axis of hyphal polarity since a hyperactive form of Cdc42 (*Cdc42^{G14V}*) and overexpression of Cdc42 resulted in reduced hyphal growth, swollen hyphal tips and conidiophore defects (Virag 2007).

Rga1 functions as a GAP of Cdc42

In *S. cerevisiae*, there are one GEF (Cdc24) and three GAPs of Cdc42p including Rga1p, Bem3p, and Rga2p (Smith, Givan et al. 2002). Each GAP appears to regulate a specific function of Cdc42p. Bem3p plays a role in septin organization at the mother-bud neck for cytokinesis, whereas Rga1p and Rga2p, which have high sequence similarity, mediate interactions between Ste20p (p21-activated kinase, PAK) and Cdc42p for haploid invasive growth (Smith *et al.* 2002). Rag1p (Rho GTPase activating protein) has

two LIM domains at N-terminus and the GAP domain at C-terminus (Stevenson, Ferguson et al. 1995). Mutation of Lys-872 in the GAP domain of Rga1p can drastically decrease the direct interaction between Rga1p and Cdc42, and decrease its GTPase activating protein function (Gladfelter, Bose et al. 2002). Moreover, deletion of Rga1 will decrease the interaction between Cdc42 and Ste20 (PAK of the MAP3K Ste11). Gladfelter's lab also proved that Rga1p^{K872A} was unable to suppress the septin-specific cdc42 alleles as loss of GAP activity and the lack of suppressor function of Rga1p^{K872A} might simply reflect its inability to interact normally with Cdc42p. Moreover, non-axial budding patterns have been found for $\Delta Rga1$ but not for $\Delta Bem3$ and $\Delta Rga2$, which indicates Rga1 has a distinct function in bud site selection that is not shared by Rga2 and Bem3 (Smith, Givan et al. 2002).

Effectors of Cdc42p for MAP kinase pathway

Cdc42 is the general component which functions upstream of MAP kinase pathways for cell wall integrity, pheromone response, osmolarity stress, and invasive hyphal growth. Moreover, the MAP kinase pathways are also involved in production of secondary metabolism, oxidative stress and sexual development (Csank, Schroppel et al. 1998; Gustin, Albertyn et al. 1998; Wei, Requena et al. 2003; Cullen, Sabbagh et al. 2004; Bardwell 2006; Tatebayashi, Yamamoto et al. 2006; Valiante, Heinekamp et al. 2008). When Cdc42p is activated, it signals effector proteins including septins, actins and the upstream kinases Ste50 and Ste20 for MAP kinase pathways. Cdc42p interacts with the effector proteins through an eight amino acid CRIB binding motif (Posas, Witten et al. 1998). PAK family members share a CRIB sequence motif (Peterson, Penkert et al. 2004).

In fungi, the PAK kinase family includes yeast homologous of Cla4p and Ste20p. Cla4p is involved in vegetative growth and Ste20p is involved in the mating pathway (Tatebayashi, Yamamoto et al. 2006; Abdullah and Cullen 2009).

Locally recruiting components of the Cdc42 GTPase module by G protein sensing is required for the *S. cerevisiae* mating pheromone response (Park and Bi 2007). The mating landmark, pheromone reception, signals to Cdc42p through Far1p. Far1p recruits Bem1p, Cdc24p and Ste20p (PAK, p21-activated kinase) to Cdc42p and polarizes the actin cytoskeleton (Butty *et al.* 1998; Leeuw *et al.* 1998; Nern *et al.* 1999). Ste50 acts as an adaptor that links the G protein-associated Cdc42p-Ste20p complexes to the effector Ste11p (Posas, Witten et al. 1998; Jansen, Buhring et al. 2001). The interaction between Ste50 and Cdc42 could be detected in both the two-hybrid system and the pull-down assay (Ramezani-Rad 2003). Cdc42 GAPs Rga1 and Rga2 may facilitate the interaction between Ste20 and Cdc42-GTP (the active form), which has been proved by two-hybrid interaction (Smith, Givan et al. 2002). In addition, Rga1 functions negatively between the G protein sensing pathway and the MAP kinase pathway in the pheromone response pathway (Saito, Fujimura-Kamada et al. 2007).

MAPkinase pathway in yeast and filamentous fungi

The MAPK (mitogen-activated protein kinase) signaling pathway is found in almost all eukaryotic organisms including animal, fungi and plants. The MAPK cascade is a set of three sequentially acting protein kinases starting from the top MAP3K (MAPK kinase kinase) which phosphorylates MAP2k or MAPKK (MAPK kinase), which in turn

phosphorylates the terminal protein kinase in the cascade, which is MAP kinase, regulates cellular responses to environmental change.

The yeast *S.cerevisiae* MAP kinase pathways are the most clearly studied model which contains three fully elaborated MAPK cascades (Bardwell 2006). They have established functions in mating-pheromone responses, maintaining cell wall integrity, responding to changes in osmolarity and nutrient sensing. Ste11MEKK is activated by PAK Ste20 and is shared by all three pathways: the Mkk1/2 → Slr2 (Mpk1^{MAPK}), Pbs2 → Hog1 and Ste7 → Fus3/Kss1 cascades (Gustin, Albertyn et al. 1998). Mpk1^{MAPK} regulates the integrity of the yeast cell wall, and Hog1^{MAPK} regulates the response to high osmolarity and various other stresses (Gustin, Albertyn et al. 1998). Fus3^{MAPK} and Kss1^{MAPK} both participate in the mating pheromone response, with Fus3 playing the major role (Farley, Satterberg et al. 1999; Sabbagh, Flatauer et al. 2001). However, Kss1 regulates the filamentous invasive growth programme (Cook, Bardwell et al. 1997) (**Fig 4-1**). The three pathways share key components, for example, Ste7 is activated during mating and invasive growth, and activates both Fus3 and Kss1 during mating, but only Kss1 during invasive growth.

When exposed to hyperosmotic extracellular environments, the budding yeast activates the HOG (high osmolarity glycerol) signaling pathway, which culminates in phosphorylation, activation, and nuclear translocation of the Hog1 MAP kinase (MAPK). As the upstream regulator of the HOG pathway, Cdc42 not only binds and activates the PAK-like kinases Ste20 and Cla4 but also binds to the Ste11–Ste50 complex to bring activated Ste20/Cla4 to their substrate Ste11. In the HOG pathway, the Ste11–Ste50 complex binds to the cytoplasmic domain of Sho1 and then activates the MAPK Pbs2.

Thus, Cdc42, Ste50, and Sho1 act as adaptor proteins that control the flow of the osmostress signal from Ste20/Cla4 to Ste11, then to Pbs2 (Tatebayashi, Yamamoto et al. 2006).

Genome sequencing analyses revealed that *Aspergillus* has orthologous genes to almost all of the mitogen-activated protein kinase (MAPK) pathway genes in *S. cerevisiae* (Ma, Qiao et al. 2008; Hagiwara, Asano et al. 2009). Other than the function in yeast, many reports showed that MAP kinase pathway function with more diversity in filamentous fungi. For example, the pheromone response kinase MpkB is involved in secondary metabolism by regulating Lae1 (Atoui, Bao et al. 2008; Chang, Yu et al. 2009). In *A. nidulans*, the central MAPKK kinase SteC, a homologous to yeast Ste11, has been shown to regulate growth rate, hyphal branching, conidiophore morphology, and $\Delta steC$ deletion mutants can inhibit heterokaryon formation and block cleistothecium development (Wei, Requena et al. 2003). MAP kinase pathways that respond to osmotic stress in *Aspergillus fumigatus* are also involved in nutritional sensing (Pitoniak, Birkaya et al. 2009). MPKA regulates conidial germination in response to the nitrogen source and is activated upon starvation for either carbon or nitrogen during vegetative growth (Fujioka, Mizutani et al. 2007; Valiante, Heinekamp et al. 2008). Fujioka, et al also show that the mitogen-activated protein (MAP) kinase pathway that responds to osmotic stress conserved in *Aspergillus fumigatus*, is also involved in nutritional sensing (Fujioka, Mizutani et al. 2007). Moreover, this MAP kinase pathway negatively regulates conidial germination and is activated in response to starvation for nitrogen or carbon sources (Xue, Nguyen et al. 2004).

Msb2 and Sho1 is upstream of MAP kinase pathway

In yeast, Msb2p is a glycosylated membrane protein which was first identified as a multicopy suppressor of *cdc24ts* mutant (Bender and Pringle 1992) and interacts with Sho1 and Cdc42 (Tatebayashi, Tanaka et al. 2007). Sho1 is an adaptor membrane protein that attaches the kinase complex to regions of polarized growth at the plasma membrane (Cullen, Schultz et al. 2000; Roman, Nombela et al. 2005). Msb2 and Hkr1 are the putative osmosensors of the HOG pathway in *S. cerevisiae* and act coordinately with Sho1 to promote osmotic adaptation (Tatebayashi, Tanaka et al. 2007). Recently, Msb2 and Sho1 have been shown to function together upstream of PAK Ste20p for the filamentous growth (FG) pathway in *S. cerevisiae* and for invasive hyphal response in *C. albicans* (Roman, Cottier et al. 2009). Although it is not entirely clear how nutritional information connects to FG pathway signaling, activation of the FG pathway requires processing and release of the extracellular inhibitory domain of Msb2p by the aspartyl protease Yps1p, which occurs preferentially under nutrient-limiting conditions (Vadaie, Dionne et al. 2008).

The Cullen lab uses Msb2* to mimic hyperactive Msb2. Msb2* protein lacks its mucin domain, thus it is underglycosylated and migrates more rapidly than wild type. Phosphorylation of Kss1 is Msb2 dependent and induced by both Msb2* and the overexpression of Sho1. However phosphorylation of Fus3 (the MAPK works with Kss1 in the mating pathway) was not influenced by Msb2* or Sho1. This indicates that Msb2 is solely required for FG pathway where it works through Kss1 by associated with Sho1 and activated Cdc42 (Cullen, Sabbagh et al. 2004).

In *Candida albicans*, Cek1 MAPK (phosphorylated by Hst7 MAPKK) is homologous to Kss1 and involved in invasive hyphal growth response (Csank, Schroppel et al. 1998; Chen, Lane et al. 2002). A recent report indicated that *Candida* Msb2 is not involved in the HOG pathway for the oxidative stress response, but plays an important role in FG (filamentous growth) and cell wall biogenesis by controlling the phosphorylation of the Cek1 MAPK in cooperation with Sho1. In addition, overexpression of Cdc42^{G12V} (the hyperactive form) can also result in hyperphosphorylation of Cek1 in a Sho1/Msb2/Hst7-dependent manner (Roman, Cottier et al. 2009).

MATERIALS and METHODS

Strains, media, growth conditions and staining

Aspergillus nidulans strains used in this study are listed in Table 1. MNV (minimal + vitamins) media were made according to KAFER (1977). MNV-glycerol and MNV-threonine media were made as described in PEARSON et al (2004). MAG (malt extract agar) and YGV (yeast extract glucose + vitamins) media were made as described previously (HARRIS et al 1994). For septation and hyphal growth studies, conidia from appropriate stains were grown at 28 °C for 12h on coverslips. Hyphae attached to the coverslip were fixed using a modified standard protocol (HARRIS et al 1994) for 20 min and then stained with staining solution [fixing solution and staining solution were made according to the recipe in the previous chapters].

Construction of gene replacement strains

The Rga1 (An1025.3) and Msb2 (An7041.3) genes from strains AHS11, AHS14 were replaced with the *pyroA*^{A.f.} marker from *A. fumigates*. All gene replacements were generated using the gene targeting system developed by NAYAK et al (2006) and the gene replacement generation strategy developed by YANG et al (2004). Oligonucleotides used in this study are listed in table 2. *pyroA*^{A.n.} DNA marker, the DNA fragments upstream and downstream of AnRga1 and were amplified from the wild-type strain FGSC28. *pyroA*^{A.f.} DNA marker fragment was PCR amplified from plasmid pTN1 (available through the Fungal Genetics Stock Center, Kansas City, MO) and the DNA fragments upstream and downstream of High Fidelity and Long Template PCR systems (Roche Diagnostics Corporation, Indianapolis, IN) were used for amplifications of individual and fusion fragments, respectively, using a Px2 Hybaid or an Eppendorf Mastercycler gradient thermal cycler. The amplification conditions were according to the manufacturer's recommendations. PCR products were gel purified using the QIAquick gel extraction kit (QIAGEN Inc., Valencia, CA). The gene replacement constructs were transformed into strain TNO2A3, and plated on supplemented minimal medium with 0.6 M KCl. Transformations were performed according the protocol described by OSMANI et al. (2006). Transformation candidates were tested for homologous integration of the gene replacement construct and the absence of the wild-type gene by diagnostic PCR as described by YANG et al (2004).

Construction of GFP fusions to AnRga1

To localize AnRga1, a GFP-pyr4 fragment was amplified from plasmid pFNO3 (available through the Fungal Genetics Stock Center, Kansas City, MO). A 1.2kb

AnRga1 fragment and a 1.5kb AnRga1 downstream fragment were amplified from strain TNO2A3. The same approach described by NAYAK et al. (2006) was used to make the gene targeting system. The fusion PCR construct was transformed to strain TNO2A3 and the transformants were verified by PCR to ensure the homologous gene insertion.

An N-terminus GFP- AnRga1 stain was also been construct using the five-piece fusion PCR approach described in the previous chapters. In addition to the retention of native promoter sequences, final constructs also contained a short linker of five glycines and alanines inserted between the GFP and AnRga1 coding sequences. In brief, the following five fragments were amplified (primers described in Table 2); (1) a 1.3-kb sequence upstream of the target gene, (2) the GFP coding sequence (minus the stop codon) derived from plasmid pMCB17apx, (3) the target gene plus 400-bp of downstream sequence, (4) the *N. crassa* pyr-4 selectable marker, also derived from pMCB17apx, and (5) a 1.3-kb sequence extending from about 400 to 1700-bp downstream of target gene. Fragments (1) and (5) were amplified by specific primers with 30bp tails that were reverse complements of the adjacent fragments. Finally, the forward primer used to amplify fragment (1) and the reverse primer used to amplify fragment (5) were used to fuse the entire five-fragment gene replacement construct. The resulting *gfp::AnRga1::pyr-4* cassettes was used to replace its respective wild type gene in strain TNO2A3.

Conidiophore observation and GFP localization on conidiophores

Conidiophore development was monitored by using the sandwich coverslip method described in the previous chapters. To localize GFP-AnRga1, cellophane stripes were used to synchronize and prepare conidiophore observation from solid medium culture.

Briefly, sterilized cellophane stripes were placed on MAG plates, and then diluted spore suspension (10^4 /ml) was spread on the top of stripes. After 24 hrs incubating at 28 °C, conidiophores start to form on the surface of cellophane stripes. Every one to two hours, a stripe can be peeled from plates and mounted with YGV liquid media for fluorescent microscope for each developmental stage. Submerged merged culture also been used to localize AnRga1-GFP on reduced conidiophores grown in liquid media since the localization is relatively easy to be observed. Briefly, the same coverslip culture method was used to grow spores in MNV with glucose substituted by 100mM threonine. After incubating at 28 °C for 3 days, hyphae and reduced conidiophores attached to coverslips were observed by the fluorescent microscope every 24 hours.

Microscopy

Digital images of plates were collected with an Olympus C-3020ZOOM digital camera. Differential interference contrast (DIC) and fluorescent images were collected with either an Olympus BX51 microscope with a reflected fluorescence system fitted with a Photometrics CoolSnap HQ camera or an Olympus Fluoview confocal laser-scanning microscope. Images were processed with IPLab Scientific Image Processing 3.5.5 (Scanalytics Inc., Fairfax, VA) and Adobe Photoshop 6.0 (Adobe Systems Incorporated, San Jose, CA).

Results

Identification of A. nidulans Msb2 and Rga1

Gene sequence annotation uncoverd the potential homologues of MSb2 and Rga1 by BLASTp search in Aspergillus genome database (broad institute genome database)

using the cognate proteins from *Saccharomyces cerevisiae* as query. AnMSb2 (An7041.3) is a predicted 822 amino acid (AA) protein with no protein domains were found. AnBud3 possesses limited homology to *S. cerevisiae* (33% identity over the predicted HMH domain about 132 AAs and about 60 AAs in the C-terminus as predicted transmembrane domain). AnRga1 (AN1025.3) is a predicted 1076 AA protein that contains an N-terminal LIM domain and a C-terminal GAP domain (**Fig. 4-2**). Similarity between AnRga1 and its *S. cerevisiae* homologue is relatively high (60% identity) and is confined to the LIM and GAP domains at each ends and about 90 AAs in the middle of protein sequence.

Rga1 is not required for vegetative growth but is essential for normal conidiophore development.

Coverslip cultures were used to examine AnRga1 knock out mutant for defects in hyphal morphogenesis. The timing and pattern of spore germination and polarity were not affected in $\Delta Anrga1$ deletion mutants. On minimal media, the colony of the $\Delta Anrga1$ deletion mutant was slightly smaller, and spore production severely reduced compared to wildtype (**Fig. 4-3**). To determine the possible basis of the conidiation defects, conidiophores of $\Delta Anrga1$ mutants and wildtype controls were imaged using the “sandwich slides” protocol. A variety of defects were found, including fused and elongated metulae and phialides (**Fig 4-4E**), loss of vesicles, and large sterigmata (**Fig 4-4D**). The sterigmata were larger and longer than wildtype (about two times longer and wider). Notably, septa were found in sterigmata (**Fig 4-4C**) and phialides branched in a

row (**Fig 4-4B**). These results indicate that AnRga1 is required for normal vesicle generation and the organization of metulae and phialides.

Rga1 localize to the top of phialides before the spore generation.

As a further test for the function of AnRga1, I used GFP fusion proteins to characterize its localization pattern. I constructed strains in which the sole functional source of AnRga1 was supplied by *AnRga1-GFP* or *GFP-AnRga1* fusions expressed under the control of the native promoter sequence. No AnRga1-GFP localization was found in hyphae. The cellophane stripe method was used to examine the localization in conidiophores. AnRga1-GFP localized to the top of phialides, where it formed a ring, but the localization is not prevalent and disappeared before spores generated (**Fig. 4-5A.B**). The submerged culture had also been used to localize AnRga1-GFP to the reduced conidiophores. Bright AnRga1-GFP rings localized to the top of phialide as expected in MNV-Thr submerged culture (**Fig. 4-5E**). As expected, AnRga1-GFP localization disappeared after the first spore generated (**Fig. 4-5C.D**).

ΔAnMsb2 affects timing and structure of hyphal growth and cell wall integrity.

To determine the possible role of AnMsb2 during hyphal and conidiophore morphogenesis, *Anmsb2::pyroA^{A.f.}* strains were generated using gene replacement. On minimal media, colonies of $\Delta Anmsb2$ mutants have restricted growth and dramatically reduced spore production (**Fig 4-6**). The coverslip culture was used to determine hyphal morphology. We found $\Delta Anmsb2$ spore germination had been delayed for about 4-5 hours, but no later hyphal development defects were observed. In *Candida albicans*, $\Delta msb2$ mutants had low tolerance for Congo red (a compound that interacts with chitin

and interferes with cell wall construction) and caspofungin (an inhibitor of β -glucan synthase) (Roman, Cottier et al. 2009). To gain further insight into the possible nature of cell wall defects in the $\Delta Anmsb2$ mutant strain, we tested the strain for defects in the cell wall such as increased sensitivity toward elevated Calcofluor white (CFW) and Congo red (CR) (Ram and Klis 2006). Gradient diluted conidia were inoculated to MNV plate with 10, 50 and 100mg/ml of CFW or CR to test susceptibility of cell wall integrity. We found the sensitivity of $\Delta Anmsb2$ cell wall to both CFW and Congo red increased with treatment concentration and spore inoculum (**Fig 4-7**). Accordingly, these results suggest that AnMsb2 must be involved in cell wall integrity.

DISCUSSION

In our study, Msb2 has been shown to have essential function for cell wall integrity, and the deletion of the Msb2 gene can severely delay spore germination which may result from the defect of chitin organization in the cell wall. In the next experiment, a test of capsosfungin will give us more information for cell wall component change in $\Delta msb2$. Moreover, cell wall integrity defects in $\Delta msb2$ may also be correlated with the small GTPases Cdc42, Rac and Ras through the MAP kinase pathway because the direct regulation between Cdc42 and Msb2 for the FG pathway has been reported in budding yeast. In *S. cerevisiae*, MMK1/2 \rightarrow Mpk1 pathway is related to cell wall stress response which is activated by Rho1 GTPase (Zarzov, Mazzoni et al. 1996; Chen and Thorner 2007) and a recent report indicates MpkA, the Mpk1^{MAPK} homolog (68% similarity), regulates cell wall assembling in *A. fumigates* (Valiante, Jain et al. 2009). In addition, the interaction of Msb2 with the Rho-like GTPase Cdc42 may also suggest an intimate relationship between the control of polarity and the function of membrane mucins

(Clevers 2004). Thus the possible function of Msb2 for regulating small GTPases on cell wall integrity could be examined by testing multicopy suppression of small GTPases to $\Delta Anmsb2$ mutants.

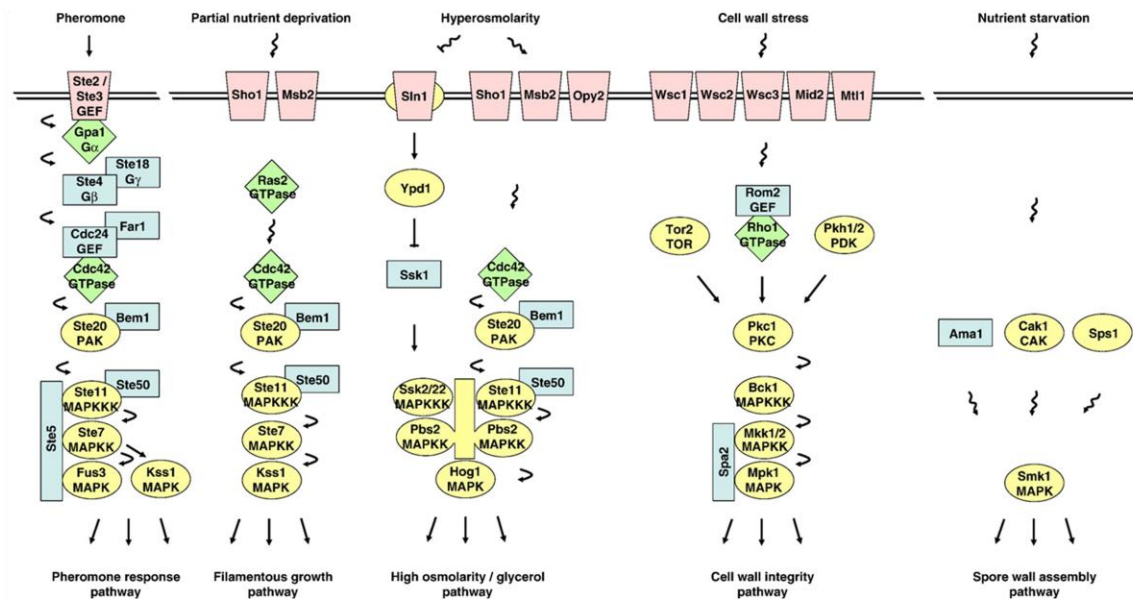
In yeast, upstream signaling of the HOG and filamentous growth (FG) pathway is functionally redundant including Sln1 and Sho1 signaling branches (O'Rourke and Herskowitz 2002). For the Sho1 branch, Msb2 and Hkr1 are the two most upstream osmosensors belong to the highly glycosylated mucin family, which bind Sho1 but function differently (Tatebayashi, Tanaka et al. 2007). According to this, AnMsb2 may also be involved in the HOG pathway response for osmotic stress. High osmotic condition such as sorbital and high salt media can be used to test this hypothesis. In addition, deletion of the mucin domain (Msb2*) have been used to mimic hyperactive Msb2 (Cullen, Sabbagh et al. 2004). Interestingly, both Hkr1 and Msb2 share the common Hkr1-Msb2 Homology (HMH) domain, which is the only essential protein part for osmosensing (Tatebayashi, Tanaka et al. 2007). By doing a preliminary two sequence alignment with yeast Msb2, the conserved HMH region also exists in the AnMsb2, but may not be the mucin and STR (Ser-Thr rich) domains. Fraction from different regions of AnMsb2 will be tested for their interaction with Cdc42 and Sho1 on the top of the MAPK pathways.

Since there are three Cdc42 GAPs in *S. cerevisiae*, GAP regulation of Cdc42 in *A. nidulans* could be complex. Seven GAPs have been found by BLASTp from our preliminary study. As one of the Cdc42 GAP, deletion of *AnRgal* is expected to increase the Cdc42-GTP bound active form. Smith et al. reported that $\Delta rgal$ displayed an elongated yeast cell, and the $\Delta rgal \Delta bem3$ double mutant strain will exacerbate the

phenotype. Moreover, $\Delta rga1$ also causes yeast hyperinvasive growth and septin disorganization paralleled by disorganization of the type II myosin Myo1p (Caviston, Longtine et al. 2003; Gladfelter, Zyla et al. 2004). In our research, we found $\Delta Anrga1$ displayed unique defects on conidiophores with elongated sterigmata, which may result from defects in septin organization due to the aberrant Cdc42-GTP level. On the other hand, Rga2 and Bem3 may also have specific functions through regulating the activity of Cdc42. Thus double mutation of Cdc42 and GAPs will help to examine morphological development in *A. nidulans*.

Interestingly, Lrg1, Rga1 and Rga2 all have a similar pattern of domain organization: tandemly arranged two LIM domains on the N-terminus and a GAP domain on the C-terminus. LIM domains are Zinc finger domains which act in protein-protein interactions. Our lab data also show that deletion of AnLrg1 in *A. nidulans* results in hyper-branching hyphal development. Making truncated GAPs with LIM domain deletion will help to understand their GAP function and interaction pattern with other proteins.

Fig. 4-1 Function and regulation in MAPK signaling pathways



Raymond E. Chen, Jeremy Thorner. *Biochimica et Biophysica Acta* 1773 (2007) 1311–1340

Figure 4-1. Function and regulation in MAPK signaling pathways

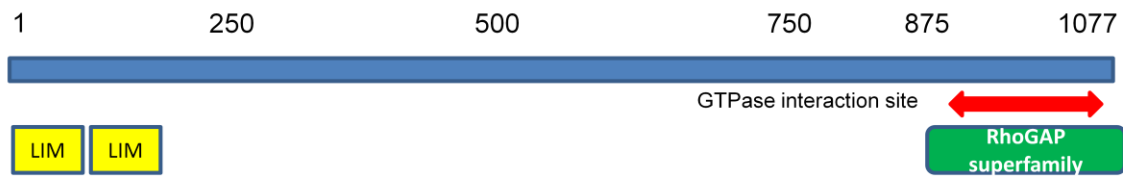
Fig 4-2. Amino acid sequence of AnRga1**Figure 4-2.** Amino acid sequence of AnRga1.

Fig 4-3. Colony phenotype of $\Delta Anrga1$

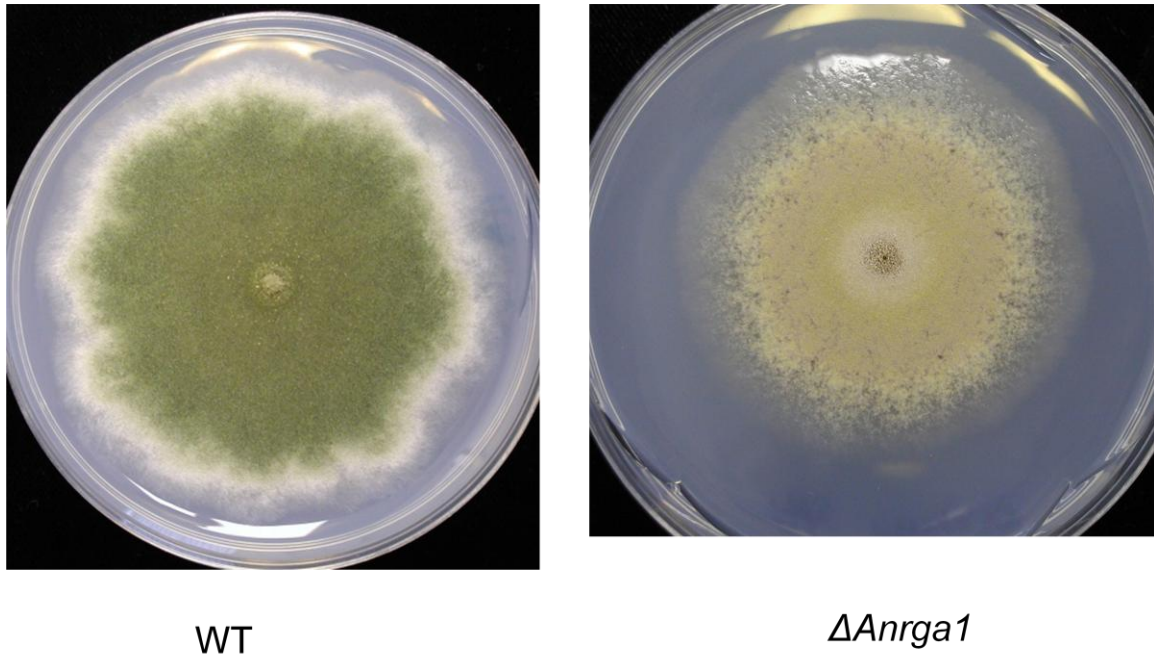


Figure 4-3. Effect of the *Anrga1* deletion on colony morphology. A. (wildtype) and B. ($\Delta Anrga1$) were grown on minimal medium for nine days.

Fig. 4-4 conidiophore morphology of $\Delta Anrga1$

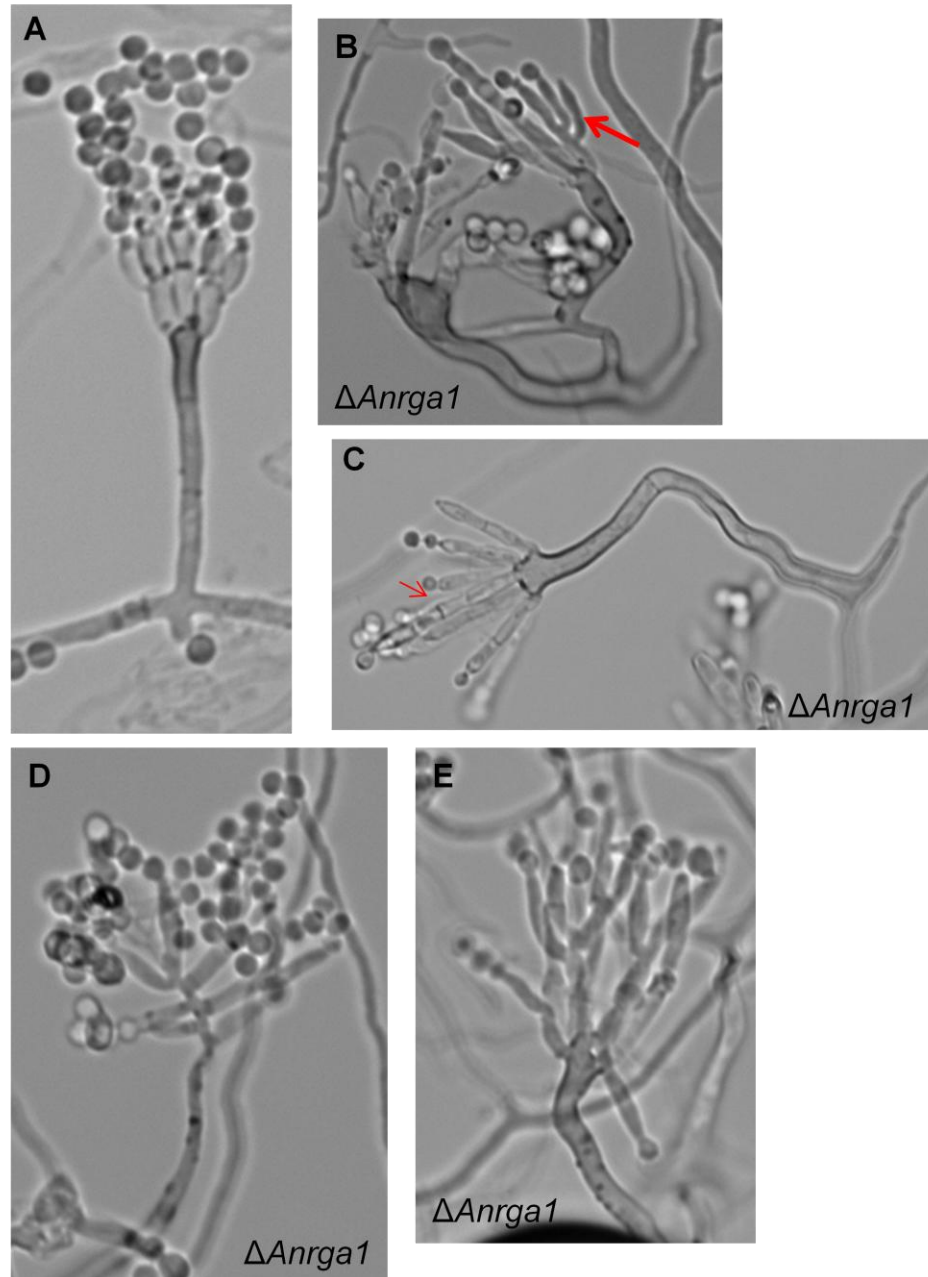


Figure 4-4. Effect of the *Anrgal* deletion on conidiophore development. Δ *Anrgal* deletion strains were grown on minimal medium for three days by the “sandwich” method. Red arrows indicate a branching metula (B) and a septum on sterigmata (C).

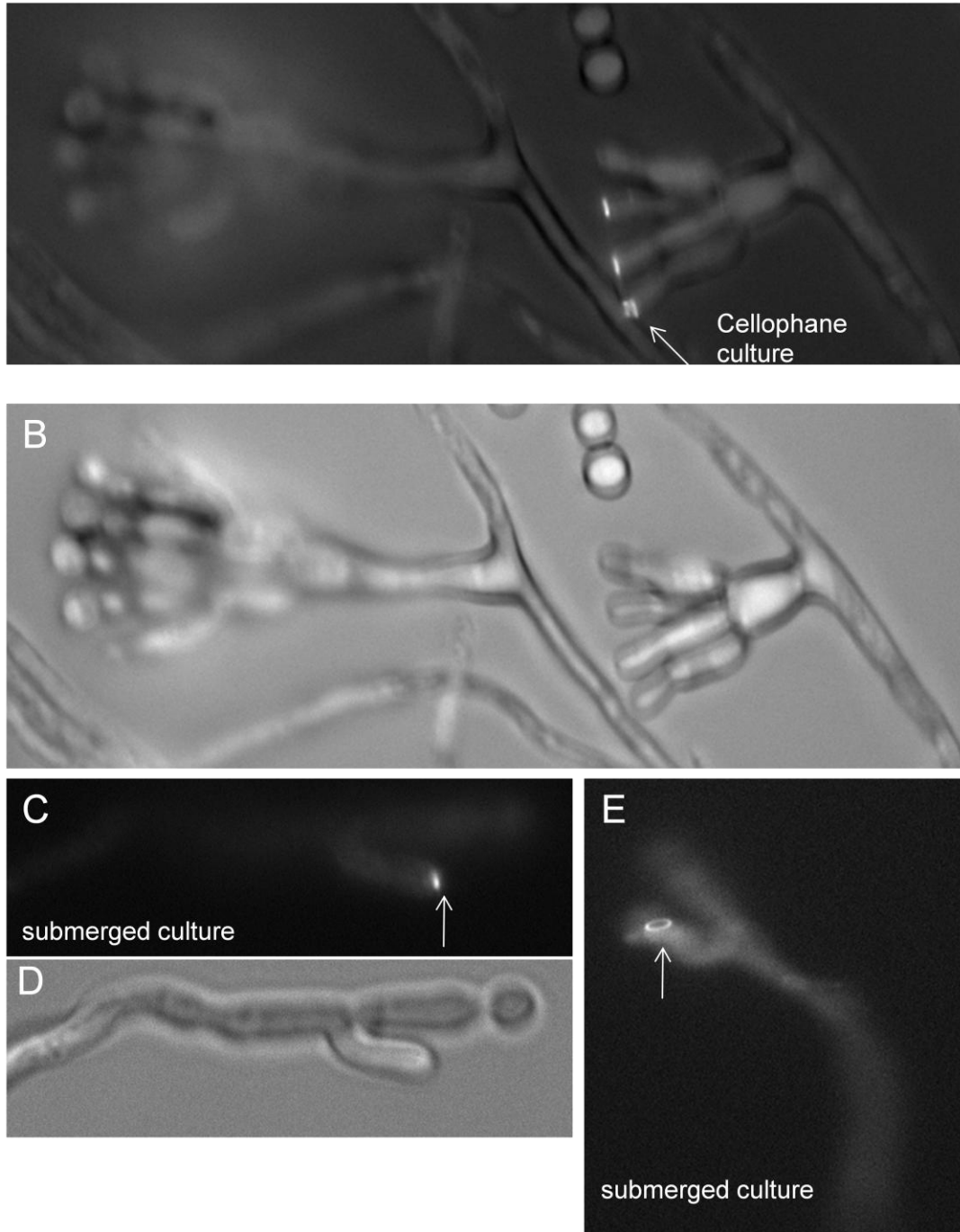
Fig 4-5

Figure 4-5. Localization of AnRga1-GFP in conidiophore development. The AnRga1-GFP strains were grown on cellophane (A and B) for 24 hours and MNV-Thr submerged culture (C-E) for 3 days. White arrows indicate AnRga1-GFP localization.

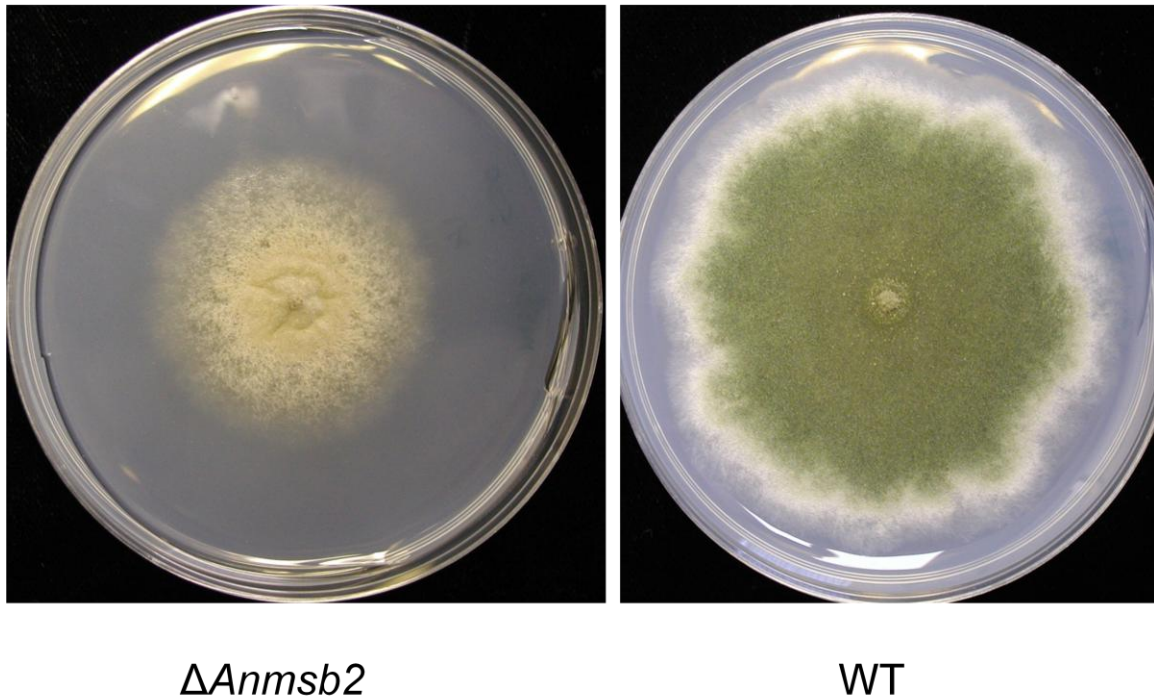
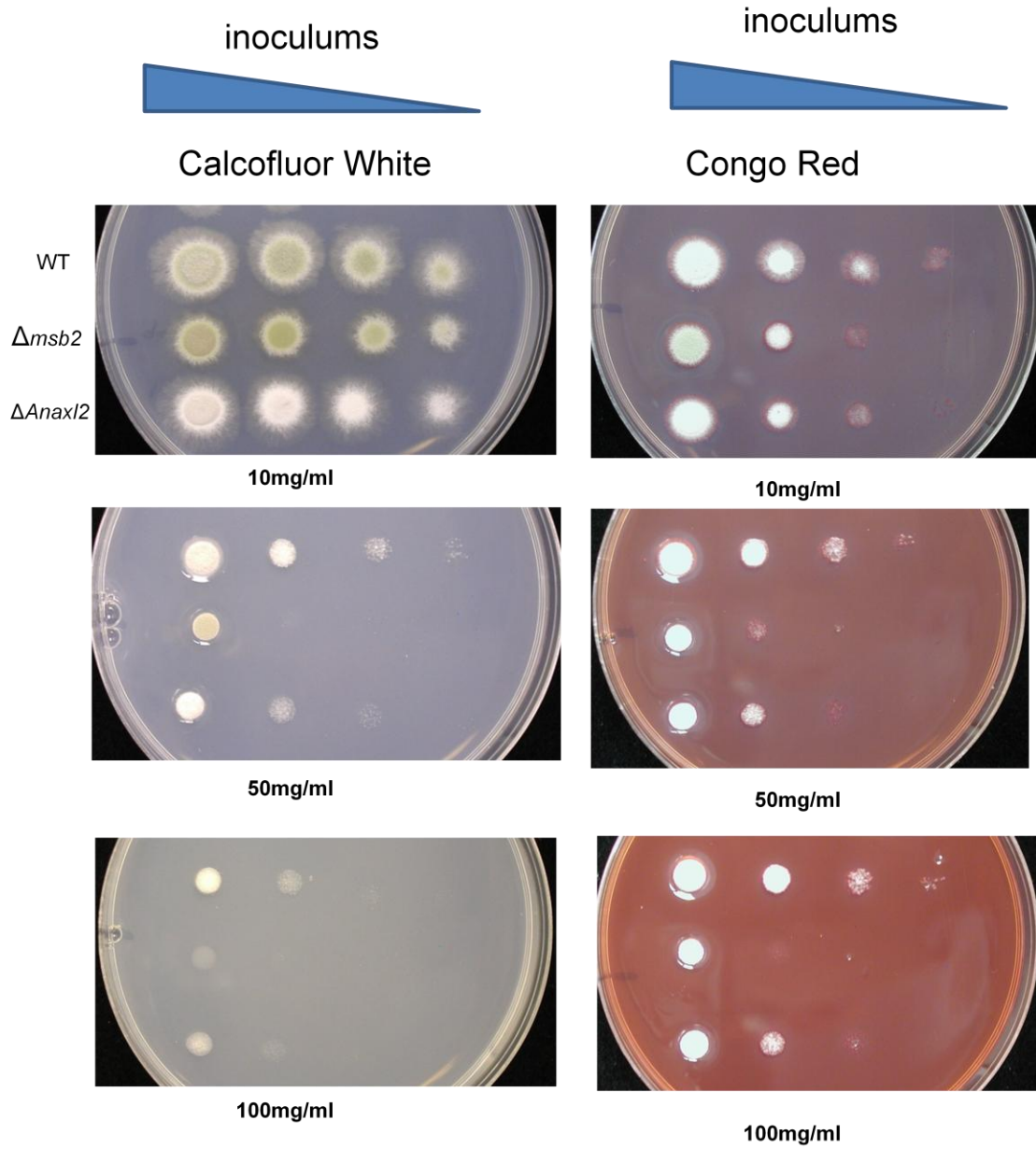
Fig 4-6.

Figure 4-6. Effect of the *Anmsb2* deletion on colony morphology. A. (wildtype) and B. ($\Delta Anmsb2$) were grown on minimal medium for nine days.

Fig 4-7**Figure 4-7.** Cell wall integrity test on *Anmsb2* deletion mutants.

REFERENCES

- Abdullah, U. and P. J. Cullen (2009). "The tRNA modification complex elongator regulates the Cdc42-dependent mitogen-activated protein kinase pathway that controls filamentous growth in yeast." *Eukaryot Cell* **8**(9): 1362-1372.
- Araujo-Bazan, L., M. A. Penalva, et al. (2008). "Preferential localization of the endocytic internalization machinery to the hyphal tips underlies polarization of the actin cytoskeleton in *Aspergillus nidulans*." *Molecular Microbiology* **67**: 891-905.
- Asnaghi, L., W. C. Vass, et al. (2010). "E-cadherin negatively regulates neoplastic growth in non-small cell lung cancer: role of Rho GTPases." *Oncogene*.
- Atoui, A., D. Bao, et al. (2008). "Aspergillus nidulans natural product biosynthesis is regulated by mpkB, a putative pheromone response mitogen-activated protein kinase." *Appl Environ Microbiol* **74**(11): 3596-3600.
- Bardwell, L. (2006). "Mechanisms of MAPK signalling specificity." *Biochem Soc Trans* **34**(Pt 5): 837-841.
- Bender, A. and J. R. Pringle (1992). "A Ser/Thr-rich multicopy suppressor of a cdc24 bud emergence defect." *Yeast* **8**(4): 315-323.
- Boyce, K. J., M. J. Hynes, et al. (2001). "The CDC42 homolog of the dimorphic fungus *Penicillium marneffeii* is required for correct cell polarization during growth but not development." *J Bacteriol* **183**(11): 3447-3457.
- Boylan, M. T., P. M. Mirabito, et al. (1987). "Isolation and physical characterization of three essential conidiation genes from *Aspergillus nidulans*." *Mol Cell Biol* **7**(9): 3113-3118.
- Burford, H., Z. Baloch, et al. (2009). "E-cadherin/beta-catenin and CD10: a limited immunohistochemical panel to distinguish pancreatic endocrine neoplasm from solid pseudopapillary neoplasm of the pancreas on endoscopic ultrasound-guided fine-needle aspirates of the pancreas." *Am J Clin Pathol* **132**(6): 831-839.
- Casselton, L. and M. Zolan (2002). "The art and design of genetic screens: filamentous fungi." *Nat Rev Genet* **3**(9): 683-697.
- Caviston, J. P., M. Longtine, et al. (2003). "The role of Cdc42p GTPase-activating proteins in assembly of the septin ring in yeast." *Mol Biol Cell* **14**(10): 4051-4066.
- Chang, C. H., F. Y. Yu, et al. (2009). "Activation of ERK and JNK signaling pathways by mycotoxin citrinin in human cells." *Toxicol Appl Pharmacol* **237**(3): 281-287.
- Chang, M.-H., K.-S. Chae, et al. (2004). "The GanB Gα-protein negatively regulates asexual sporulation and plays a positive role in conidial germination in *Aspergillus nidulans*." *Genetics* **167**: 1305-1315.
- Chang, Y. C. and W. E. Timberlake (1993). "Identification of *Aspergillus* brlA response elements (BREs) by genetic selection in yeast." *Genetics* **133**(1): 29-38.
- Chen, C., Y. S. Ha, et al. (2006). "Cdc42 is required for proper growth and development in the fungal pathogen *Colletotrichum trifolii*." *Eukaryot Cell* **5**(1): 155-166.
- Chen, J., S. Lane, et al. (2002). "A conserved mitogen-activated protein kinase pathway is required for mating in *Candida albicans*." *Mol Microbiol* **46**(5): 1335-1344.
- Chen, R. E. and J. Thorner (2007). "Function and regulation in MAPK signaling pathways: lessons learned from the yeast *Saccharomyces cerevisiae*." *Biochim Biophys Acta* **1773**(8): 1311-1340.

- Cho, R. J., M. J. Campbell, et al. (1998). "A genome-wide transcriptional analysis of the mitotic cell cycle." Mol Cell **2**(1): 65-73.
- Cid, V. J., L. Adamikova, et al. (2001). "Cell cycle control of septin ring dynamics in the budding yeast." Microbiology **147**(Pt 6): 1437-1450.
- Clevers, H. (2004). "Signaling mucins in the (S)limelight." Dev Cell **7**(2): 150-151.
- Cook, J. G., L. Bardwell, et al. (1997). "Inhibitory and activating functions for MAPK Kss1 in the *S. cerevisiae* filamentous-growth signalling pathway." Nature **390**(6655): 85-88.
- Csank, C., K. Schroppel, et al. (1998). "Roles of the *Candida albicans* mitogen-activated protein kinase homolog, Cek1p, in hyphal development and systemic candidiasis." Infect Immun **66**(6): 2713-2721.
- Cullen, P. J., W. Sabbagh, Jr., et al. (2004). "A signaling mucin at the head of the Cdc42- and MAPK-dependent filamentous growth pathway in yeast." Genes Dev **18**(14): 1695-1708.
- Cullen, P. J., J. Schultz, et al. (2000). "Defects in protein glycosylation cause SHO1-dependent activation of a STE12 signaling pathway in yeast." Genetics **155**(3): 1005-1018.
- d'Enfert, C., B. M. Bonini, et al. (1999). "Neutral trehalases catalyse intracellular trehalose breakdown in the filamentous fungi *Aspergillus nidulans* and *Neurospora crassa*." Molecular Microbiology **32**: 471-483.
- d'Enfert, C. and T. Fontaine (1997). "Molecular characterization of the *Aspergillus nidulans* *treA* gene encoding an acid trehalase required for growth on trehalose." Molecular Microbiology **24**: 203-216.
- de Vries, R. P., S. J. Flitter, et al. (2003). "Glycerol dehydrogenase, encoded by *gldB* is essential for osmotolerance in *Aspergillus nidulans*." Molecular Microbiology **49**: 131-141.
- Efimov, V. P. (2003). "Roles of NUDE and NUDF proteins of *Aspergillus nidulans*: insights from intracellular localization and overexpression effects." Mol Biol Cell **14**(3): 871-888.
- Fares, H., L. Goetsch, et al. (1996). "Identification of a developmentally regulated septin and involvement of the septins in spore formation in *Saccharomyces cerevisiae*." J Cell Biol **132**(3): 399-411.
- Farley, F. W., B. Satterberg, et al. (1999). "Relative dependence of different outputs of the *Saccharomyces cerevisiae* pheromone response pathway on the MAP kinase Fus3p." Genetics **151**(4): 1425-1444.
- Fillinger, S., M.-K. Chaverroche, et al. (2002). "cAMP and ras signalling independently control spore germination in the filamentous fungus *Aspergillus nidulans*." Molecular Microbiology **44**: 1001-1016.
- Fillinger, S., G. Ruitijter, et al. (2001). "Molecular and physiological characterization of the NAD-dependent glycerol 3-phosphate dehydrogenase in the filamentous fungus *Aspergillus nidulans*." Molecular Microbiology **39**: 145-157.
- Fujioka, T., O. Mizutani, et al. (2007). "MpkA-Dependent and -independent cell wall integrity signaling in *Aspergillus nidulans*." Eukaryot Cell **6**(8): 1497-1510.
- Gao, X. D., L. M. Sperber, et al. (2007). "Sequential and distinct roles of the cadherin domain-containing protein Axl2p in cell polarization in yeast cell cycle." Mol Biol Cell **18**(7): 2542-2560.

- Garrod, D. and T. E. Kimura (2008). "Hyper-adhesion: a new concept in cell-cell adhesion." Biochem Soc Trans **36**(Pt 2): 195-201.
- Gladfelter, A. S., I. Bose, et al. (2002). "Septin ring assembly involves cycles of GTP loading and hydrolysis by Cdc42p." J Cell Biol **156**(2): 315-326.
- Gladfelter, A. S., L. Kozubowski, et al. (2005). "Interplay between septin organization, cell cycle and cell shape in yeast." J Cell Sci **118**(Pt 8): 1617-1628.
- Gladfelter, A. S., T. R. Zyla, et al. (2004). "Genetic interactions among regulators of septin organization." Eukaryot Cell **3**(4): 847-854.
- Gustin, M. C., J. Albertyn, et al. (1998). "MAP kinase pathways in the yeast *Saccharomyces cerevisiae*." Microbiol Mol Biol Rev **62**(4): 1264-1300.
- Hage, B., K. Meinel, et al. (2009). "Rac1 activation inhibits E-cadherin-mediated adherens junctions via binding to IQGAP1 in pancreatic carcinoma cells." Cell Commun Signal **7**: 23.
- Hagiwara, D., Y. Asano, et al. (2009). "Transcriptional profiling for *Aspergillus nidulans* HogA MAPK signaling pathway in response to fludioxonil and osmotic stress." Fungal Genet Biol **46**(11): 868-878.
- Jansen, G., F. Buhring, et al. (2001). "Mutations in the SAM domain of STE50 differentially influence the MAPK-mediated pathways for mating, filamentous growth and osmotolerance in *Saccharomyces cerevisiae*." Mol Genet Genomics **265**(1): 102-117.
- Johnson, D. I. (1999). "Cdc42: An essential Rho-type GTPase controlling eukaryotic cell polarity." Microbiol Mol Biol Rev **63**(1): 54-105.
- Kikuma, T., M. Ohneda, et al. (2006). "Functional analysis of the ATG8 homologue Aoa8 and role of autophagy in differentiation and germination in *Aspergillus oryzae*." Eukaryot Cell **5**(8): 1328-1336.
- Kim, H., K. Han, et al. (2002). "The veA gene activates sexual development in *Aspergillus nidulans*." Fungal Genet Biol **37**(1): 72-80.
- Lindsey, R. and M. Momany (2006). "Septin localization across kingdoms: three themes with variations." Curr Opin Microbiol **9**(6): 559-565.
- Longtine, M. S., D. J. DeMarini, et al. (1996). "The septins: roles in cytokinesis and other processes." Curr Opin Cell Biol **8**(1): 106-119.
- Lord, M., M. C. Yang, et al. (2000). "Cell cycle programs of gene expression control morphogenetic protein localization." J Cell Biol **151**(7): 1501-1512.
- Ma, Y., J. Qiao, et al. (2008). "The sho1 sensor regulates growth, morphology, and oxidant adaptation in *Aspergillus fumigatus* but is not essential for development of invasive pulmonary aspergillosis." Infect Immun **76**(4): 1695-1701.
- Marston, A. L., T. Chen, et al. (2001). "A localized GTPase exchange factor, Bud5, determines the orientation of division axes in yeast." Curr Biol **11**(10): 803-807.
- McCrea, P. D. and D. Gu (2010). "The catenin family at a glance." J Cell Sci **123**(Pt 5): 637-642.
- Momany, M. (2002). "Polarity in filamentous fungi: establishment, maintenance and new axes." Curr Opin Microbiol **5**(6): 580-585.
- Momany, M., P. J. Westfall, et al. (1999). "*Aspergillus nidulans* swo mutants show defects in polarity establishment, polarity maintenance and hyphal morphogenesis." Genetics **151**: 557-567.

- Momany, M., J. Zhao, et al. (2001). "Characterization of the *Aspergillus nidulans* septin (asp) gene family." *Genetics* **157**(3): 969-977.
- Mooney, J. L. and L. N. Yager (1990). "Light is required for conidiation in *Aspergillus nidulans*." *Genes Dev* **4**(9): 1473-1482.
- Nelson, W. J. and R. Nusse (2004). "Convergence of Wnt, beta-catenin, and cadherin pathways." *Science* **303**(5663): 1483-1487.
- O'Rourke, S. M. and I. Herskowitz (2002). "A third osmosensing branch in *Saccharomyces cerevisiae* requires the Msb2 protein and functions in parallel with the Sho1 branch." *Mol Cell Biol* **22**(13): 4739-4749.
- Osherov, N. and G. May (2000). "Conidial germination in *Aspergillus nidulans* requires RAS signalling and protein synthesis." *Genetics* **155**: 647-656.
- Peterson, F. C., R. R. Penkert, et al. (2004). "Cdc42 regulates the Par-6 PDZ domain through an allosteric CRIB-PDZ transition." *Mol Cell* **13**(5): 665-676.
- Peyrieras, N., D. Louvard, et al. (1985). "Characterization of antigens recognized by monoclonal and polyclonal antibodies directed against uvomorulin." *Proc Natl Acad Sci U S A* **82**(23): 8067-8071.
- Pitoniak, A., B. Birkaya, et al. (2009). "The signaling mucins Msb2 and Hkr1 differentially regulate the filamentation mitogen-activated protein kinase pathway and contribute to a multimodal response." *Mol Biol Cell* **20**(13): 3101-3114.
- Posas, F., E. A. Witten, et al. (1998). "Requirement of STE50 for osmostress-induced activation of the STE11 mitogen-activated protein kinase kinase in the high-osmolarity glycerol response pathway." *Mol Cell Biol* **18**(10): 5788-5796.
- Prade, R. A. and W. E. Timberlake (1993). "The *Aspergillus nidulans* brlA regulatory locus consists of overlapping transcription units that are individually required for conidiophore development." *EMBO J* **12**(6): 2439-2447.
- Ram, A. F. and F. M. Klis (2006). "Identification of fungal cell wall mutants using susceptibility assays based on Calcofluor white and Congo red." *Nat Protoc* **1**(5): 2253-2256.
- Ramezani-Rad, M. (2003). "The role of adaptor protein Ste50-dependent regulation of the MAPKKK Ste11 in multiple signalling pathways of yeast." *Curr Genet* **43**(3): 161-170.
- Roemer, T., K. Madden, et al. (1996). "Selection of axial growth sites in yeast requires Axl2p, a novel plasma membrane glycoprotein." *Genes Dev* **10**(7): 777-793.
- Roman, E., F. Cottier, et al. (2009). "Msb2 signaling mucin controls activation of Cek1 mitogen-activated protein kinase in *Candida albicans*." *Eukaryot Cell* **8**(8): 1235-1249.
- Roman, E., C. Nombela, et al. (2005). "The Sho1 adaptor protein links oxidative stress to morphogenesis and cell wall biosynthesis in the fungal pathogen *Candida albicans*." *Mol Cell Biol* **25**(23): 10611-10627.
- Sabbagh, W., Jr., L. J. Flatauer, et al. (2001). "Specificity of MAP kinase signaling in yeast differentiation involves transient versus sustained MAPK activation." *Mol Cell* **8**(3): 683-691.
- Saito, K., K. Fujimura-Kamada, et al. (2007). "Transbilayer phospholipid flipping regulates Cdc42p signaling during polarized cell growth via Rga GTPase-activating proteins." *Dev Cell* **13**(5): 743-751.

- Sanders, S. L. and I. Herskowitz (1996). "The BUD4 protein of yeast, required for axial budding, is localized to the mother/BUD neck in a cell cycle-dependent manner." J Cell Biol **134**(2): 413-427.
- Scott, S. V., D. C. Nice, 3rd, et al. (2000). "Apg13p and Vac8p are part of a complex of phosphoproteins that are required for cytoplasm to vacuole targeting." J Biol Chem **275**(33): 25840-25849.
- Shaw, B. and C. Momany (2002). "*Aspergillus nidulans* polarity mutant *swaA* is complemented by protein *O*-mannosyltransferase *pmtA*." Fungal Genetics and Biology **37**: 263-270.
- Sheu, Y. J., B. Santos, et al. (1998). "Spa2p interacts with cell polarity proteins and signaling components involved in yeast cell morphogenesis." Mol Cell Biol **18**(7): 4053-4069.
- Smith, G. R., S. A. Givan, et al. (2002). "GTPase-activating proteins for Cdc42." Eukaryot Cell **1**(3): 469-480.
- Spellman, P. T., G. Sherlock, et al. (1998). "Comprehensive identification of cell cycle-regulated genes of the yeast *Saccharomyces cerevisiae* by microarray hybridization." Mol Biol Cell **9**(12): 3273-3297.
- Stevenson, B. J., B. Ferguson, et al. (1995). "Mutation of RGA1, which encodes a putative GTPase-activating protein for the polarity-establishment protein Cdc42p, activates the pheromone-response pathway in the yeast *Saccharomyces cerevisiae*." Genes Dev **9**(23): 2949-2963.
- Taheri-Talesh, N., T. Horio, et al. (2008). "The tip growth apparatus of *Aspergillus nidulans*." Molecular Biology of the Cell **19**: 1439-1449.
- Takeshita, N., Y. Higashitsuji, et al. (2008). "Apical sterol-rich membranes are essential for localizing cell end markers that determine growth directionality in the filamentous fungus *Aspergillus nidulans*." Molecular Biology of the Cell **19**: 339-351.
- Tatebayashi, K., K. Tanaka, et al. (2007). "Transmembrane mucins Hkr1 and Msb2 are putative osmosensors in the SHO1 branch of yeast HOG pathway." EMBO J **26**(15): 3521-3533.
- Tatebayashi, K., K. Yamamoto, et al. (2006). "Adaptor functions of Cdc42, Ste50, and Sho1 in the yeast osmoregulatory HOG MAPK pathway." EMBO J **25**(13): 3033-3044.
- Tazebay, U. H., V. Sophianopoulou, et al. (1995). "Post-transcriptional control and kinetic characterization of proline transport in germinating conidiospore of *Aspergillus nidulans*." FEMS Microbiology Letters **132**: 27-37.
- Tazebay, U. H., V. Sophianopoulou, et al. (1997). "The gene encoding the major proline transporter of *Aspergillus nidulans* is upregulated during conidiospore germination and in response to proline induction and amino acid starvation." Molecular Microbiology **24**: 105-117.
- Timberlake, W. E. (1990). "Molecular genetics of *Aspergillus* development." Annu Rev Genet **24**: 5-36.
- Upadhyay, S. and B. Shaw (2008). "The role of actin, fimbrin and endocytosis in growth of hyphae in *Aspergillus nidulans*." Molecular Microbiology **68**: 690-705.

- Vadaie, N., H. Dionne, et al. (2008). "Cleavage of the signaling mucin Msb2 by the aspartyl protease Yps1 is required for MAPK activation in yeast." J Cell Biol **181**(7): 1073-1081.
- Valiante, V., T. Heinekamp, et al. (2008). "The mitogen-activated protein kinase MpkA of *Aspergillus fumigatus* regulates cell wall signaling and oxidative stress response." Fungal Genet Biol **45**(5): 618-627.
- Valiante, V., R. Jain, et al. (2009). "The MpkA MAP kinase module regulates cell wall integrity signaling and pyomelanin formation in *Aspergillus fumigatus*." Fungal Genet Biol **46**(12): 909-918.
- van Drogen, F. and M. Peter (2002). "Spa2p functions as a scaffold-like protein to recruit the Mpk1p MAP kinase module to sites of polarized growth." Curr Biol **12**(19): 1698-1703.
- Virag, A., M. P. Lee, et al. (2007). "Regulation of hyphal morphogenesis by cdc42 and rac1 homologues in *Aspergillus nidulans*." Mol Microbiol **66**(6): 1579-1596.
- Wei, H., N. Requena, et al. (2003). "The MAPKK kinase SteC regulates conidiophore morphology and is essential for heterokaryon formation and sexual development in the homothallic fungus *Aspergillus nidulans*." Mol Microbiol **47**(6): 1577-1588.
- Weis, W. I. and W. J. Nelson (2006). "Re-solving the cadherin-catenin-actin conundrum." J Biol Chem **281**(47): 35593-35597.
- Wendland, J. and P. Philippsen (2001). "Cell polarity and hyphal morphogenesis are controlled by multiple rho-protein modules in the filamentous ascomycete *Ashbya gossypii*." Genetics **157**(2): 601-610.
- Xue, T., C. K. Nguyen, et al. (2004). "A mitogen-activated protein kinase that senses nitrogen regulates conidial germination and growth in *Aspergillus fumigatus*." Eukaryot Cell **3**(2): 557-560.
- Zarzov, P., C. Mazzoni, et al. (1996). "The SLT2(MPK1) MAP kinase is activated during periods of polarized cell growth in yeast." EMBO J **15**(1): 83-91.

Chapter IV Future Directions

GAP(s) of the Bud3-Rho4 module

We have proved AnBud3 is the guanine exchange factor (GEF) that activates AnRho4 into GTP bound form. However, the AnRho4 GAP(s) still need to be identified. We have found seven hypothetical GAPs in the *A. nidulans* genome by BLASTp with the conservative GAP domain. Unfortunately, none of these hypothetical GAPs can be identified by multicopy suppression of the $\Delta Anbud3$ suppressor strain which is suspected to have a mutation in the Rho4 GAP. This suggests that the regulation of Rho4 is complicated and it can be more than one GAP exists for AnBud3-Rho4 module. Thanks to the Illumina sequencing for the $\Delta Anbud3$ suppressor strain, we can narrow down the Rho4 GAP(s) to a few candidates. We intend to knock out these candidate genes and make double mutants with $\Delta Anbud3$ in order to genetically identify the GAP because the double mutants should exhibit a near wildtype phenotype. A hyperactive mutant Rho4 constructed by point amino acid substitution can be also constructed to trap Rho4 in the GTP-bound active form. This hyperactive GTP-Rho4 can be used to pull down its interacting GAP(s) partners by small GTP-GTPase beads. The yeast two-hybrid method might be used to test the interaction between hyperactive Rho4 and its GAP candidates.

The roles of AnAxl2 and Anbud4 in septin organization

Septins play key roles in cytokinesis, organize contractile actin rings (CAR) and SepA localization during septum formation. As reported in Chapter II, we proved an interaction occurs between septins and Anbud4 or AnAxl2, but further studies need to be done to elucidate their specific interactions. As I showed in the discussion, Anbud4 can

specifically interact with AspE for cell viability. An N-terminal S-Tag-Anbud4 fusion protein can be used to pull down components that interact with it during both hyphal and asexual growth. A tagged AspE can be then detected by western blot. Moreover, if AnBud4 functions as a scaffold to organize septins, expressing multicopies of AspE may suppress the $\Delta Anbud4$ phenotype and restore septation and conidiation.

The specific interaction between AspD and AnAxl2 also needs to be determined. Unfortunately, AnAxl2 is a transmembrane protein and only expressed during conidiation, thus purification of AnAxl2 is a challenge. Before performing an *in vitro* assay to detect the possible interaction of AspD-AnAxl2, a pilot experiment can be done to first examine the hypothesis. In yeast, AnAxl2 had been identified as the multicopy suppressor of the $\Delta spa2 \Delta Cdc10$ double mutant. A similar $\Delta spaA \Delta aspD$ double mutant can be constructed by normal sexual crosses from lab stocks ($\Delta aspD$ is provided by Momany's lab). Multicopies of *AnAxl2* can be transformed into the $\Delta spaA \Delta aspD$ double mutant and be capable of suppressing the double mutation phenotype as in budding yeast. We can also localize AnAxl2-GFP in the septin gene deletion mutants, especially in $\Delta aspE$ and $\Delta aspD$ mutants since they have less of a defect in conidiation compared with the others. Mislocalization of AnAxl2-GFP in any of the mutants will give a genetic proof for the possible direction of interaction. In the same way, Septin-GFP(s) can be localized in the $\Delta AnAxl2$ background.

In yeast, Cla4 is a p21-activated kinase (PAK) involved in septin ring assembly by phosphorylating Cdc3p (AspB) and Cdc10p (AspD). Thus AnCla4 may also be involved in AnAxl2 assembly with septins at the incipient site of conidiation. AnCla4-GFP and $\Delta Ancla4$ can be used to test its function during conidiophore development.

Since Cla4 phosphorylates Cdc3p, the key septin, its localization can be universal but the localization pattern on conidiophore in $\Delta AnAxl2$ background will help us to understand the organization of septins at the neck between phialides and nascent spores. $\Delta Ancla4 \Delta AnAxl2$ double mutants can also be generated to examine conidiophore morphogenesis.

Cell cycle related AnAxl2, Bud3 and Anbud4 expression

We have indicated that contractile actin ring (CAR) assembly is associated with mitosis and nuclear division. A functional SIN pathway is required for AnBud3 localization to the septation site. These results suggest AnBud3 expression can be cell cycle related. Moreover, results from promoter swap experiments between *AnAxl2* and *Anbud4* also indicate that proper expression of *Anbud4* and *AnAxl2* during cell division may be required for their correct localization and even cell viability. I suspect that not only the spatial signal involved in the organization of Bud3, Anbud4 and AnAxl2, but also timing of delivery during cell division will be important.

A series of experiments can be done to investigate the timing of their expression. Microarray experiments can achieve this but will be expensive. Then, northern blot analysis can be used to examine expression levels during cell cycle arrest in the SIN pathway mutants. For example, cell cycle is arrested at G2/M in NIMA mutants and arrested at G1/S in bimE7 mutants. Other nuclear division mutants can also be constructed to precisely arrest the cell cycle. Placing *AnBud3*, *Anbud4* and *AnAxl2* under the control of inducible promoters, such as *alcA*(p), can introduce a pulsed expression during induction. If their pulsed expression can restore correct localization or normal growth in cell cycle arrest mutants, the timing of their delivery will help us to learn

precisely the role of cell cycle-specific transcription as landmark proteins in fungal morphogenesis.

In addition, proper expression of *Anbud4* is essential for cell viability since wrong timing of delivery under the *AnAxl2* promoter resulted in a near lethal phenotype. Pulsed expression will generate high local concentration of Anbud4, which can be used to precisely investigate its interaction with septins, SepA and actin rings by pull down assay and co-immunofluorescence.

Roles of Vac8 and AnAxl2 during sexual development

Our results suggest AnAxl2 may be involved in sexual development through its cadherin domain which interacts with the catenin domain of AnVac8. The upregulated genes in sexual development should be determined in $\Delta AnAnAxl2$ and $\Delta AnVac8$ mutants by microarray or Illumina sequencing. The expression of several key genes needs to be analyzed: VeA, the transcriptional factor for sexual development, may not be expressed in the dark; nsdD, the transcriptional factor for asexual development, may be down-regulated; other sexual related genes RosA (Repressor of sexual development), NosA (Number of sexual spores), SteA (MAPK) and StuA (transcriptional factor) should also be analyzed for expression.

To test the hypothesis of an AnAxl2-AnVac8 interaction, an AnAxl2 intracellular fraction can be cloned and their interactions determined by *in vitro* assay in *E.coli* or yeast two-hybrid, since the β -catenin binds to the cytoplasmic domain cadherins.

Noticeably, AnVac8 and AnAxl2 block sexual development at different stages; double

mutants are also worth generating, which may abolish asexual development. As discussed, the signal through AnAxl2-AnVac8 may transduce to the small GTPases Cdc42 and RacA; thus sexual development in the double or triple mutants of Axl2, Vac8 and Cdc42/RacA will be also interesting to explore. Since $\Delta cdc42$ has a systematic defect, conditional mutants such as *alcA(p)::cdc42^{G14V}* can be used for that purpose.

Further testing the function of Msb2 in cell wall integrity

Functions of Msb2 for cell wall integrity and osmolarity should be tested further by other cell wall inhibitors and osmotic stress chemicals such as caspofungin, 1M sorbitol, 0.8M NaCl, and 1M KCl. As the co-regulator with AnMsb2, AnSho1 is worth investigating as well by gene deletion, localization of GFP fusion protein and protein interaction assay with Msb2. Sho1 can be expected to co-localize with AnMsb2 and $\Delta Ansho1$ would increase the cell wall sensitivity to the integrity inhibitor and osmotic stress like $\Delta msb2$. When I aligned AnMsb2 and yeast Msb2, the conserved HMH region can be found in *AnMsb2*, which is the only essential sequence for osmosensing. After the HMH region is identified in AnMsb2, it should be cloned and tested for protein-protein interactions with Cdc42 and AnSho1 under osmotic stress.

Cell wall integrity defects in $\Delta Anmsb2$ may be correlated with the small GTPases Cdc42, Rac and RhoA, which activate the corresponding HOG and FG MAP kinase pathway. For testing this hypothesis, the intracellular portion of Msb2 can be identified and tested *in vivo* for the direct interaction between Cdc42 and Msb2. CoIP analysis can also be employed to confirm their interaction by labeling Msb2 and its suspected associating proteins with different peptide tags.

Functions of GAPs in *Aspergillus* morphogenesis

A. nidulans homologues of Rga2 and Bem3 may also have specific function through regulating the activity of Cdc42. Knockout mutants, GFP fusion and double mutants can be generated for examining the morphological defects in *A. nidulans*.

Lrg1, Rga1 and Rga2 have a similar pattern of domain organization: tandemly arranged two LIM domains at the N-terminus and GAP domain at the C-terminus. The future study can focus on examining functions of their *Aspergillus* ancestral homologues in both hyphal branching and conidiophore morphogenesis. The three GAPs can bind with other proteins through their LIM domains and activate small GTPase in a similar pattern. Since the interaction between GAPs and small GTPase is dynamic, truncated GAPs without LIM domain can be easier to manipulate for detecting their specific targets. And the LIM domain may also be cloned to for examining interaction pattern with other proteins by the protein pull down assay.